Universitat de Barcelona

Departament de Química Física

Laboratori d'electrodeposició i corrosió (Electrodep)

L'electrodeposició com a mètode de preparació de capes primes heterogènies de cobalt-coure

Albert Llorente Mola

Barcelona, Desembre de 2003

Programa de Doctorat de Tecnología de Materials. Química Física.

Bienni 1999-2001

L'electrodeposició com a mètode de preparació de capes primes heterogènies de cobalt-coure

Tesi que presenta Albert Llorente Mola

per optar al títol de Doctor en Química

Directores de la Tesi:

Dra. Elvira Gómez Valentín
Professora Titular de Química Física
Universitat de Barcelona

Dra. Elisa Vallés Giménez
Professora Titular de Química Física
Universitat de Barcelona

Agraïments

Agraeixo a totes aquelles persones que durant aquests anys de feina m'han ajudat i han estat al meu costat.

En primer lloc agraeixo a les Dres. Elvira Gómez i Elisa Vallés, les meves directores de Tesi, el seu suport i la seva ajuda, sense la qual no hagués estat possible la realització d'aquesta tesi.

Als meus companys i amics del laboratori, que no han estat pocs durant aquest temps!
3A, Evapé, Musta, EvaG & Paco, JC, Isma, Miki, RafaB, RafaN, AnnaA, Birame,
Zergio, Guidon, LauraS, Lidia & Ramón, Carlos & Maria...Amílcar i altre cop a
E & E (les millors 'jefas' que es poden tenir: això és un agraïment, no un
compliment!).

A l'Òscar, Largo i Fernando, i a la resta dels impresentables dels
meus amics, de la facultat, de castefa...de tot arreu.

Fins i tot a Sugelabor i a Panreac! Per la seva confiança en el
camp professional.

Al Tennis Taula, la bici, el futbol, nedar,...al mar i la muntanya.

A Londres, Düsseldorf, La Costa Brava, Cuba, Argentina, Menorca,
l'Ebre, el Pedra i Puigmal, Madrid, Praga i Budapest, Pais Basc,
Eivissa & Formentera,...el Garraf
& any other beatiful place on earth.

A Pérez-Reverte & Paulo Coelho...Als Doors, System of a
Down, Manic Street Preachers, Metallica, Suede, KoRn...
als div al Paraíso de radio 3.

A la conciència social, la llibertat i igualtat, l'ecologia,
rollo hippie, moltes beers, a enjoy life i a
treballar per viure, mai a l'inrevés!...
a l'amistat i a l'amor.

Als meus pares, als meus germans Jordi i Montse i tb a la Marta, Roger i David.

A l'Emma.

Barcelona, Desembre de 2003

‘El miracle de la senzillesa’

Paulo Coelho

Índex

1.- Introducció 1

Referències 7

2.- Objectius 11

3.- Instrumentació i metodologia de treball 13

3.1.-Estudis electroquímics 13

3.1.1.- Instrumentació 13

3.1.2.- Dissolucions 14

3.1.3.- Cel·la i elèctrodes 14

3.1.4.- Tècniques electroquímiques 16

3.1.4.1.- Voltametria cíclica 16
3.1.4.2.- Cronomètodes 16
3.1.4.3.- Deposició polsant 17
3.1.4.4.- Tècniques de redissolució anòdica (stripping) 18

3.2.- Mètodes de caracterització ex-situ 21

3.2.1.- Anàlisi morfològic 21

3.2.2.- Anàlisi composicional 23

3.2.3.- Anàlisi estructural 25

3.2.4.- Mesures magnètiques 27

3.2.5.- Mesures de magnetoresistència 27

3.3.- Tractament tèrmic de les mostres 28

4.- Resultats 31

4.1. Estudi de l'electrodeposició d'aliatges Co-Cu sobre diferents substrats 31

Obtention and characterisation of cobalt+copper electrodeposits from a citrate bath 33

Electrodeposited cobalt+copper thin films on ITO substrata 41

4.2. Control de la heterogeneïtat dels dipòsits Co-Cu mitjançant electrodeposició 47

Electrodeposition for obtaining homogeneous and heterogeneous Co-Cu films 51

4.3. Estudi de la influència del recuit en làmines Co-Cu obtingudes per electrodeposició 73

Annealing of Co-Cu films obtained by electrodeposition 77

4.4. Preparació i caracterització de multicapes de cobalt/coure electrodipositades 101

Characterisation of cobalt/copper multilayers obtained by electrodeposition 103

Electrochemical behaviour and physical properties of Cu/Co multilayers 109

5. Discussió i anàlisi de resultats 119

6.- Situació actual 129

Referències 132

7.- Conclusions 135

1.- Introducció

Durant els darrers anys s'han trobat noves propietats de les làmines metàl·liques primes que amplien sensiblement el camp d'aplicació dels recobriments metàl·lics, restringits durant molt de temps a aplicacions decoratives, de protecció contra la corrosió o d'augment de la duresa dels materials. Actualment hi ha molt interès en les propietats que presenten les capes magnètiques, les multicapes, els aliatges heterogenis i les nanoestructures. Una d'aquestes noves propietats és la magnetoresistència gegant (*giant magnetoresistance*-GMR), que va ser descoberta el 1988 per dos científics europeus que treballaven independentment, Peter Gruenberd [1] de l'institut d'investigació KFA de Julich a Alemanya i Albert Fert [2] de la universitat de Paris-Sud.

Aquest dos grups d'investigadors van trobar que materials composats de tres capes alternes molt primes de Fe/Cr/Fe crescudes per epitàxia de feix molecular (*molecular beam epitaxy*-MBE) canviaven el valor de la resistència elèctrica – un 6 % [1] i un 50 % [2] - aplicant un camp magnètic de 20 kOe en experiments duts a terme a baixes temperatures. Aquesta descoberta va agafar la comunitat científica per sorpresa, ja que els físics mai havien pensat en la possibilitat que aquest fenomen fos possible.

La GMR descoberta d'aquesta manera es pot definir com un canvi acusat en la resistència elèctrica d'un sistema heterogeni que té lloc quan s'aplica un camp magnètic. Una característica comuna dels materials en els quals s'ha detectat GMR és l'existència de zones de mida nanomètrica no homogènies magnèticament.

Encara que els primers resultats es van obtenir en presència de camps magnètics molt alts i amb materials de difícil fabricació, la magnitud d'aquest descobriment va portar a intentar aprofitar l'efecte de la GMR en sistemes d'emmagatzematge d'informació i de tecnologia de sensors. L'objectiu seria el disseny de dispositius magnetoresistius, basats en la relació camp magnètic - resistència elèctrica de determinades làmines

metàl·liques. Aquest fet pot ser aprofitat per aplicar-lo en àrees de mesura de corrent elèctric, sensors de posició, sensors de rotació o per a capçals magnetoresistius de lectura d'informació [3-9].

Els primers treballs en aquesta línia van estar adreçats a estudiar la magnetoresistència que presentaven algunes multicapes metàl·liques constituïdes per una repetitiva alternança de metalls amb propietats magnètiques diferents [10-20]. La MR es va observar en algunes estructures de multicapes de la forma F/NM en les quals F és una capa d'un metall ferromagnètic (Co, Ni, Fe o els seus aliatges) i NM és un metall no magnètic (Cr, Cu, Ag, Au, etc), sempre que les capes magnètiques i no magnètiques siguin d'uns quants nanòmetres de gruix.

D'altra banda, també es va detectar MR en determinats dipòsits heterogenis constituïts per grànuls ferromagnètics de mida nanomètrica inserits dins d'una matriu metàl·lica d'un metall no magnètic, com Cu, Au, Ag, cosa que va estimular la preparació i estudi d'aquest tipus de materials. Aquests dipòsits heterogenis són materials que presenten fases separades o espècies immiscibles. En aquests materials, després d'un tractament tèrmic adequat, és possible aconseguir la precipitació de partícules de mida nanomètrica de material ferromagnètic dins la matriu no magnètica [21-29].

D'aquesta manera, les pel·lícules d'aliatges heterogenis, i no únicament les multicapes F/NM, són potencialment útils per a les aplicacions de MR, especialment en l'àmbit dels sensors magnètics. La preparació de pel·lícules d'aliatges heterogenis presenta l'avantatge de ser generalment més simple i econòmica que la preparació de pel·lícules de multicapes.

Els primers estudis de materials magnetoresistius es van centrar en capes primes preparades per mètodes físics de deposició. Aquests mètodes permeten obtenir materials sòlids per "deposició": per transferència d'energia tèrmica [19,24-25,27] o cinètica [17,18,23,29,30], de manera que els metalls flueixen en un entorn de baixa pressió i condensen quan arriben al substrat. Manipulant convenientment els

paràmetres d'aquests processos es poden obtenir dipòsits amorfs, policristal·lins o fins i tot monocristal·lins, de composició, estructura, morfologia i gruix variables.

S'ha trobat que les propietats d'aquestes capes primes depenen de la seva estructura i, per tant, del seu mètode de preparació. Materials de la mateixa composició poden presentar valors de les propietats magnètiques i magnetoresistives ben diferents [31-34]. Tanmateix, una lleugera diferència en el mètode i les condicions de preparació de les làmines pot implicar una gran variació en les seves propietats. La relació entre les condicions de preparació i les propietats químiques i físiques de les làmines no és encara clara, de manera que avui dia continua essent tema d'estudi.

Com a alternativa als mètodes de preparació físics, l'electrodeposició es presenta com una tècnica adient amb certs avantatges. La deposició en fase vapor suposa un cost elevat tant pel que fa a equipament com pel que fa al temps necessari per controlar la deposició, especialment quan l'objectiu és la deposició de capes alternades. L'electrodeposició no requereix tecnologia de buit i, per tant, és molt més econòmica. Els sistemes experimentals utilitzats són mes simples que els aparells d'evaporació o de *sputtering* i, a més, permeten treballar a temperatura ambient, factor que és molt important en aquells sistemes en què es vol evitar la interdifusió de les capes adjacents. Pot ser fàcilment escalada per aplicar-se en peces de gran àrea i permet dipositar uniformement pel·lícules en superfícies complexes, sense efectes d'ombra que sovint presenten els altres mètodes de deposició. A més, la forta tendència dels materials electrodipositats a créixer epitaxialment ofereix la possibilitat d'obtenir materials amb una textura prefixada pel substrat. De totes maneres hi ha també limitacions associades a l'electrodeposició, com ara la necessitat d'utilitzar un substrat conductor o almenys semiconductor, així com el menor nombre d'elements que poden ser dipositats.

Els primers sistemes heterogenis preparats per electrodeposició van ser multicapes. El fet que algunes multicapes electrodipositades presentessin MR va estimular la investigació, encara que sempre en menor grau que mitjançant els mètodes físics de deposició. Es van testar diferents combinacions de materials i es van utilitzar

diferents substrats a fi de millorar les propietats magnetoresistives. Com a curiositat val a dir que les primeres multicapes obtingudes per electrodeposició de les quals es va mesurar la MR es van preparar sobre coure, i van haver d'ésser retirades del substrat, amb la complicació que això comporta, per aconseguir fer-ne les mesures [35].

En les primeres multicapes electrodipositades la dificultat va raure en la preparació de capes de gruix ben definit i de baixa rugositat [36-39], de la qual cosa es dedueix que per a cada sistema és necessari realitzar un estudi previ de la influència dels paràmetres de deposició. El desenvolupament de les tècniques de caracterització permet visualitzar la qualitat de les capes formades, fins i tot quan les capes són de mida nanomètrica [40-42].

Atès l'interès creixent de les làmines primes de materials heterogenis en la indústria microelectrònica, vàrem plantejar en el Laboratori d'Electrodeposició i Corrosió l'estudi d'aquests tipus de sistemes. L'interès és el possible control de la heterogeneïtat dels dipòsits en funció de les condicions d'electrodeposició. Per això s'ha escollit com a primer sistema d'estudi el cobalt-coure, a fi d'analitzar les possibilitats que presenta l'electrodeposició per a la preparació de làmines primes heterogènies amb propietats magnetoresistives.

El sistema cobalt-coure és potencialment útil per a produir-ne mostres heterogènies, ja que el seu diagrama de fases mostra una pràcticament nul·la solubilitat de cobalt en coure i de coure en cobalt [43], no revela la formació de dissolució sòlida per sota de 900°C ni la formació de cap compost intermetàl·lic encara que els radis atòmics dels dos metalls són similars. Segons això, làmines que contenen cobalt i coure podrien ser heterogènies immediatament després de la seva preparació, la qual cosa podria fer innecessari un tractament tèrmic posterior. A més, les possibles multicapes Co/Cu tindrien com a avantatge respecte a les d'altres metalls la seva possible limitada interdifusió. Un altre avantatge del sistema cobalt-coure és que aquests elements són relativament econòmics i de fàcil abast en el mercat.

Els primers treballs publicats sobre capes primes que contenen cobalt i coure es refereixen a capes alternes de Co/Cu obtingudes mitjançant diferents mètodes físics com l'evaporació amb feix d'electrons (*electron beam evaporation*) [44,45], la deposició per bombardeig d'ions d'argó (*sputtering*) [9,46-50], la deposició amb feix d'ions de baixa energia (*low energy ion-assisted deposition*) [51] o la deposició per bombardeig d'ions d'argó induïda magnèticament (*magneton sputtering*) [52-54]. Aquests estudis analitzen la possible magnetoresistència [9,47,52-55], insisteixen en estudiar la interdifusió entre capes [44-46] i la influència de l'estructura en les propietats magnètiques [48,51].

També hi ha diferents treballs basats en la preparació directa de làmines heterogènies per diferents mètodes físics: *sputtering* [21,56-59], piròlisi d'esprai nebulitzat (*nebulized spray pyrolysis*) [60], *electron beam evaporation* [61,62], refredament ràpid (*rapid quenching*) [63] o molturació mecànica (*mechanical milling*) [64]. Encara que el diagrama de fases del sistema Co-Cu reveli la immiscibilitat d'ambdós metalls [43], s'han trobat condicions que condueixen a dipòsits homogenis [56]. Uns altres estudis determinen que no tots els dipòsits heterogenis de cobalt-coure presenten magnetoresistència [21,58,59,61,62].

S'ha testat la possibilitat de preparació per electrodeposició de làmines Co-Cu [65-69] i de multicapes alternades Co/Cu utilitzant deposició polsant amb un únic bany [70-78]. Tal com succeeix en alguns dipòsits obtinguts per *sputtering*, l'electrodeposició pot conduir a dipòsits metaestables [67-69]. S'han utilitzat diferents banys que contenen els cations metàl·lics en forma de sulfats o sulfamats i alguns d'ells clorur sòdic, àcid bòric o altres additius. Per a la preparació de capes Co-Cu s'han utilitzat banys electrolítics que contenen determinats complexants, necessaris per aconseguir la deposició conjunta dels metalls, a causa de la gran diferència que existeix entre els potencials de deposició del cobalt i del coure. En cada cas la composició concreta del bany (electròlits, pH, additius…) i les condicions d'electrodeposició escollides condueixen a dipòsits amb propietats diferents. Aquests treballs sobre electrodeposició de capes cobalt-coure se centren normalment en l'anàlisi de les característiques de dipòsits obtinguts en condicions prefixades, però

en ells no s'ha trobat una relació directa entre les condicions de preparació i les propietats dels dipòsits. Probablement no s'ha dedicat prou esforç a determinar el paper dels paràmetres electroquímics, com ara el potencial, la composició de l'electròlit i el pH sobre el procés de nucleació i creixement, factors que podrien ser essencials en les propietats finals de les làmines.

L'interès d'aquest treball serà analitzar al nostre laboratori les possibilitats que presenta l'electrodeposició per a la preparació de làmines primes que continguin cobalt i coure per les seves propietats, especialment les magnetoresistives. Simultàniament, es testarà la viabilitat de les tècniques electroquímiques com a eina de caracterització in-situ dels dipòsits obtinguts, comparant els resultats de la caracterització electroquímica amb els de la caracterització ex-situ: microscòpia electrònica de rastreig (*scanning electron microscopy*-SEM), microscòpia electrònica de transmissió (*transmission electron microscopy*-TEM), difracció de raigs X (*X-ray diffraction*-XRD), microsonda electrònica (*electron probe microanalysis*-EPMA). Normalment aquests mètodes ex-situ requereixen una dificultosa preparació de les mostres per a la seva observació.

Es pretén dissenyar un tipus de bany amb suficient versatilitat per explorar la influència dels paràmetres de deposició sobre la heterogeneïtat dels dipòsits obtinguts. Com a complexant s'ha escollit el citrat ja que influeix en l'electrocristal·lització del coure de manera que en adsorbir-se sobre l'elèctrode inhibeix la reducció de les espècies complexades de coure [79].

Referències

1.- M.N. Baibich, J.M. Broto, A. Fert, F.Nguyen van Dau, F. Petroff, P. Eitenne, G. Creuset, A. Friederich and J. Chazclas, Phys. Rev. Lett. 61 (1988) 2472

2.- G. Binasch, P. Gruenberg, F. Saurenbach, W. Zinn, Phys. Rev. B. Condens. Mat. and Mater. Phys. 39 (1989) 4828

3.- J.A. Brug, L. Tran, M. Bhattacharyya, J. H. Nickel, T.C. Anthony, A. Jander, J. Appl. Phys. 79 (1996) 4491

4.- J.P. Spallas, M. Mao, B. Law, F. Grabner, D. O'Kane, C. Cerjan, IEEE T. Magn. 33 (1997) 3391

5.- K. Y. Kim, W.E. Booij, R.W. Moseley, Z.H. Barber, M.G. Blamire, J.E. Evetts, IEEE T. Magn. 35 (1999) 3646

6.- K. Ludwig, J. Hauch, R. Matteis, K.U. Barholz, G. Rieger, Sensors Actuat. A-Phys. A106 (2003) 15

7.- A.E. Mahdi, L. Paruna, D. Mapas, Sensors Actuat. A-Phys.A105 (2003) 271

8.- H. Takahashi, S. Soeya, J. Hayakawa, K. Ito, A. Kida, C. Yamamoto, H. Asano, M. Matsui, J. Appl. Phys. 93 (2003) 8029

9.- M. Suzuki, T. Ohwaki and Y. Taga, Thin Solid Films 304 (1997) 333

10.- T. Shinjo, S. Araki, N. Hosoito J. Magn. Magn. Mater. 90-91 (1990) 753

11.- L. Piraux, A. Fert, P.A. Schroeder, R. Loloee, P. Etienne, J. Magn. Magn. Mater. 110 (1992) L 247-L253

12.- R.B. van Dover, E.M. Gyorgy, R.J. Cava, J.J. Krajwski, R.J. Felder, W.F. Peck, Phys. Rev. B Condens. Mat. and Mat. Phys. 47 (1993) 6134

13.- J. Inoue, H. Itoh, S. Maekawa, J. Magn. Magn. Mater. 121 (1993) 344

14.- N. Kataoka, K. Saito, H. Fujimori, J. Magn. Magn. Mater. 121 (1993) 378

15.- D. Yin, J. Magn. Magn. Mater. 126 (1993) 605

16.- T. Dei, R. Nakatani, H. Hoshiya, K. Hoshino, Y. Sugita, J. Magn. Magn. Mater. 126 (1993) 492

17.- J.D. Jarratt, T. J. Klemmer, J.A. Barnard, IEEE T. Magn. 33 (1997) 3511

18.- A. Tsoukatos, S. Gupta, Y. Huai, IEEE T. Magn. 33 (1997) 3514

19.- K. Wellock, J. Caro, B.J. Hickey, J. Magn. Magn. Mater. 198-199 (1999) 27

20.- E. Majkova, M. Spasova, M. Jergel, S. Luby, S. Okayasu, A. Luches, M. Martino, E.N. Zubarev, M. Brunel, Thin Solid Films 343 (1999) 214
21.- J.Q. Xiao, J.S.Jiang and C.L. Chien, Phys. Rev. Lett. 68 (1992) 3749
22.- J. Xiao, J.S. Jiang, C.L. Chien, IEEE T. Magn. 29 (1993) 2688
23.- J. Q. Wang, G. Xiao, Phys. Rev. B Condens. Mat. and Mat. Phys. 49 (1994) 3982
24.- Ch. Peng, Sh. Zhang, G. Li, D. Dai, J. Appl. Phys. 76 (1994) 998
25.- C. Bellouard, C. Senet, B. George, G. Marchal, J. Phys. Condens. Mat. 7 (1995) 2081
26.- A. Gerber, A. Milner, B.Groisman, M. Karpovsky, A. Gladkikh, Phys. Rev. B Condens. Mater 55 (1997) 6446
27.- L. Dimesso, H. Hahn,, J. Appl. Phys. 84 (1998) 953
28.- J.H. Du, W. Liu, Q. Li, H. Sang, S.Y. Zhang, Y.W. Du, D. Feng, J. Magn. Magn. Mater. 191 (1999) 17
29.- A.M. Zeltser, N. Smith, J. Appl. Phys. 79 (1996) 9224
30.- M. Xu, Ch. Chai, G. Wo, T. Yang, Z. Mai, W. Lai, Thin Solid Films 375 (2000) 205
31.- M. Doi, T. Kanbe, M. Matsui, J. Magn. Magn. Mater. 126 (1993) 443
32.- U. Miyamoto, T. Yoshitani, S. Nakagawa, M. Naoe, IEEE T. Magn. 32 (1996) 4719
33.- H.P. Sun, Z. Zhang, V.D. Wang, H.W. Jiang, W.Y. Lai, J. Appl. Phys. 87 (2000) 2835
34.- H.Wang, X. Lu, X. Yang, S.P. Wong, W.Y. Cheung, N. Ke, J.B. Xu, S.J. Hu, D.C. Zeng, Z.Y. Liu, J. Appl. Phys. 88 (2000) 4216
35.- M. Alper, K. Attenborough, R. Hart, S.J. Lane, D.S. Lashmore, C. Younes, W. Schwarzacher, Appl. Phys. Lett. 63 (1993) 2144
36.- I. Kirilova, I. Ivanov and St. Rashkov, J.Appl.Electrochem.28 (1998) 637, 1359.
37.- J.D. Jensen, D.R. Gabe and G.D. Wilcox, Surf. Coat. Tech. 105 (1998) 240
38.- G. Chawa, G.D. Wilcox and D.R. Gabe, Trans. IMF 76 (1998) 117
39.- M.R. Kalantary, G.D. Wilcox and D.R. Gabe, J. British Corrosion 33 (1998) 197
40.- A.A. Pasa and W. Schwarzacher, Phys. Status Solidi 173 (1999) 73

41.- Y. Jyoko, S. Kashiwabara, Y. Hayashi and W. Schwarzacher, Electrochem. Solid-State Lett. 2 (1999) 67

42.- E. Toth Kadar, L. Peter, T. Becsei and W. Schwarzacher, J. Electrochem. Soc. 147 (2000) 3311

43.- Alloy phase diagrams, Hugo Baker (Eds), ASM Handbook vol 3, ASM Internacional, Ohio, 1992

44.- H. Awano, Y. Suzuki, T. Katayama, A. Itoki, J. Appl. Phys. 68 (1990) 4569

45.- J. Figuera, J.E. Prieto, G. Kostka, S. Müller, C. Ocel, R. Miranda, K. Heinz, Surf. Sci. 349 (1996) L139,

46.- P. Wu, E.Y. Jiang, Y.G. Lin, C.D. Wang, Thin Solid Films 301 (1997) 90

47.- S.S.P. Parkin, R. Bhadra, K. Roche, Phys. Rev. Lett. 66 (1991) 2152

48.- L. Albini, G. Carlotti, G. Gubbiotti, L. Pareti, G. Socino, G. Tioulli, J. Magn. Magn. Mater. 198 (1999) 363

49.- A.M. Shukh, D.H. Shin, H. Hoffmann, J. Appl. Phys. 76 (1994) 6507

50.- R.J. Pollard, M.J. Wilson, P.J. Guindy, , J. Magn. Magn. Mater. 146 (1995) L1, 151 (1995) 139

51.- N.D. Telling, M.D. Crapper, D.R. Lowett, S.J. Gulfoyle, C.C. Tang, M. Petty, Thin Solid Films 317 (1998) 278

52.- L. Malkinski, J.Q. Wang, W.Zhou, T. Kondenkandath, Thin Solid Films 375 (2000) 59

53.- D.J. Kubinski, H. Holloway, J. Magn. Magn. Mater. 165 (1997) 104

54.- M.J. Hall, D.B. Jardine, J.E. Evetts, J.A. Leake, R.E. Somekh, , J. Magn. Magn. Mater. 173 (1997) 253

55.- Y. Ueda, T. Houga, H. Zaman and A. Yamada, J. Solid State Chem. 147 (1999) 274

56.- Childress JR, Chien CL, Phys. Rev. B 43 (1991) 8089

57.- Childress JR, Chien CL, J. Appl. Phys. 70 (1991) 5885

58.- A.E. Berkowitz, J.R. Mitchell, M.J. Carey, A.P. Young, S. Zhang, F.E. Spada, F.T. Parker, A. Hutten, G. Thomas, Phys. Rev. Lett. 68 (1992) 3745

59.- M. Tsunoda , K. Okuyama, M. Ooba, M. Takahashi, J. Appl. Phys. 83 (1998) 7004

60.- Parashar S, Raju AR, Rao CNR, Mat. Chem. Phys. 61 (1999) 46

61.- A.D.C. Viegas, J. Geshev, J.E. Schmidt, E.F. Ferrari, J. Appl. Phys. 83 (1998) 7007
62.- G.N. Kakazei, A.F. Krovetz, N.A. Lesnik, M.M. Pereira de Azevedo, Yu.G. Pogorelov, G.V. Bondorkova, V.L. Silantiev, J.B. Sousa, J. Magn. Magn. Mater. 196 (1999) 29
63.- D. Schmool, A. García-Arribas, E. Abad, J.S. Garitaonandia, M.L. Fdez-Gubieda, J.M. Barandiaran, J. Magn. Magn. Mater. 203 (1999) 73
64.- Liu BX, Ma E, Li J, Huang LJ, Nuc. Instr. Meth. Phys. Res. B 19/20 (1997) 682
65.- H. Zaman, A. Yamada, H. Fukuda, Y. Ueda, J. Electrochem. Soc. 145 (1998) 565 66.- H.J. Blythe, V.M. Fedosyuk, J. Magn. Magn. Mater. 155 (1996) 352.
67.- H.J. Blythe, V.M. Fedosyuk, Phys. Condens. Mater 7 (1995) 3461
68.- V.M. Fedosyuk, O.I. Kasyutich, D. Ravinder, H.J. Blythe, J. Magn. Magn. Mater. 156 (1996) 345
69.- R. López, J. Herreros, A. García Arribas, J.M. Barandiarán, M.L. Fdez-Gubieda, J. Magn. Magn. Mater. 196-197 (1999) 53
70.- M.Schlesinger, K.D. Bird, en M. Paunovic (Eds), Electrochemically Deposited Films II, vol 94-31, Proceedings of The Electrochemical Soc., Pennington, 1995
71.- K.D. Bird, M.Schlesinger, J. Electrochem. Soc. 142 (1995) L65
72.- P. Nallet, E. Chassaing, M.G. Walls, M.J. Hÿtch, J. Appl. Phys. 79 (1996) 6884
73.- Y. Jyoko, S. Kashiwabara, Y. Hayashi, J. Electrochem. Soc. 144 (1997) L5
74.- E. Chassaing, A. Morrone, J.E. Schmidt, J. Electrochem. Soc. 146 (1999) 1794
75.- E. Chassaing, P. Nallet, M.F. Trichet, Journal de Physique IV 6 (1996) C7-13
76.- H. El Fanity, K. Rahmouni, M. Bouanani, A. Dinia, G. Schmerber, C. Mény, P. Panisod, A. Cziraki, F. Cherkaoui, A. Berrada, Thin Solid Films 318 (1998) 227
77.- Y Ueda, N.Kikuchi, S. Ikeda and T. Houga, J. Magn. Magn. Mater. 198-199 (1999) 740.
78.- P.E. Bradley, D. Landolt, Electrochim. Acta 45 (1999) 1077
79.- E. Chassaing, K. Vu Quang, R. Wiart, J. Appl. Electrochem. 16 (1986) 591

2.- Objectius

L'objectiu general del treball és realitzar un estudi de les possibilitats que ofereix l'electrodeposició en la preparació de làmines metàl·liques heterogènies de cobalt-coure i provar la utilitat, per a aquest sistema, de diferents mètodes de caracterització tant electroquímics com físics.

Amb l'objectiu d'aconseguir dipòsits heterogenis de cobalt-coure i/o multicapes alternades de Co/Cu serà necessari:

- Escollir el tipus de bany que permeti l'obtenció d'aquests sistemes i estudiar el procés de deposició en funció de la composició del bany, del substrat i del potencial/corrent aplicat a fi de poder dissenyar les característiques dels dipòsits obtinguts.

- Establir la possible relació entre la informació obtinguda a partir de les tècniques de caracterització electroquímiques i les tècniques de caracterització físiques de les pel·lícules formades.

- Comprovar si l'electrodeposició tant de dipòsits Co-Cu com de multicapes alternades Co/Cu és possible sobre substrats que permetin la mesura directa de la magnetoresistència i, en el seu cas, establir les condicions d'electrodeposició que portin a l'obtenció de dipòsits que presentin magnetoresistència.

3.- Instrumentació i metodologia de treball

3.1.-Estudis electroquímics

3.1.1.-Instrumentació

Els experiments electroquímics s'han realitzat amb un potenciostat/galvanostat EG&G 273 controlat per el programa Echem 270 i amb un equip Autolab amb equipament PGSTAT30 i software GPES.

EG&G 273

Autolab PGSTAT30

Les multicapes s'han preparat amb un sistema analògic Belport 105 potenciostat juntament amb un generador de senyal EG&G 175 o amb un equip Autolab amb equipament PGSTAT30 i software GPES.

S'ha utilitzat un termòstat de flux regulat Haake FS o Julabo 5.

3.1.2.- Dissolucions

Totes les dissolucions han estat preparades el mateix dia de l'experiment, amb aigua desionitzada, bidestil·lada i tractada amb un sistema Millipore Milli Q. Les dissolucions s'han preparat amb reactius ($CuSO_4 \cdot 5H_2O$, $CoSO_4 \cdot 7H_2O$, citrat de sodi ($Na_3C_6H_5O_7 \cdot 2H_2O$) i H_3BO_3) de puresa analítica. El pH de les dissolucions electrolítiques ha estat ajustat, en cas necessari, per addició de H_2SO_4 . Abans i durant els experiments, les dissolucions han estat desoxigenades utilitzant argó (99,99%).

3.1.3.- Cel·la i elèctrodes

S'ha utilitzat una cel·la convencional termostatitzada de tres elèctrodes.

Cel·la termostatitzada de tres elèctrodes

S'han utilitzat diferents tipus d'elèctrodes de treball en funció del tipus d'experiment:

- Carboni vitri, Ni, Cu: Barres de carboni vitri (Metrohm), níquel i coure (John Matthey, 99,99%.) de 2 mm de diàmetre i barra de coure de 7 mm diàmetre.
- Grafit: Barra de grafit (Alfa Aesar) de 0.45 mm de diàmetre.

- Vidre/Au, vidre/Cr: Plaques de vidre de 1.1-1.3 cm^2 recobertes, per *sputtering*, de capes d'or o de crom de 200 nm.
- Vidre/ITO: Fines capes (25 nm) d'òxid de indi i estany (ITO) dipositades per *sputtering* sobre substrats de vidre d'àrea 1.5 cm^2.
- Si/capa llavor: Peces de silici d'àrea 1.1 cm^2 recobertes amb una capa llavor de titani/níquel (100nm/50nm).

Diferents tipus d'elèctrodes utilitzats

En cada cas, l'àrea del elèctrode de treball s'ha controlat utilitzant cinta de tefló: 0.0314 cm^2 per carboni vitri i Ni, 0.0314 o 0.39 cm^2 per Cu, 0.25 cm^2 per grafit, 0.27 cm^2 per vidre/Au i vidre/Cr i 0.7 cm^2 per vidre/ITO i Si/capa llavor.

Com a elèctrode auxiliar s'ha emprat una espiral de platí. Com a elèctrode de referència s'ha utilitzat un elèctrode de Ag|AgCl|1 mol dm^{-3} NaCl. El contacte de l'elèctrode de referència amb la dissolució s'ha realitzat via un capil·lar de Luggin ple d'una dissolució de Na_2SO_4 0.5 mol dm^{-3} per al contacte amb la dissolució. Tots els potencials es refereixen a aquest elèctrode.

Depenent de la naturalesa de l'elèctrode de treball, s'ha trobat la manera més adequada de preparació abans de cada experiment, amb l'objectiu d'aconseguir una superfície el més reproduïble possible: Els elèctrodes de carboni vitri s'han polit manualment fins a acabat especular sobre draps de polir DP-Mol i OP-Nap Struers, amb alúmina de diferent mida de gra (3.75 i 1.87 μm) i posteriorment rentats

ultrasònicament durant dos minuts en aigua. Els elèctrodes de níquel s'han polit fins a acabat especular fent servir pasta de diamant de 6 i 1 μm sobre draps de polir Struers DP-Nap en una polidora mecànica Struers Dap-7 i a continuació manualment sobre draps DP Mol Struers amb alúmina de 0.3 μm suspesa en aigua destil·lada i posteriorment rentat ultrasònicament durant dos minuts en aigua. Els elèctrodes de coure s'han polit manualment fins a acabat especular fent servir primer paper de grau 4000 i desprès alúmina (0.3 i 0.05 μm) suspesa en aigua destil·lada sobre draps Buehler Masterdex. Posteriorment es renten ultrasònicament durant dos minuts en aigua. Els elèctrodes de vidre/ITO, vidre/Au, vidre/Cr i Si/capa llavor han estat rentats primer amb acetona i a continuació amb aigua.

3.1.4.- Tècniques electroquímiques

3.1.4.1.- Voltametria cíclica

La voltametria cíclica ha permès realitzar l'estudi general del procés de deposició. Els experiments voltamètrics s'han realitzat a diferents velocitats d'escombrat, partint sempre d'un potencial al qual no es detecta corrent. S'ha registrat únicament un cicle per a cada experiment voltamètric. Durant l'escombrat catòdic es produeix la electrodeposició de coure i cobalt, i durant l'escombrat anòdic té lloc l'oxidació dels metalls prèviament dipositats. Cal establir els límits de potencial per evitar la evolució de hidrogen (escombrat catòdic) i l'evolució d'oxigen/oxidació del substrat (escombrat anòdic). També es pot obtenir informació de l'eficiència del procés de deposició o de la passivació del dipòsit, comparant les càrregues dels processos d'oxidació i reducció.

3.1.4.2.- Cronomètodes

S'ha analitzat la deposició també mitjançant tècniques potenciostàtiques i galvanostàtiques a diferents potencials o densitats de corrent, tant en condicions

estacionàries com d'agitació. L'agitació s'ha controlat per bombolleig d'argó o per agitació magnètica a diferents velocitats (entre 60 i 500 rpm).

3.1.4.3.- Deposició polsant

Les multicapes Co/Cu s'han fet créixer a partir d'un únic bany contenint els ions metàl·lics, mitjançant corrent polsant sota control potenciostàtic. Durant la deposició s'ha utilitzat una moderada agitació de la dissolució per mantenir la contribució del coure(II), minoritari a la dissolució, cap a l'elèctrode. Degut a que el coure és un metall molt noble es requereix un potencial baix per dipositar-lo, mentre que el cobalt requereix un potencial més negatiu. S'aplica un potencial E_{Cu} durant un temps t_{Cu} per a dipositar la capa de coure i un potencial E_{Co} durant un temps mes curt t_{Co} per a dipositar la capa de cobalt. Aquest cicle es repeteix varies vegades, registrant simultàniament la resposta densitat de corrent-temps, el que permet calcular la càrrega de cada capa.

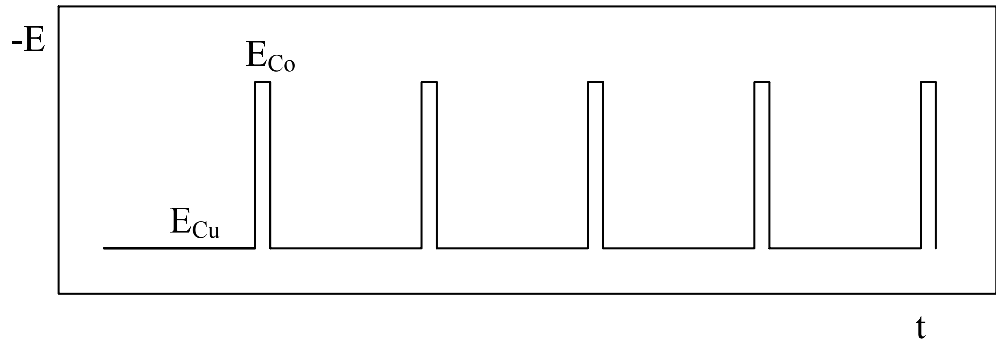

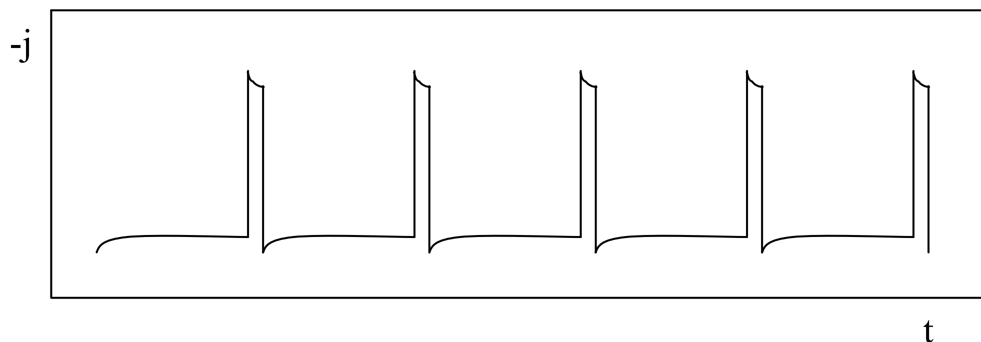

3.1.4.4.- Tècniques de redissolució anòdica (stripping)

Per analitzar in-situ els dipòsits mitjançant mètodes electroquímics s'han utilitzat les tècniques de *stripping*. Amb la redissolució anòdica es pretén caracteritzar electroquímicament les diferents fases que constitueixen un dipòsit gràcies al fet que l'oxidació d'aquestes fases pot tenir lloc a valors de potencial diferents. L'anàlisi per *stripping* s'ha realitzat sempre immediatament després de la deposició, obtenint-se resultats similars tant si l'*stripping* es duu a terme en la pròpia dissolució o bé en una dissolució blanc (sense Cu(II) i Co(II)).

S'han utilitzat diferents possibilitats tant per la formació del dipòsit com per la seva oxidació.

a) Deposició potenciostàtica + oxidació potenciodinàmica.

Es registra la corba cronoamperomètrica durant la formació del dipòsit a potencial constant i la corba potenciodinàmica durant l'oxidació. Des d'un potencial inicial en el que no hi ha deposició s'escombra cap a potencials positius a una velocitat de 10 mV s^{-1}. Un exemple de la senyal aplicada i de la resposta obtinguda en el cas de deposició en condicions d'agitació i oxidació d'un únic tipus de dipòsit format seria:

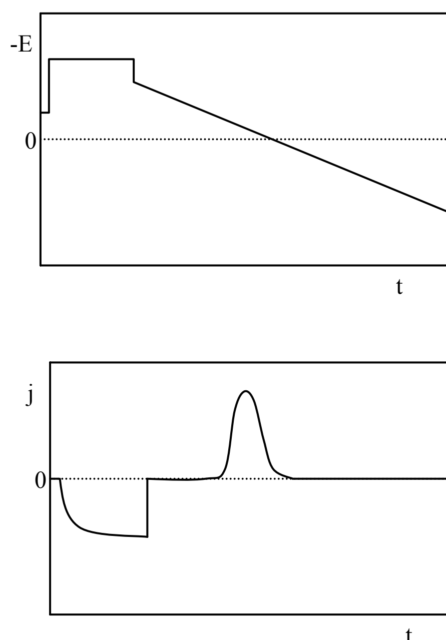

b) Deposició galvanostàtica + oxidació potenciodinàmica.

El dipòsit es prepara aplicant, durant un cert temps, un corrent constant i a continuació s'oxida mitjançant un escombrat de potencial, en les mateixes condicions que en el cas anterior. Es registra la resposta potencial-temps durant la deposició i la resposta densitat de corrent-potencial durant l'oxidació.

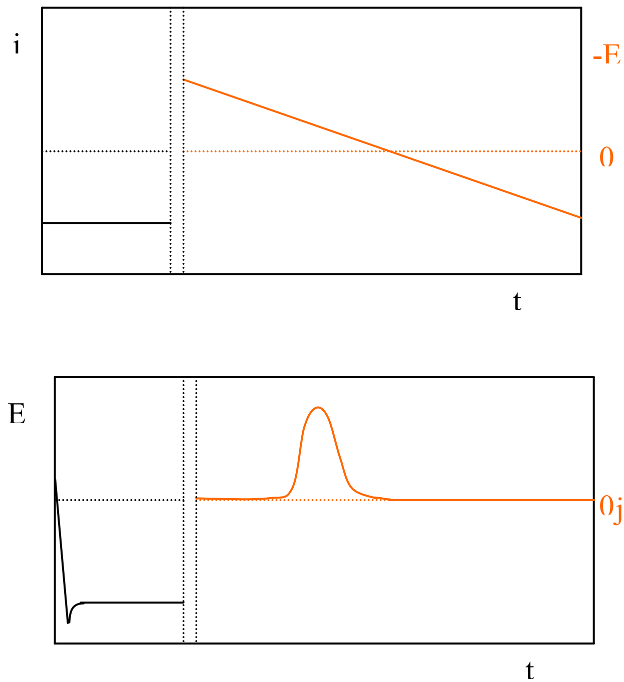

c) Deposició potenciostàtica + oxidació galvanostàtica.

S'analitza la resposta densitat de corrent-temps durant la deposició a potencial constant i posteriorment l'oxidació a densitat de corrent constant i positiva. S'escullen densitats de corrent d'oxidació moderadament positives per afavorir l'oxidació lenta del dipòsit preparat.

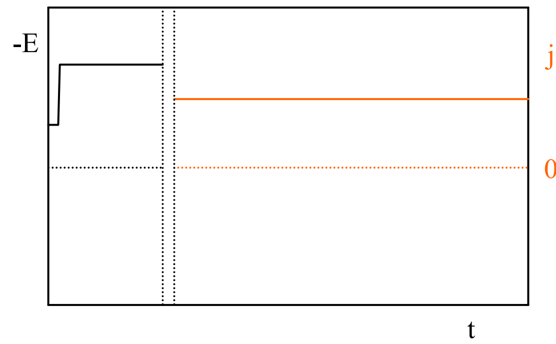

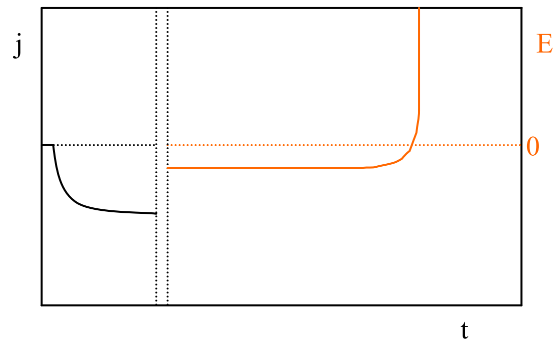

A l'exemple presentat s'observa un únic *plateau* a la corba d'oxidació, corresponent a l'oxidació d'un únic tipus de dipòsit format. La brusca pujada en la resposta E-t indica la complerta oxidació del dipòsit.

d) Deposició i oxidació galvanostàtica.

En aquest cas s'oxida a densitat de corrent positiva i constant un dipòsit preparat a densitat de corrent negativa i constant. Es registra i analitza la resposta potencial-temps tant durant la deposició con durant l'oxidació.

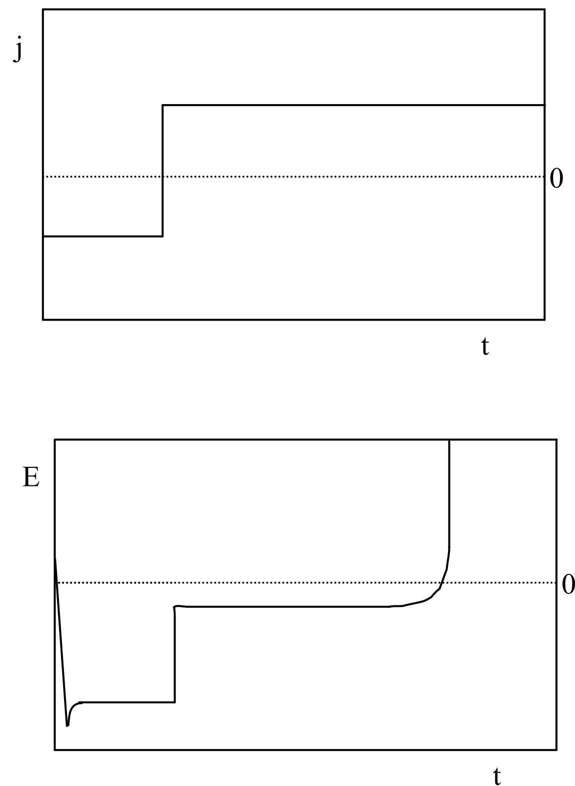

3.2.- Mètodes de caracterització ex-situ

3.2.1.- Anàlisi morfològic

Per al seguiment de la preparació de la superfície dels elèctrodes i per a una observació preliminar dels dipòsits obtinguts s'ha utilitzat un microscopi òptic Olympus PM GC3.

La caracterització morfològica dels dipòsits s'ha realitzat amb diferents equips de SEM: Hitachi S-2300 i Leica Stereoscan 360. El microscopi electrònic de rastreig permet obtenir imatges de gran resolució de la topografia superficial dels dipòsits.

L'observació dels dipòsits preparats sobre elèctrodes de carboni vitri o metall s'ha dut a terme directament, sense necessitat de recobrir la superfície de les mostres. En canvi, per observar les mostres obtingudes sobre els elèctrodes base-vidre o silici, degut a que aquests elèctrodes tenen un substrat no conductor, ha estat necessari

aplicar “pistes” de laca de plata per fer contacte elèctric entre el suport del microscopi i la mostra.

Leica Stereoscan 360

L’observació per SEM de les multicapes obtingudes sobre elèctrode de coure ha requerit una acurada preparació. Les multicapes s’han protegit dipositant-hi al damunt una capa de coure d’unes 40 μm. La mostra va ser tallada lentament a 1mm per sota de la superfície per evitar danys a les multicapes i a continuació va ser emmotllada en una resina polimèrica. Amb l’objectiu de deixar a la vista la secció transversal de la mostra, es comença a polir el motlle, tenint en compte que les multicapes quedin en posició perfectament transversal: primerament es poleix amb papers de gra gruixut (grau 1000 i 2400) i just en el moment en què apareix la secció de les multicapes, es passa a polit manual acurat amb papers de grau 4000. A continuació s’utilitza alúmina de 0.3 i 0.05 μm suspesa en aigua destil·lada. Les mostres són rentades amb aigua destil·lada entre cada una de les etapes del polit. Degut a que la resina no és conductora s’hi ha d’aplicar una pista de laca de plata per a l’observació.

L’estudi de les multicapes per microscòpia de forces atòmiques en mode dinàmic (*tapping mode atomic force microscopy*-TMAFM) es va portar a terme amb un microscopi Multimode controlat per una electrònica Nanoscope III, ambdós equips de Digital Instruments. Les puntes d’observació són de silici i fabricades per

Nanosensors. La microscòpia de forces atòmiques permet fer una perfilometria tridimensional amb resolució entre 1mm i 1 nm.

DI Multimode

Per realitzar l'observació per TMAFM de les multicapes va ser necessari, després de realitzar la mateixa preparació de mostra que per a l'observació per SEM, atacar selectivament una de les capes, creant així un relleu de la superfície que permet distingir les capes individuals. L'atac químic selectiu del coure es fa submergint la mostra durant 5 segons en dissolució de Nital (dissolució de HNO_3 65 % en etanol). Les mostres es van rentar en aigua destil·lada prèviament a l'observació per TMAFM.

3.2.2.- Anàlisi composicional

La composició dels dipòsits s'ha analitzat amb la microsonda electrònica, en un equip Cameca SX-50. La microsonda electrònica, basada en la detecció de la radiació X generada en bombardejar la mostra amb un feix d'electrons energètics focalitzats, permet determinar la composició elemental de petites regions (poques micres quadrades) de la mostra. Permet així comprovar si la composició és constant en diferents punts de la mostra.

Els substrats base vidre o silici es varen analitzar prèviament a fi d'obtenir la resposta del substrat (necessària per analitzar les capes primes de Co-Cu). Per a les mostres obtingudes sobre aquests elèctrodes, el microanàlisi s'ha realitzat utilitzant la tècnica de voltatge variable als següents potencials: 10, 12, 15, 18, i 20 keV. Las línies de raigs X analítiques han estat les de Co-K_α i Cu-K_α. La composició i el gruix s'han estimat a partir de raigs X utilitzant el programa informàtic Layerf per a caracterització de capes primes (Pouchou and Pichoir model, Cameca SX-50).

En algun cas concret s'ha determinat la composició mitjançant l'analitzador de raigs X incorporat en un Leica Cambridge Stereoscan S-360.

La determinació de la composició dels dipòsits en funció del gruix s'ha realitzat amb un espectròmetre de raigs X (*X ray photoelectron spectroscopy*-XPS), PHI 5600 utilitzant la radiació Al-K_α amb una resolució de 0.1 eV. L'espectrometria de fotoelectrons s'utilitza per a l'anàlisi elemental, semiquantitatiu i de l'estat químic de la superfície de les mostres. Fent un atac de la superfície durant diferents temps és possible fer l'anàlisi a diferents profunditats.

PHI 5600

Les mesures d'espectroscòpia Auger s'han realitzat amb un sistema PHI 670. L'espectrometria d'electrons Auger és complementària a l'anterior ja que és també

una tècnica superficial, però localitza amb precisió subatòmica. Només es aplicable a materials conductors.

3.2.3.- Anàlisi estructural

L'estudi de la microestructura dels dipòsits s'ha realitzat mitjançant microscòpia electrònica de transmissió en un equip Phillips CM-30. Els microscopis de HRTEM (TEM d'alta resolució) també permeten obtenir difractogrames electrònics de feix convergent de zones nanomètriques de les mostres. El seu anàlisi permet la determinació de paràmetres de xarxa cristal·lina i el grup d'espai de l'estructura.

Phillips CM-30

L'observació dels dipòsits per TEM precisa d'una preparació específica segons el tipus de mostra.

Per a l'observació planar d'un dipòsit la mostra es talla amb una serra Buehler Isomet lentament a 1mm per sota de la superfície del substrat per evitar danys al dipòsit. Es col·loca la mostra invertida sobre un cilindre metàl·lic i s'hi fixa amb la resina. Es poleix en la polidora mecànica Struers Labopol-5 amb paper gruixut (grau 600) fins a deixar un gruix de mostra de unes 70 μm (el dipòsit queda intacte, ja que

queda a la part inferior); el gruix es controla per enfocament de la imatge amb un microscopi òptic. Es continua amb un polit més fi amb paper de grau 4000 fins a fer desaparèixer les ratlles del polit gruixut. A continuació es separa la mostra del cilindre i s'enganxa (també invertida) a una arandella de Cu amb cola M-Bond 610. A continuació es passa a un polit més acurat amb la polidora còncava Gatan 656 Dimple Grinder: primer amb una roda de Cu utilitzant pasta de diamant de 0.3 μm, fins a un gruix de unes 20-30 μm en la part central de la concavitat formada. Es fa un polit fi durant pocs minuts amb una roda amb drap i alúmina fina de 0.05 μm. Es trasllada la mostra a l'aprimador iònic Gatan 691 Ion Pollishing System: s'aprima amb un doble feix a 4.5 keV i angles de +8º, la mostra en rotació de 2 rpm, fins a l'aparició del forat. En aquest moment es passa a fer un aprimament simultani per la part superior i inferior (angles = +6º i –8º) durant cinc minuts, a fi d'aconseguir que les vores del forat tinguin el menor gruix possible i així facilitar l'observació en el microscopi.

La preparació per a l'observació transversal de les mostres de multicapes requereix el mateix tipus de preparació que les mostres planars però amb la variant que es tallen dues mostres de multicapes i s'enganxen, de manera que les superfícies dels dipòsits de multicapes quedin encarades. Assegurant que les multicapes quedin en posició perfectament perpendicular, es realitza el mateix tipus de polit (ara per ambdues cares) i aprimament que en el cas de les mostres planars.

Els experiments de difracció de raigs X s'han realitzat en els difractòmetres: Phillips MRD i Siemens D-500, en funció de la geometria de la mostra. A la XRD s'utilitzen longituds d'ona dels raig X del mateix ordre que les distàncies interatòmiques dels cristalls, que actuen com a xarxes de difracció, difractant els raig X en direccions i amb intensitats determinades. El difractòmetre Siemens D-500 s'ha utilitzat per a estudiar els recobriments preparats sobre substrats plans, mentre que el difractòmetre Phillips MRD s'ha utilitzat per l'estudi dels dipòsits obtinguts sobre carboni vitri o barretes metàl·liques. En ambdós casos es va seleccionar la radiació Cu-K_{α} (λ=1.5406 Å). Els difractogrames es registren en diferents intervals de 2θ, mesurant cada 2θ=0.05^{o} i utilitzant un temps de mesura variable entre 3 i 14 s per punt.

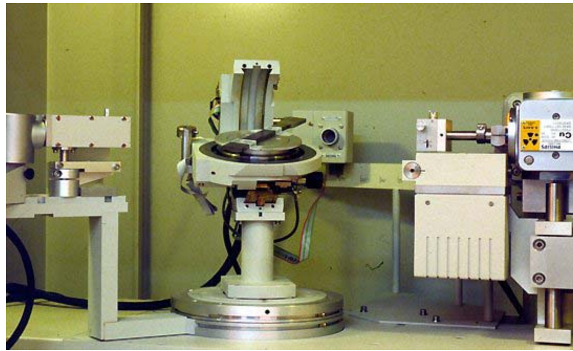

Phillips MRD

3.2.4.- Mesures magnètiques

La determinació de la magnetització de saturació i de la coercitivitat dels dipòsits s'ha realitzat en un magnetòmetre tipus pèndol Manics DSM-8 a temperatura ambient. L'instrument va ser calibrat mesurant la magnetització d'una ferrita standard.

3.2.5.- Mesures de magnetoresistència

Les mesures de magnetoresistència (MR) s'han realitzat mitjançant la tècnica de corrent altern i sondes de quatre punts a temperatura ambient i a 27 K amb camps magnètics fins a 11 kOe, utilitzant equipament de Oxford Instruments.

L'electroimant permet variar el camp magnètic des de -11 kOe a 11 kOe, amb un sensor que mesura el camp magnètic real al centre de les bobines de l'electroimant amb una precisió de ±2Oe. Un amplificador *lock-in* mesura el voltatge i el corrent que circula per la mostra per a la freqüència seleccionada. El criostat acoblat al centre de l'electroimant permet variar la temperatura de la mostra. S'ha utilitzat un criostat de cicle tancat de Air Products que permet baixar la temperatura fins a 27 K. S'han aplicat intensitats de corrent baixes (<10mA) per tal d'evitar l'escalfament de les mostres. Els contactes elèctrics (4 fils de Cu) s'han fet per pressió amb la mostra.

El valor de la magnetoresistència s'ha calculat com a $|\Delta R/R_0|$, on ΔR=R(H)-R_0 és la variació de la resistència elèctrica deguda al camp magnètic aplicat i R_0 és la resistència màxima en el camp coercitiu.

Sistema de mesura de la magnetoresistència

3.3.- Tractament tèrmic de les mostres

Per realitzar el recuit de les mostres s'ha dissenyat i construït un forn de les següents característiques: Construït a partir de la mecanització d'un bloc d'alumini, consta d'un bloc de coure aïllat de la base del forn per unes potes d'un material ceràmic; dins el bloc de coure hi ha tres orificis a on s'hi posen tres làmpares halògenes; també té un petit orifici on hi va el termoparell; les làmpares dins el bloc de coure constitueixen el sistema calefactor. Els cables del termoparell i les làmpares passen cap a l'exterior del forn a través d'un passamurs, connector elèctric que tanca hermèticament el buit. El forn està connectat a una bomba rotatòria de buit a fi de mantenir una atmosfera lliure d'oxigen per evitar que les mostres s'oxidin durant el recuit. S'ha d'arribar a una pressió mínima de 10^{-2} atm abans de començar a pujar la temperatura. El forn disposa d'una tapa superior amb una petita finestra de metacrilat

que permet observar la mostra durant el recuit. El control de la temperatura es fa seleccionant el nombre de làmpares en funcionament.

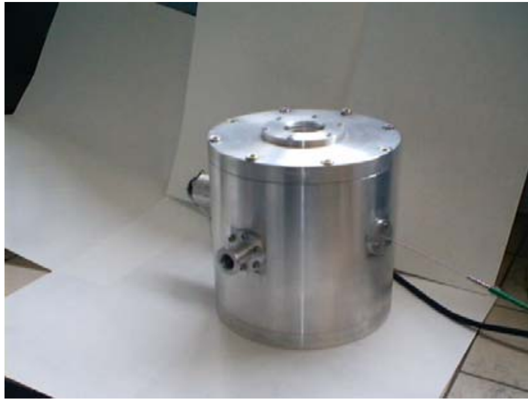

Forn per el tractament tèrmic de les mostres

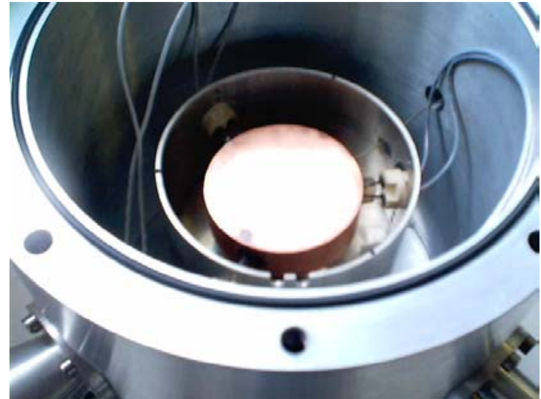

Vista del sistema calefactor

4.- Resultats

4.1. Estudi de l'electrodeposició d'aliatges Co-Cu sobre diferents substrats

En aquest capítol s'ha estudiat la electrodeposició del sistema Co-Cu a partir de dissolucions que contenen $CuSO_4$ i $CoSO_4$, amb una concentració total d'ions metàl·lics de 0,2 mol dm^{-3}, en medi citrat (0.5 mol dm^{-3} de citrat sòdic) i en presència de H_3BO_3 (30 g dm^{-3}). El pH de les dissolucions ha estat de 5.3 i la temperatura s'ha mantingut a 20ºC. S'han utilitzat diferents elèctrodes com carboni vitri, Ni, Cu o vidre/ITO.

S'ha dut a terme un estudi bàsic del procés a partir dels banys de relació de [Co(II)]/[Cu(II)] en solució 1:1, 3:1 i 9:1, majoritàriament sobre elèctrode de carboni vitri per ampliar la zona de potencials en la que no hi ha resposta del propi elèctrode. Es comprovarà si el comportament observat és extensiu a qualsevol relació de [Co(II)]/[Cu(II)] en solució i pot ser aplicat a diferents substrats.

Per a cada bany electrolític emprat s'han preparat dipòsits Co-Cu, normalment en condicions galvanostàtiques i amb agitació de la dissolució, a diferents condicions d'electrodeposició. S'ha analitzat si el tipus de bany i el control de les condicions d'electrodeposició permeten obtenir dipòsits uniformes i coherents de diferent composició (EPMA) i morfologia (SEM).

S'estudia si la tècnica d'*stripping* (tant potenciodinàmic com galvanostàtic) permet obtenir informació sobre el tipus i composició dels dipòsits, i es comprovarà si els resultats concorden amb les observacions de XPS i XRD. S'intentarà establir les característiques estructurals dels dipòsits.

Amb l’objectiu de mesurar la magnetoresistència dels dipòsits, aquests es preparen sobre vidre/ITO, ja que és un elèctrode suficientment conductor com per permetre l’ electrodeposició i alhora no ho és prou com per interferir en les mesures de MR. Es mesurarà la MR d’aquests dipòsits, i s’intentarà establir una relació amb el %Co.

L’anàlisi dels valors de MR, i els resultats de XRD, TEM i *stripping*, permetrà estudiar la possible heterogeneïtat dels dipòsits.

Els resultats detallats d’aquest capítol s’inclouen en els següents articles:
-*Obtention & Characterisation of Co+Cu electrodeposits from a citrate bath*
J. Electroanal. Chem. 495 (2000) 19-26
-*Electrodeposited Co+Cu thin films on ITO substrata*
J. Electroanal. Chem. 517 (2001) 63-68

ELSEVIER

www.elsevier.nl/locate/jelechem

Journal of Electroanalytical Chemistry 495 (2000) 19–26

Journal of Electroanalytical Chemistry

Obtention and characterisation of cobalt + copper electrodeposits from a citrate bath

E. Gómez, A. Llorente, E. Vallés *

Laboratori de Ciència i Tecnologia Electroquimica dels Materials (LCTEM), Departament de Química Física, Facultat de Química, Universitat de Barcelona, Martí i Franquès 1, 08028 Barcelona, Spain

Received 15 May 2000; received in revised form 4 August 2000; accepted 9 September 2000

Abstract

The electrodeposition of cobalt + copper alloy on vitreous carbon, copper and nickel electrodes in a citrate bath at pH ca. 5 has been studied for two [Co(II)]/[Cu(II)] ratios in solution. Voltammetric and stripping results on vitreous carbon show that co-deposition of the two metals takes place under these conditions. Electrodeposition leads to the formation of a solid solution of cobalt in copper, detected by only one oxidation peak that shifts from the copper to the cobalt position as the applied current density–applied potential is made more negative. Structural XRD analysis and compositional analyses, confirm the formation of a cobalt–copper solid solution of face-centred-cubic (fcc) structure. Diffractograms show peaks that appear at diffraction angles between the lines corresponding to copper and fcc cobalt. The value of the fcc lattice constant a of the alloy decreases linearly with the increase in the cobalt percentage in the deposits, following Vegard's law. Deposits obtained at the same charge and current density from the same bath on different substrates have similar morphology: nodular-grained deposits at low deposition current densities–applied potentials, which evolve gradually to more fine-grained and structured deposits as the cobalt percentage in the deposits is increased. © 2000 Elsevier Science B.V. All rights reserved.

Keywords: Electrodeposition; Cobalt + copper alloy; Stripping analysis; XRD

1. Introduction

Recently, the preparation of coatings of transition metals such as Co, Fe or Ni (ferromagnetic metals) in a metallic matrix of Cu, Cr, Au or Ag (non magnetic metals), both in the form of coupled metallic multilayers and in the form of heterogeneous alloys, has attracted considerable attention for its potential applicability to magnetoresistive devices.

The cobalt + copper system is at the moment an object of study in this field due to its possible applications for magnetic sensing. It has been found that some Co + Cu multilayers [1–7] and some heterogeneous Co + Cu alloys [8–12] present a high magnetoresistance value.

The equilibrium phase diagram of Co + Cu allows negligible solubility at room temperature [13]; however homogeneous films can be obtained by sputtering [14]. Recently electrodeposition has also been demonstrated as a useful tool for the preparation of these homogeneous films [15]. Therefore, the Co + Cu system is well suited as a candidate for the production of such metastable alloys.

In this study we attempt to obtain electrodeposited Co + Cu alloy films. As it is observed that a slight difference in the preparation can introduce a large difference in physical properties, a systematic study of the influence of electrodeposition parameters was made. It is necessary to understand the deposition mechanism in order to control the characteristics and properties of the alloy deposits. Due to the different standard electrode potentials of cobalt and copper, a complexing agent is required in order to codeposit the two metals more readily.

The purpose was threefold: (a) to produce cobalt + copper deposits from a single solution; (b) to examine the influence of different parameters on the alloy composition and (c) to characterise these materials as a function of the electrochemical conditions.

* Corresponding author. Tel.: +34-93-4021234; fax: +34-93-4021231.

E-mail address: e.valles@qf.ub.es (E. Vallés).

0022-0728/00/$ - see front matter © 2000 Elsevier Science B.V. All rights reserved.
PII: S0022-0728(00)00376-4

The characterisation was made in-situ by means of electrochemical stripping and ex-situ by X-ray diffraction in order to assure the alloy formation, due to the possibility that the two metals could have been deposited separately, according to the phase diagram.

2. Experimental

Chemicals used were $CuSO_4 \cdot 5H_2O$, $CoSO_4 \cdot 7H_2O$, sodium citrate ($Na_3C_6H_5O_7 \cdot 2H_2O$) and H_3BO_3. All solutions were freshly prepared with water first doubly distilled and then treated with a Millipore Milli Q system. In all experiments solutions contained 0.5 mol dm^{-3} Na_3citrate + 30 g dm^{-3} H_3BO_3 and the total metallic ion concentration was maintained at 0.2 mol dm^{-3}. The [Co(II)]/[Cu(II)] ratio in solution was either 3:1 or 1:1. A prior study of the electrodeposition of both metals separately, was also made. The pH was adjusted to 5.3 in all cases by suitable addition of H_2SO_4.

Before and during the experiments, solutions were de-aerated with argon. Deposition was performed at 20°C.

Electrochemical experiments were carried out in a conventional three-electrode cell using an EG&G 273 potentiostat/galvanostat controlled by a microcomputer. Working electrodes (0.0314 cm^2) were: vitreous carbon rod (Metrohm) and nickel and copper rods (John Matthey 99.99%). Vitreous carbon electrodes were polished to a mirror finish before each experiment using alumina of different grades (3.75 and 1.87 μm) and cleaned ultrasonically for 2 min in water. Nickel and copper electrodes were polished to a mirror finish before each experiment using diamond (6 and 1 μm) and alumina (0.3 μm) suspended in distilled water and cleaned ultrasonically for 2 min in water. The counter electrode was a platinum spiral. The reference electrode was Ag | AgCl | 1 mol dm^{-3} NaCl mounted in a Luggin capillary containing 0.5 mol dm^{-3} Na_2SO_4 solution. All potentials are referred to this electrode.

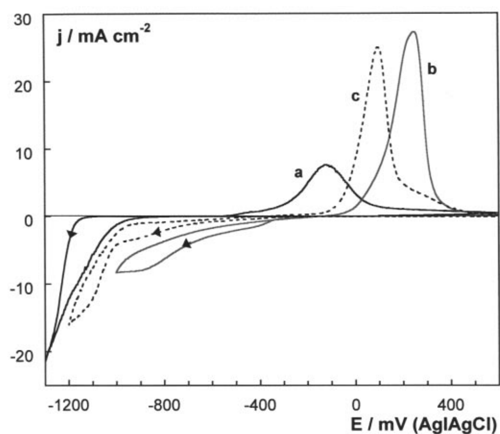

Fig. 1. Cyclic voltammograms: (a) 0.2 mol dm^{-3} $CoSO_4$ solution. Lower limit −1300 mV. (b) 0.2 mol dm^{-3} $CuSO_4$ solution. Lower limit −1000 mV. (c) 3:1 ratio of a [Co(II)]/[Cu(II)] solution. Lower limit −1200 mV. Stationary conditions.

The morphology of the deposits was examined with a Hitachi S 2300 scanning electron microscope. The electrodeposits were analysed using a Cameca SX-50 electron microprobe and an X-ray photoelectron spectrometer (XPS), PHI 5600 multitechnique system, using standard Al–K_α radiation, with a resolution of 0.1 eV.

X-ray diffraction (XRD) analysis was performed on a Phillips MRD diffractometer on its low resolution parallel beam optics. The Cu–K_α radiation ($\lambda = 1.5406$ Å) was monochromatised by means of a diffracted beam flat graphite crystal. $2\theta/\theta$ diffractograms were obtained in the range of $2\theta = 20–100°$ with a step range of $2\theta = 0.05°$ and a measuring time of 5 s per step.

Magnetic measurements were performed with a pendulum type-magnetometer (MANICS DSM 8) at room temperature. The instrument was calibrated by magnetisation measurement of standard ferrite.

Voltammetric experiments were carried out at 50 mV s^{-1}, scanning at first to negative potentials. Only one cycle was run in each voltammetric experiment. Stripping analysis was always performed immediately after deposition, without removing the electrode from the solution. All potentiodynamic stripping experiments were made at a scan rate of 10 mV s^{-1} and an initial potential at which deposition did not occur was chosen. All deposits were obtained under stirred conditions.

3. Results and discussion

Prior to the study of cobalt + copper electrodeposition, a study of the deposition of both individual metals was performed in the same citrate medium. The analysis of the individual metals forming the basis of the alloy included all electrochemical and morphological techniques used in the study of the alloy electrodeposition.

3.1. Cobalt + copper alloy deposition

3.1.1. Voltammetric data

Fig. 1 shows the voltammetric curves for the individual metals deposition (curves a and b) and for the alloy deposition (curve c). For the Co + Cu system the voltammograms show in all cases one oxidation peak, ranged between the individual cobalt and copper oxidation peaks. The shape of the reduction zone at less negative potentials, where cobalt does not deposit, is not modified by the presence of cobalt in the solution (the decay of intensity in the figure is due to a lower

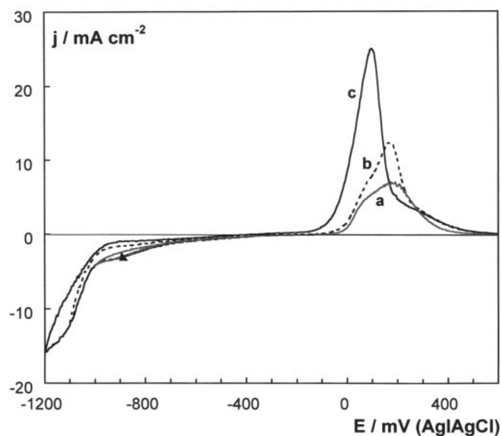

Fig. 2. Cyclic voltammograms of a 3:1 ratio of a [Co(II)]/[Cu(II)] solution at different lower limits: (a) −1000; (b) −1100 and (c) −1200 mV. Stationary conditions.

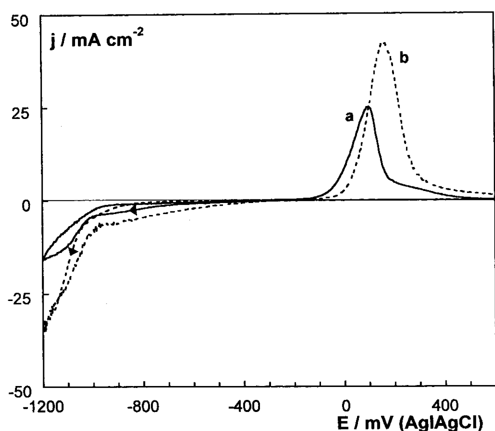

Fig. 3. Cyclic voltammograms of a 3:1 ratio of a [Co(II)]/[Cu(II)] solution: (a) stationary (b) stirring conditions. Lower limit −1200 mV.

Cu(II) concentration in solution). The sharp fall of the current density in the negative scan is related to the start of the alloy deposition process.

Stationary cyclic voltammograms at different lower limits (Fig. 2) show oxidation peak displacement from copper towards the cobalt oxidation position as the lower potential limit is made more negative, which could be related to the increase of cobalt percentage in the deposit.

For any [Co(II)]/[Cu(II)] ratio in solution, stirring conditions and scan rate, a defined limiting potential from which displacement of the voltammetric oxidation peak from copper towards cobalt position begins, can be described, which is clearly related to the start of the alloy deposition. A greater shift of the oxidation peak for higher [Co(II)]/[Cu(II)] ratio solutions can also be observed, due to a higher cobalt percentage in the deposit formed during the negative scan.

Fig. 3 shows the comparison of cyclic voltammograms under stationary and stirred conditions. Under stirred conditions (curve b) the start of the electrodeposition process occurs at a more negative potential than that observed in quiescent solution (curve a). Also, under stirred conditions, the j/E slope in the negative going sweep becomes pronounced. These results indicate, as expected, more difficult nucleation and easier growth of the nuclei with stirring of the solution. There is also a shift of the oxidation peak in curve b in Fig. 3 towards the copper oxidation position, due to the enhanced Cu(II) transport towards the electrode. The latest shift is not so marked for a 1:1 ratio of [Co(II)]/[Cu(II)] in solution, due to the low Co(II) concentration.

3.1.2. Voltammetric and galvanostatic strippings

In order to analyse the deposits in situ, both potentiodynamic and galvanostatic strippings were performed, since these methods have been proved to be highly useful for the characterisation of electrodeposited alloys [16–20].

Voltammetric stripping experiments for deposits obtained galvanostatically or potentiostatically (same reduction potentials as the stabilisation potentials of the galvanostatic ones) give the same information, always showing one oxidation peak that shifts from the copper towards the cobalt position as the applied current density–applied potential is made more negative, which is in agreement with the previous cyclic voltammometric results.

A series of galvanostatic deposits obtained at different current densities followed by its corresponding voltammetric and galvanostatic strippings were performed for 3:1 and 1:1 ratios of [Co(II)]/[Cu(II)] solutions.

Fig. 4 shows the galvanostatic curves of the deposition process at different current densities and fixed charge (Fig. 4(1)) and the corresponding potentiodynamic (Fig. 4(2)) and galvanostatic (Fig. 4(3)) strippings. Galvanostatic transients for the deposition process show a nucleation spike followed by stabilisation of the potential, which decreases as the current density is made more negative. Further decrease of the current density leads to deformation of the E–t transients, which can be related to hydrogen evolution.

When a less negative current density is applied (Fig. 4(1), curve a) only copper is deposited as is observed from the stripping oxidation peak at copper position (Fig. 4(2), curve a) and from the flat galvanostatic stripping related to copper oxidation (Fig. 4(3), curve a).

The oxidation of deposits obtained for gradually more negative current densities show, in the voltammetric stripping, (Fig. 4(2), curves b–d), in addition to a peak shift towards the cobalt oxidation position, a current efficiency decrease due to simultaneous hydrogen evolution.

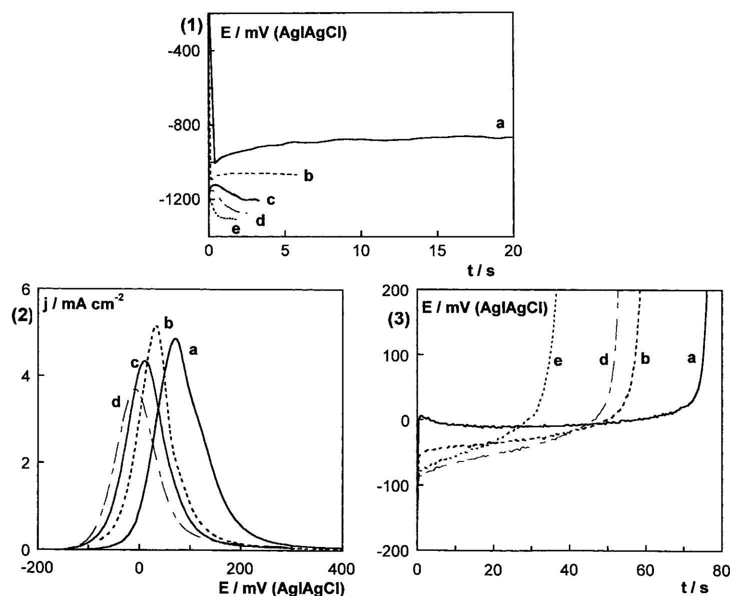

Fig. 4. (1) Galvanostatic transients of a 3:1 ratio of a [Co(II)]/[Cu(II)] solution. Current density: a, -1.6; b, -11.1; c, -19.1; d, -25.5; and e, -35.0 mA cm^{-2}. $Q = -2$ mC. Stirred conditions. (2) Stripping voltammograms of deposits corresponding to (1). $v = 10$ mV s^{-1}. (3) Galvanostatic stripping curves at 0.8 mA cm^{-2} of deposits corresponding to (1).

Galvanostatic strippings of these deposits show a gradual variation of the potential with time (Fig. 4(3), curves b,d,e), indicating that non separate oxidation of the two metals takes place. Galvanostatic strippings also confirm the decrease of the efficiency of the deposition process as the current density is made more negative, which can be seen from the shorter times needed to oxidise the deposit.

The electrochemical behaviour observed for the oxidation of deposits, a single peak in the potentiodynamic stripping and a gradual potential variation in the galvanostatic stripping, is related to the oxidation of a deposit formed by a solid solution.

Similar stripping results were obtained from a 1:1 ratio of [Co(II)]/[Cu(II)] in solution, however some predictable variations were observed: galvanostatic stripping transients show smaller slopes and stripping voltammograms show smaller oxidation peak displacements, both being related to a lower incorporation of cobalt into the deposit.

In all experiments, for fixed deposition conditions the oxidation peak position in the stripping voltammograms is not dependent on the deposition time, which could be related to invariant composition with time.

Stripping techniques could not be studied on metallic substrates, due to their oxidation in the range of potentials used.

3.2. Characterisation of deposits

Alloy deposits were galvanostatically obtained from both 1:1 and 3:1 ratios of [Co(II)]/[Cu(II)] in solution on vitreous carbon, nickel and copper substrates. The electrochemical response during the deposition was similar on different substrates (Fig. 5).

Scanning electron microscopy (SEM) was used to examine the dependence of the morphology of the alloy electrodeposits on the experimental conditions. For this purpose, at first, deposits were obtained at different current densities but fixed charge Fig. 6(A) shows a SEM micrograph of a homogeneous nodular deposit obtained at low negative current density (cobalt-free). By applying more negative current densities, the deposits gradually varied from coarse to fine morphology

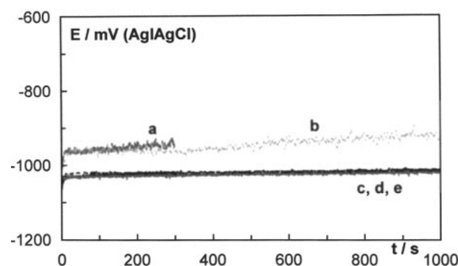

Fig. 5. Galvanostatic transients of a 3:1 ratio of a [Co(II)]/[Cu(II)] solution. (a) Vitreous carbon, -6.4 mA cm^{-2}; (b) nickel, -6.4 mA cm^{-2}; (c) vitreous carbon, -9.5 mA cm^{-2}; (d) nickel, -9.5 mA cm^{-2}; (e) copper, -9.5 mA cm^{-2}. Stirred conditions.

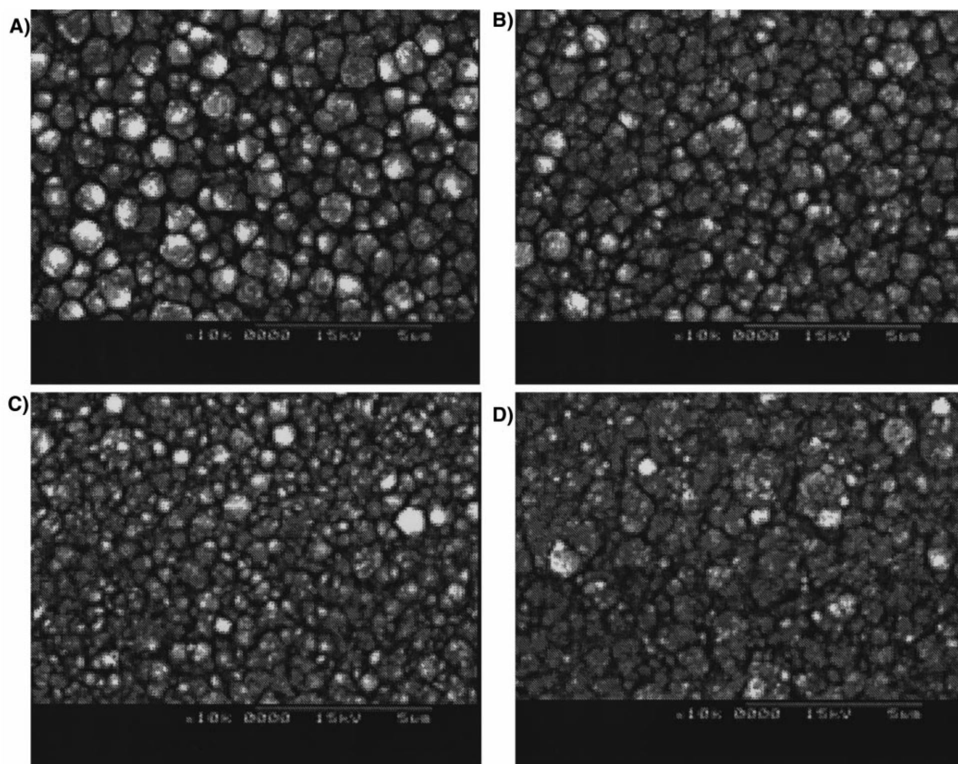

Fig. 6. SEM micrographs of deposits obtained galvanostatically from a 1:1 ratio of a [Co(II)]/[Cu(II)] solution. (A) -11.1 mA cm^{-2}, 0% Co; (B) -11.9 mA cm^{-2}, 3.8% Co; (C) -12.7 mA cm^{-2}, 8.5% Co; (D) -13.5 mA cm^{-2}, 11.8% Co. $Q = -300$ mC. Stirred conditions. Copper substrate.

(Fig. 6(B–D)). This variation is related to a gradual increase of cobalt percentage in the deposit.

On the other hand, deposits obtained under the same electrodeposition conditions on different substrates have similar morphology (Fig. 7(A,B)). From XPS experiments on these deposits it can be confirmed that, under stirring conditions, the alloy composition throughout the thickness of the deposit is constant (Fig. 7(C)).

Upon testing the deposits obtained from both 3:1 and 1:1 ratios of the [Co(II)]/[Cu(II)] solutions, the composition of the alloy has been proved to be highly dependent on the concentration of the metallic cations in solution. From a 3:1 ratio of the [Co(II)]/[Cu(II)] solution a maximum of about 30% Co can be achieved in the deposit, while just about 15% Co from a 1:1 ratio of the [Co(II)]/[Cu(II)] solution is possible, before a drastic drop in the current efficiency due to the accompanying hydrogen evolution as more negative current densities are applied.

Fig. 8 shows a SEM micrograph of a thinner alloy deposit. By comparing it with much higher charge alloy deposits, shown in Fig. 6, it can be concluded that the deposit becomes coarse as the deposition charge is increased.

Deposits obtained at fixed charge and the same stabilisation potentials during galvanostatic experiments from different bath compositions show similar morphology but different cobalt content, as can be seen by comparing the SEM micrographs of Fig. 6(C) (8.5% Co) and Fig. 7(A) (30% Co).

Alternatively, deposits obtained at the same charge from different bath compositions and different stabilisation potentials, can have similar cobalt contents; however their morphology is obviously different.

The invariant oxidation peak position observed in the potentiodynamic stripping experiments for different low charge deposits may be related to constant composition. XPS experiments showed equivalent results for high deposition charges: the alloy composition does not depend on the thickness of the deposit. Therefore, for any bath composition, the relative oxidation peak position in stripping experiments could be used to estimate the relative cobalt percentage in the deposit.

Deposits obtained on nickel electrodes with deposition charges of -300 mC were analysed using X-ray diffraction. The films obtained from different solutions and from current densities that lead to cobalt + copper alloys always present a similar type of diffractogram. Next to the lines corresponding to nickel substrate, a collection of peaks is obtained (labelled by arrows in Fig. 9(1)). These diffraction peaks correspond to a fcc structure and appear at diffraction angles between the lines corresponding to copper and fcc cobalt, as is observed in the magnified details of the diffractogram (Fig. 9(2,3)).

By comparing the diffractograms of deposits with different cobalt percentage it is observed that the position of each diffraction peak shifts towards the position of the cobalt line as the cobalt percentage in the deposit is increased (Fig. 10(1)). This behaviour is in agreement with the proposal of cobalt + copper solid solution formation from the electrochemical results. From the position of the peaks indexed as the fcc phase in the diffractograms, least-square refinements of the lattice parameter a of the fcc structure were performed. Very small differences between the measured and the calculated positions are observed. The fcc lattice constant,

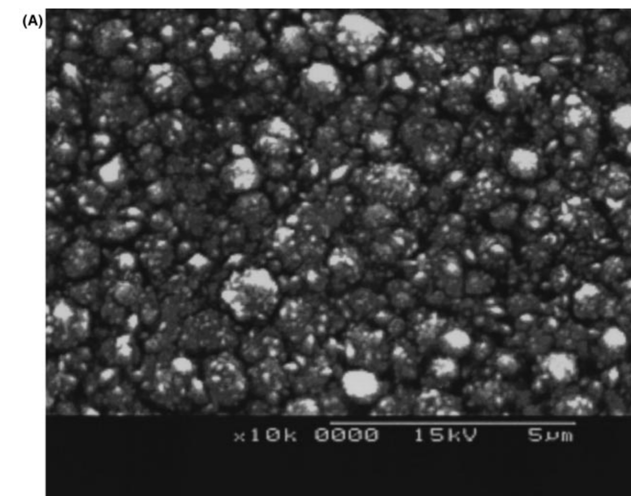

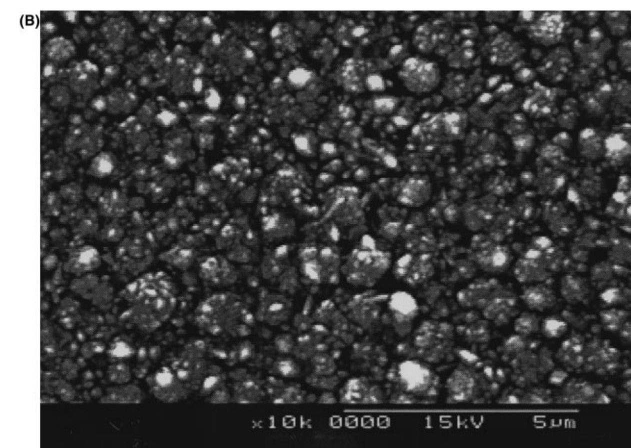

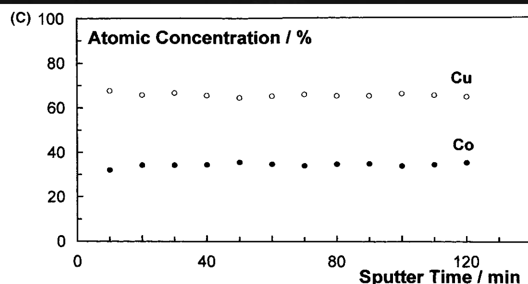

Fig. 7. SEM micrographs of deposits obtained galvanostatically at -12.7 mA cm^{-2} from a 1:1 ratio of a [Co(II)]/[Cu(II)] solution. (A) Copper and (B) nickel substrates. 30% Co. $Q = -300$ mC. Stirred conditions. (C) XPS depth profile of (B).

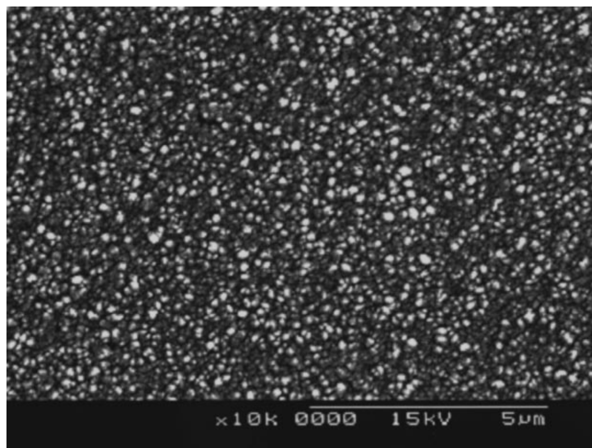

Fig. 8. SEM micrograph of a deposit obtained galvanostatically from a 1:1 ratio of a [Co(II)]/[Cu(II)] solution. Vitreous carbon substrate. 2.3% Co. $Q = -60$ mC. Stirred conditions.

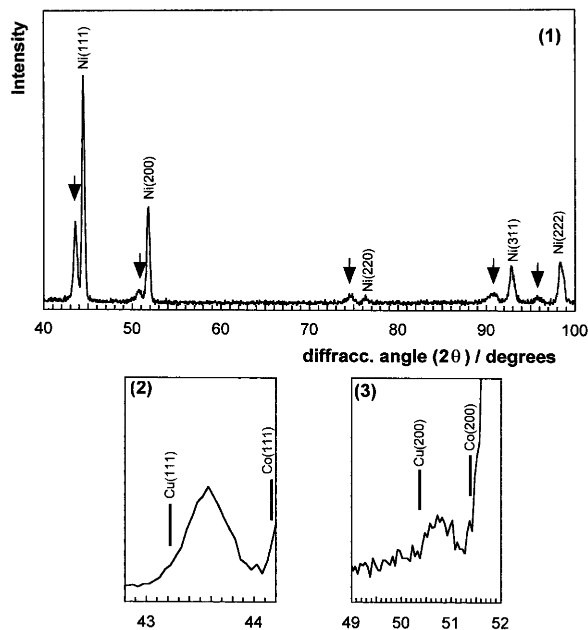

Fig. 9. (1) X-ray diffractogram of the Co + Cu deposit of Fig. 7(B); (2) and (3) magnified details.

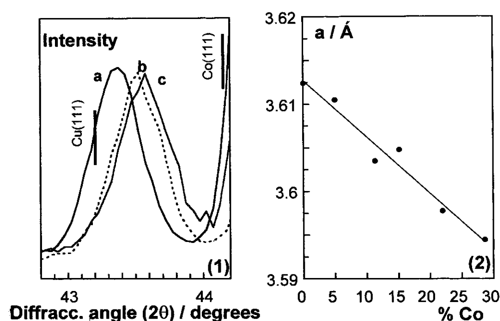

Fig. 10. (1) (111) diffraction peaks of Co + Cu films of cobalt percentage: (a) 5.0% (b) 22.0% and (c) 28.7%. (2) Lattice constant variation of the fcc phase with cobalt percentage.

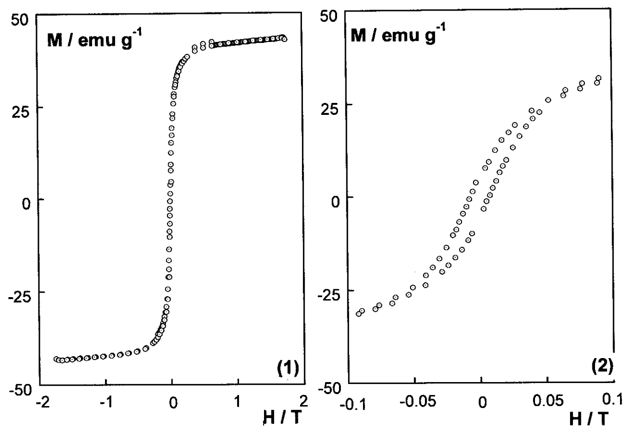

Fig. 11. Magnetic hysteresis curve of a 30% Co deposit on graphite substrate at room temperature. (1) General curve and (2) magnified detail.

calculated using a profile pattern matching, decreases linearly with the increase of cobalt concentration following Vegard's law (Fig. 10(2)), a result that is in agreement with those obtained by other authors for Co + Cu films obtained by sputtering [14] or electrodeposition [15]. Therefore, the diffraction peak shift due to a gradual variation of the lattice constant of the fcc phase, is the result of a Co + Cu solid solution formation, as occurs under other electrodeposition conditions [15].

In order to test the magnetic properties of the Co + Cu films obtained, magnetisation loops were measured at room temperature for the samples with the highest cobalt percentage. The magnetisation curve is not totally reversible: hysteretic behaviour is observed even at this temperature. For a deposit containing 30% of cobalt a saturation magnetisation of around 40 emu g^{-1} and, from the magnetisation loop a coercitivity value of a few oersted are obtained (Fig. 11). On the contrary, other electrodeposition conditions [21,22] lead to heterogeneous Co + Cu films that present a complete reversible magnetisation curve, for similar cobalt content in the deposits, at room temperature. For these films, it was necessary to decrease the temperature in order to detect a hysteresis loop.

Electrodeposition is therefore promising to obtain Co + Cu films with different properties as a function of electrodeposition conditions (bath composition, pH, temperature, current density).

4. Conclusions

The experimental results show that non-separate metal deposition occurs from the bath tested. A citrate bath at pH ca. 5 permit deposits of cobalt + copper alloy over different substrates to be obtained, provided that a minimum value of current density or potential is applied.

The control of the electrodeposition conditions allows Co + Cu deposits of different composition and morphology to be obtained. As the applied current density–applied potential is decreased gradually, more finely grained deposits with a higher cobalt percentage are obtained. However, a clear influence of the bath composition is observed since it is possible to obtain deposits with similar morphology but different cobalt percentage from different [Co(II)]/[Cu(II)] ratios in solution.

Although the thermal phase diagram reveals high inmiscibility of the two metals, using electrodeposition under our experimental conditions, the formation of a solid solution of cobalt in copper, of fcc structure, is detected.

Potentiodynamic strippings are a rapid method to obtain information about the inclusion of cobalt in the deposit. Moreover, the technique is useful to check whether the composition of the deposit remains constant with the deposition charge. Initial (low charge) deposition has been studied by stripping techniques, while final (high charge) deposits have been characterised by ex-situ techniques. Comparison between both methods shows that stripping results can be extended to higher deposition times.

The baths and experimental conditions studied lead to the formation of homogeneous deposits. In order to test the possibility of a high value of magnetoresistance of these deposits a further study must be planned in which the annealing of the samples will lead to a granular heterogeneous structure.

Acknowledgements

The authors thank to Serveis Científico-Tècnics (Universitat de Barcelona) for equipment availability. This research was supported financially by contract MAT 97-0379 of the Comisión Interministerial de Ciencia y Tecnología (CICYT) and by the Comissionat of the Generalitat de Catalunya under Research Project SGR98-027.

References

[1] M. Schlesinger, K.D. Bird, in: M. Paunovic (Eds.), Electrochemically Deposited Films II, vol. 94–31, Proceedings of The Electrochemical Soc., Pennington, 1995.
[2] K.D. Bird, M. Schlesinger, J. Electrochem. Soc. 142 (1995) L65.
[3] E. Chassaing, P. Nallet, M.F. Trichet, J. Phys. IV 6 (1996) C7–13.
[4] P. Nallet, E. Chassaing, M.G. Walls, M.J. Hÿtch, J. Appl. Phys. 79 (1996) 6884.
[5] Y. Jyoko, S. Kashiwabara, Y. Hayashi, J. Electrochem. Soc. 144 (1997) L5.
[6] H. El Fanity, K. Rahmouni, M. Bouanani, A. Dinia, G. Shmerber, C. Mény, P. Panissod, A. Cziraki, F. Cherkaoui, A. Berrada, Thin Solid Films 318 (1998) 227.

[7] E. Chassaing, A. Morrone, J.E. Schmidt, J. Electrochem. Soc. 146 (1999) 1794.

[8] A.E. Berkowitz, J.R. Mitchell, M.J. Carey, A.P. Young, S. Zhang, F.E. Spada, F.T. Parker, A. Hutten, G. Thomas, Phys. Rev. Lett. 68 (1992) 3745.

[9] J.Q. Xiao, J.S. Jiang, C.L. Chien, Phys. Rev. Lett. 68 (1992) 3749.

[10] R.P. Setna, A. Cerezo, J.M. Hyde, G.D.W. Smith, Appl. Surf. Sci. 76/77 (1994) 203.

[11] V.M. Fedosyuk, O.I. Kasyutich, D. Ravinder, H.J. Blythe, J. Magn. Magn. Mat. 156 (1996) 345.

[12] W. Schwarzacher, D.S. Lashmore, IEEE Trans. Magn. 32 (1996) 3133.

[13] Alloy phase diagrams, in: Hugh Baker (Eds.), ASM Handbook, vol. 3, ASM International, Ohio, 1992.

[14] J.R. Childress, C.L. Chien, Phys. Rev. B 43 (1991) 8089.

[15] H. Zaman, A. Yamada, H. Fukuda, Y. Ueda, J. Electrochem. Soc. 145 (1998) 565.

[16] E. Gómez, J. Ramírez, E. Vallés, J. Appl. Electrochem. 28 (1998) 71.

[17] E. Gómez, E. Peláez, E. Vallés, J. Electroanal. Chem. 469 (1999) 139.

[18] V.D. Jovic, R.M. Zejnilovic, A.R. Despic, J.S. Stevanovic, J. Appl. Electrochem. 18 (1988) 511.

[19] M.L. Alcalá, E. Gómez, E. Vallés, J. Electroanal. Chem. 370 (1994) 73.

[20] E. Gómez, X. Alcobé, E. Vallés, J. Electroanal. Chem. 475 (1999) 66.

[21] H.J. Blythe, V.M. Fedosyuk, Phys. Status Solidi A 146 (1994) K13.

[22] H.J. Blythe, V.M. Fedosyuk, J. Magn. Magn. Mat. 155 (1996) 355.

ELSEVIER

Journal of Electroanalytical Chemistry 517 (2001) 63–68

Journal of Electroanalytical Chemistry

www.elsevier.com/locate/jelechem

Electrodeposited cobalt + copper thin films on ITO substrata

E. Gómez [a], A. Labarta [b], A. Llorente [a], E. Vallés [a,*]

[a] Departament Química Fisica, Facultat de Química, Laboratori de Ciència i Tecnologia Electroquimica dels Materials (LCTEM), Universitat de Barcelona, Martí i Franquès 1, 08028 Barcelona, Spain

[b] Departament Física Fonamental, Facultat de Física, Universitat de Barcelona, Martí i Franquès 1, 08028 Barcelona, Spain

Received 24 March 2001; received in revised form 13 September 2001; accepted 6 October 2001

Abstract

Cobalt + copper thin films with variable composition were obtained over indium–tin oxide covered glass plates (ITO) by means of electrodeposition, from a citrate bath upon varying both the [Co(II)]/[Cu(II)] ratio in solution and the deposition conditions. The ITO/glass substrate is sufficiently conductive to allow electrodeposition directly onto it, and also allows the measurement of the magnetoresistance without separating the films. The electrochemical and structural analyses indicated that a solid solution is formed in the electrodeposition conditions studied, although TEM analysis showed the random distribution of nanometric dense particles of cobalt distributed within the deposits. These particles were responsible for the magnetoresistance (MR) signal which was observed for all the Co + Cu films. The MR value increased when the cobalt percentage increased in the deposit. © 2001 Elsevier Science B.V. All rights reserved.

Keywords: Electrodeposition; Cobalt + copper alloy; Indium–tin oxide; Magnetoresistance

1. Introduction

The development of new magnetic/magnetoresistive alloy thin-films has attracted considerable attention for application to sensor devices. Although a considerable amount of work on thin films has been done, the interrelation between structure, composition and magnetism or magnetoresistive properties is still under discussion. A binary alloy cobalt + copper system is a convenient system that can be used to study magnetic [1–5] and magnetoresistive [6–13] properties, due to the possibility of continuous variation of the film composition.

Electrodeposition is one of the advantageous methods for producing alloys. Electrolytic growth of metals differs from other methods providing the possibility of depositing films with structures different from those formed from the vapor phase. Also, the electrodeposition technique allows the possibility of deposition at normal conditions of pressure and temperature, requiring relatively inexpensive equipment.

In a previous publication we developed a bath from which Co + Cu electrodeposition was studied on vitreous carbon and metallic substrates [14]. The characterisation of the deposits obtained was made by means of electrochemical methods combined with morphological and structural investigations. It was revealed that, although the thermal diagram of the Co + Cu system presents inmiscibility between components [15], the deposits obtained under our electrodeposition conditions were homogeneous and formed a solid solution in a fcc-like structure. Moreover, this solid solution formation could be followed by means of the electrochemical results and a means of estimating the cobalt content, the minor component in the alloy, was proposed.

Nevertheless, electrodeposition has one feature that can be a major disadvantage, namely the need to use a conducting substrate. This difficulty can be avoided by employing an evaporated or sputtered seed layer over a non-conducting substrate (i.e. indium–tin oxide, ITO, covered glass plates). Electrodeposition could then lead to an efficient method for fabricating thin layers of films with magnetic, or magnetoresistive properties avoiding the conductive substrate.

* Corresponding author. Tel.: +34-93-402-1324; fax: +34-93-402-1231.

E-mail address: e.valles@qf.ub.es (E. Vallés).

0022-0728/01/$ - see front matter © 2001 Elsevier Science B.V. All rights reserved.
PII: S0022-0728(01)00670-2

The purpose of this work is to produce cobalt + copper thin films from different single baths, characterising the process and the final deposits obtained over ITO substrates, which allows direct magnetoresistive measurements to be performed. The electrodeposition process will be analysed for a wide range of bath compositions, in order to test whether the behaviour previously observed [14] can be extended to any [Co(II)]/[Cu(II)] solution ratio and can also be applied to less conductive substrates such as ITO.

2. Experimental

Chemicals used were $CuSO_4 \cdot 5H_2O$, $CoSO_4 \cdot 7H_2O$, sodium citrate ($Na_3C_6H_5O_7 \cdot 2H_2O$) and H_3BO_3. All solutions were freshly prepared with water, first doubly distilled and then treated with a Millipore Milli Q system. In all experiments, solutions contained 0.5 mol dm^{-3} Na_3Citrate + 30 g dm^{-3} H_3BO_3. The citrate bath was chosen to favour simultaneous Co and Cu deposition and to control the pH medium. Boric acid, in addition to its buffer function, has been shown to be a useful additive compound, favouring the formation of low roughness deposits. The total metallic ion concentration was maintained at 0.2 mol dm^{-3} and the cobalt(II)/copper(II) ratio in solution was varied between 3 and 18. The pH was adjusted to 5.3 by suitable addition of H_2SO_4 in all cases.

Before and during the experiments, solutions were deaerated with argon. Deposition was performed at 30 °C.

Electrochemical experiments were carried out in a conventional three-electrode cell using an EG&G 273 potentiostat/galvanostat controlled by a microcomputer. Working electrodes were: a vitreous carbon rod (Metrohm, area = 0.0314 cm^2) and indium tin oxide (ITO) thin films sputtered on glass plates (area = 0.7 cm^2, thickness of ITO layer = 25 nm). The vitreous carbon electrode was polished to a mirror finish using alumina of different grades (3.75 and 1.87 μm) and cleaned ultrasonically for 2 min in water before each experiment. The ITO electrodes were first cleaned with acetone and then with water. The counter electrode was a platinum spiral. The reference electrode was Ag | AgCl | 1 mol dm^{-3} NaCl mounted in a Luggin capillary containing 0.5 mol dm^{-3} Na_2SO_4 solution. All potentials are referred to this electrode.

Voltammetric experiments were carried out at 50 mV s^{-1}, scanning first to negative potentials. Only one cycle was run in each voltammetric experiment. Stripping analysis was always performed immediately after deposition, without removing the electrode from the solution. All deposits were obtained under stirring conditions ($\omega = 500$ rpm, magnetic stirrer).

The morphology of the deposits was examined with a Hitachi S 2300 scanning electron microscope.

Electron probe microanalysis (EPMA) was performed on a Cameca SX-50 electron probe using a variable voltage technique at 10, 12, 15, 18 and 20 keV operating potentials. The analytical X-ray lines were Co–K_α and Cu–K_α. The composition and thickness were estimated from the X-ray data using the LAYERF computer program for thin film characterisation (Pouchou and Pichoir model, Cameca SX-50 default). The glass plates and ITO electrodes were previously analysed to obtain the response of the substrate, (necessary for analysing the Co + Cu thin films).

The particle size distribution and microstructure of deposits were examined with a Phillips CM-30 transmission electron microscope.

X-ray diffraction (XRD) analysis was performed on a Siemens D-500 diffractometer. The Cu–K_α radiation ($\lambda = 1.5406$ Å) monochromatiser was selected by means of a diffracted beam flat graphite crystal. $2\theta/\theta$ diffractograms were obtained in the range of $2\theta = 20–100°$ with a step range of $2\theta = 0.05°$ and a measuring time of 14 s per set.

The magnetoresistance (MR) was measured by an alternating current four-point probe technique at 27 K and in magnetic fields up to 11 kOe. The MR ratio was calculated as $|\Delta R/R_0|$, where ΔR is the change in resistance due to the applied magnetic field and R_0 is the maximum resistance at the coercitive field.

3. Results and discussion

3.1. Voltammetric results

Prior to the analysis of Co + Cu deposition, the cyclic voltammograms of ITO electrodes were recorded in a blank solution (0.2 mol dm^{-3} Na_2SO_4 + 0.5 mol dm^{-3} Na_3citrate + 30 g dm^{-3} H_3BO_3/pH = 5.3) in order to test the stability of this substrate. The ITO stability is assured in the range of 0.6 to −1.2 V, but some reduction process can be detected from potentials more negative than −1.2 V (Fig. 1, curve a), related to the reduction of indium–tin oxide (and possible hydrogen evolution).

When the ITO electrode is used as a substrate for Co + Cu deposition (Fig. 1, curve b), from the voltammetric curve it is observed that alloy deposition occurs prior to ITO reduction and then, the ITO substrate is stable in the potential range used to analyse alloy deposition. Oxidation of the alloy is detected, and only one oxidation peak is recorded, at an intermediate position between those corresponding to cobalt and copper.

A comparison between ITO and vitreous carbon (Fig. 1, curve c) shows that, despite their different

activities, both electrodes induce similar qualitative behaviour for cobalt + copper deposition: alloy formation at potentials more positive than that corresponding to pure cobalt deposition is observed, showing one clear oxidation peak corresponding to the electrodeposited alloy. In both substrates this peak shifts from the copper towards the cobalt position with increasing $[Co(II)]/[Cu(II)]$ ratio in solution and/or as the lower potential limit is made more negative.

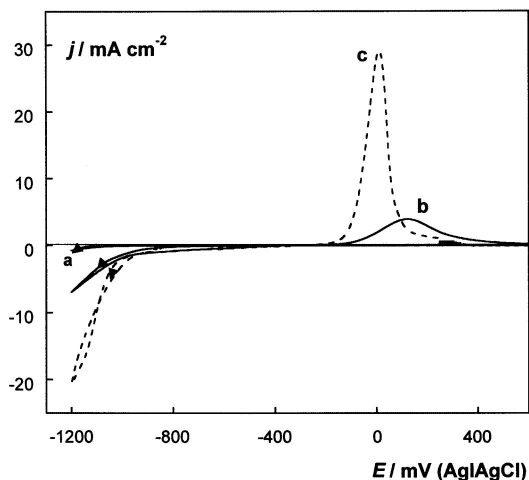

Fig. 1. Cyclic voltammograms of (a) blank solution, ITO electrode, (b) $[Co(II)]/[Cu(II)] = 9$ ratio solution, ITO electrode, (c) $[Co(II)]/[Cu(II)] = 9$ ratio solution, vitreous carbon electrode. Stationary conditions. Starting potential: 0.1 V.

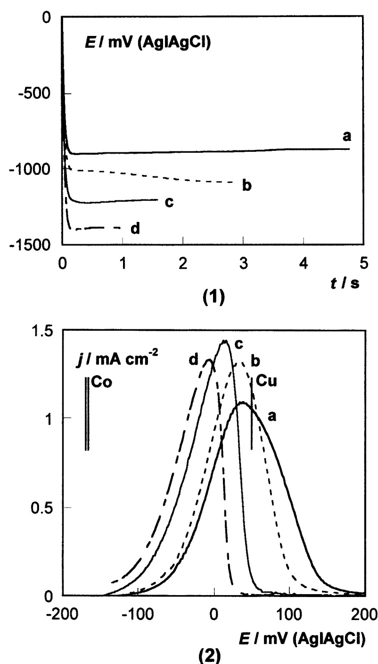

Fig. 2. (1) Galvanostatic transients of a $[Co(II)]/[Cu(II)] = 6$ ratio solution on an ITO electrode. Current density: (a) -3.0 (b) -5.0 (c) -9.0 and (d) -15.0 mA cm^{-2}. $Q = -14$ mC cm^{-2}. (2) Stripping voltammograms of deposits corresponding to (1). Single line: copper position, double line: cobalt position.

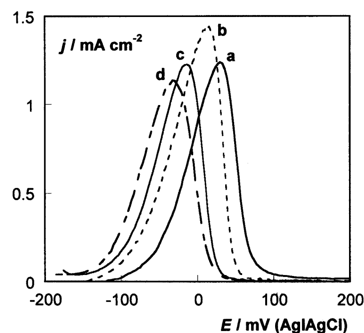

Fig. 3. Stripping voltammograms of galvanostatic deposits ($Q = -14$ mC cm^{-2}) obtained on an ITO electrode at a stabilisation potential of -1250 mV corresponding to $[Co(II)]/[Cu(II)]$ ratio solutions of: (a) 3, (b) 6, (c) 9 and (d) 18.

3.2. Voltammetric strippings

All potentiodynamic stripping experiments were performed at a scan rate of 10 mV s^{-1} immediately after galvanostatic deposition at low deposition charges, beginning the positive scan at an initial potential at which deposition did not occur.

Fig. 2 shows the galvanostatic curves of the deposition process at different current densities and fixed charge (Fig. 2(1)) and the corresponding potentiodynamic strippings of the corresponding deposits (Fig. 2(2)) for one of the $[Co(II)]/[Cu(II)]$ ratios studied. At short deposition times, galvanostatic transients for the deposition process show a nucleation spike followed by stabilisation of the potential, which decreases as the current density is made more negative.

When a less negative current density is applied (Fig. 2(1), curve a) almost only copper is obtained, as is deduced from the stripping oxidation peak (Fig. 2(2), curve a) near to the copper position (single line in Fig. 2(2)).

Stripping of the deposits obtained for gradually more negative current densities, shows (Fig. 2(2), curves b–d) a peak shift towards the cobalt oxidation position (double line in Fig. 2(2)), which could be related to a higher incorporation of cobalt into the deposit. Similar stripping behaviour was observed for different $[Co(II)]/[Cu(II)]$ ratios in solution. Only one oxidation peak was observed under all conditions, probably related to solid solution formation.

Fig. 3 shows the voltammetric stripping of deposits obtained from different $[Co(II)]/[Cu(II)]$ ratio solutions at the same stabilisation potential. To fix the stabilisation potential it is necessary to make a gradual increase (less negative) in the current densities applied when the $[Co(II)]/[Cu(II)]$ ratio in solution is increased, which makes the oxidation peak shift towards the cobalt position.

In all experiments, for fixed deposition conditions, the oxidation peak position in the stripping voltammograms is not dependent on the deposition time (at low charges, at which the stripping technique is valid), which could be related to invariant composition with time.

Therefore, there are two possible ways of gradually increasing the Co content of the deposits: by increasing the [Co(II)]/[Cu(II)] ratio in the solution and by decreasing the deposition current density.

3.3. Characterisation of deposits

The electrochemical study allowed us to establish the conditions at which neither damage of the substrate nor substantial hydrogen evolution occurs. Thus, low negative current densities/deposition potentials were selected. Therefore, in order to increase the cobalt percentage in the deposits, at a reasonable current efficiency, the [Co(II)]/[Cu(II)] ratio in solution was increased. In order to facilitate the control of the thickness of the deposits, the galvanostatic mode was chosen.

Different deposition charges were tested for all solution compositions. For the range [Co(II)]/[Cu(II)] = 3–18, adherent thin films were obtained for charges up to around -225 mC cm^{-2}.

Scanning electron microscopy (SEM) showed that fine-grained homogenous deposits were obtained under these conditions on an ITO substrate. From EPMA measurements, the composition of the deposits was proved to be highly dependent on the concentration of the metallic cations in solution. Under the previously selected conditions, a maximum of about 30, 18 and 12 wt.% Co could be achieved in the deposit from [Co(II)]/[Cu(II)] ratios of 18, 9 and 6, respectively. Therefore, the analysis of the different deposits prepared showed that it is possible, also over ITO, to modify the cobalt percentage in the Co + Cu coatings as a function of solution composition and applied current density. The cobalt percentage was increased either by increasing the [Co(II)]/[Cu(II)] ratio in solution or by the application of more negative current densities. However, a limit of the current density was detected for each solution, from which deposits were cracked and not homogeneous, due to simultaneous hydrogen evolution. For solutions with the highest [Co(II)]/[Cu(II)] ratios, this limit of the current density is attained easily.

It is important to investigate the crystallographic structure of the deposited films, because this is related directly to the properties of the film, such as the magnetoresistive properties. Co + Cu deposits of different composition obtained over an ITO substrate from different solutions and current densities were analysed using X-ray diffraction. Much effort has been devoted to obtain information from the diffractograms, due to the low thickness of the Co + Cu films and the presence of the ITO seed layer. The diffractograms corresponding to the different thin deposits were similar (Fig. 4(1)), showing only two clear peaks that could be seen over the response of the glass/ITO substrate (Fig. 4(2)). Only the first of these two peaks could be studied further by increasing the statistics, because the second has also a signal component from the ITO substrate. The peaks recorded correspond to a fcc structure and appear at diffraction angles between the lines corresponding to electrodeposited fcc copper and fcc cobalt from the same citrate bath. By comparing samples with different cobalt percentages, the position of each diffraction peak (Fig. 4(3)) shifts towards the position of the cobalt line, as the cobalt percentage in the deposit is increased. This behaviour is in agreement with the formation of a solid solution, which was found for Co + Cu deposits on nickel electrodes [14] and is in agreement with the proposal of Co + Cu solid solution formation on an ITO substrate, according to the stripping results. Then, the electrodeposited films do not seem to correspond to the structure predicted by the equilibrium diagram [15]. However, XRD analyses do not give enough definition for thin Co + Cu films on ITO, and TEM characterisation is necessary to solve the microstructure of the deposits.

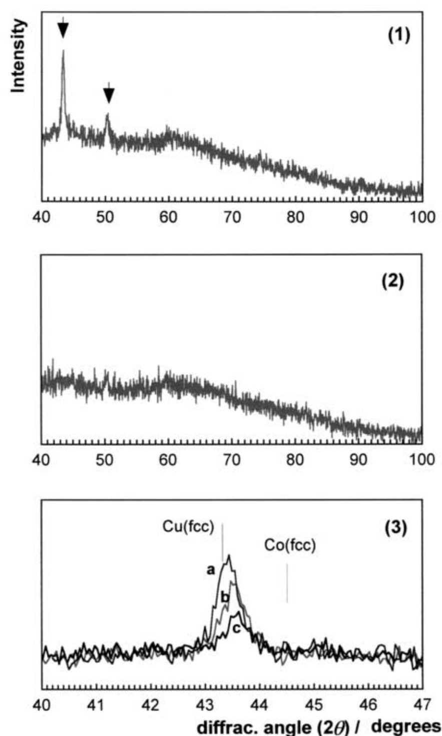

Fig. 4. (1) X-ray diffractogram of a Co + Cu deposit of 9% Co on ITO substrate. (2) X-ray diffractogram of ITO substrate. (3) Magnified detail of the (111) fcc diffraction peak of Co + Cu films of Co percentages of: (a) 9%, (b) 13% and (c) 18%.

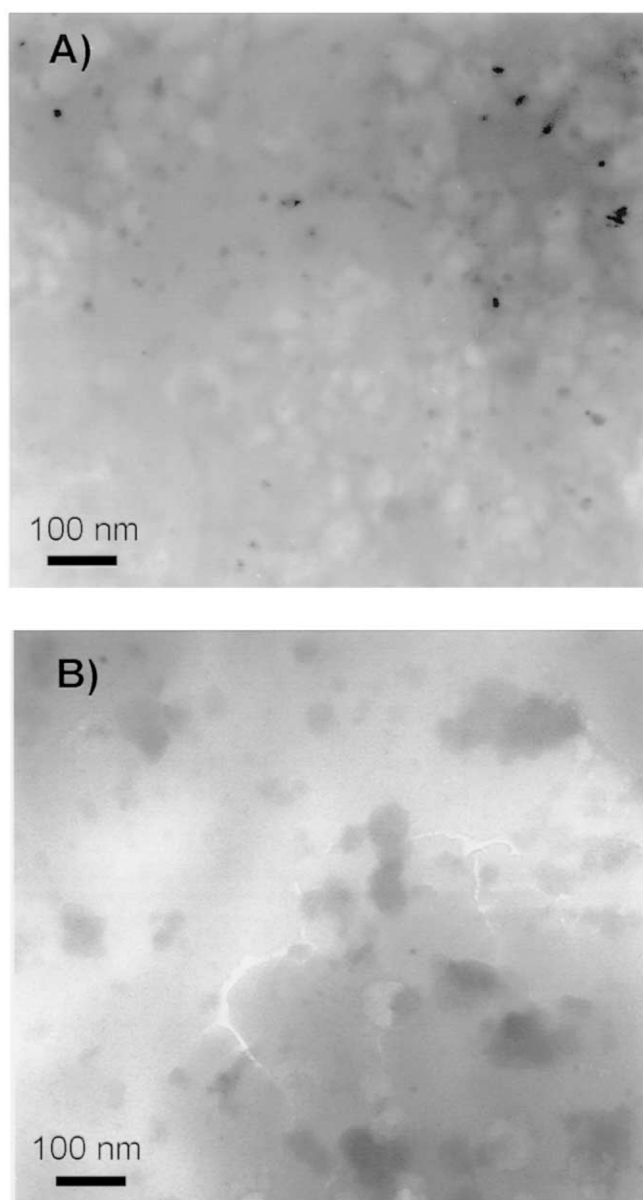

Fig. 5. Bright field TEM images of Co + Cu deposits obtained from: (A) [Co(II)]/[Cu(II)] = 6 ratio solution, 8% Co, (B) [Co(II)]/[Cu(II)] = 9 ratio solution, 15% Co.

Fig. 5A,B show TEM images of deposits obtained from [Co(II)]/[Cu(II)] = 6 and [Co(II)]/[Cu(II)] = 9 ratio solutions, respectively. A random distribution of nanometric particles can be observed on a homogeneous matrix. These particles have a higher density than the matrix and, therefore, they can be assigned to cobalt particles. The size distribution ranges from 10 to 20 nm and from 10 to 70 nm for the Co + Cu with compositions of 8 and 15 wt.% Co, respectively. Therefore, although the total number of particles does not seem to increase significantly, the mean size of the particles clearly increases as the cobalt percentage of the deposit increases, thus increasing the total percentage of non-alloyed cobalt within the Co + Cu matrix.

Fig. 6 shows a high resolution TEM image of the deposit in Fig. 5B, from which the granular nature of the samples is observed. Moreover, from some grains of the matrix the atomic planar spacing can be seen and measured, obtaining a cell parameter a that corresponds to a Co + Cu alloy, as it is a value between the cell parameters of copper and cobalt.

The electrodeposited films display giant magnetoresistance when this is measured at low temperatures and at magnetic fields up to 11 kOe, although the MR signal is below 3% for all the compositions studied. The MR curve measured at 27 K for the electrodeposited Co + Cu film with a Co content of 15 wt.% and obtained from the [Co(II)]/[Cu(II)] = 9 ratio solution, is shown in Fig. 7(1). The shape of this curve and the MR value at $H = 11$ kOe (2.4%) are quite similar to the corresponding observations in as-prepared thin films of the same composition obtained by sputtering [6–8,16,17] and electron beam co-evaporation [11,12]. In the inset of Fig. 7(1) is shown the low field region, which displays the irreversible behaviour associated with a coercitive field of about 200 Oe, a value which is in agreement with those usually found in Co + Cu based granular alloys with Co-rich clusters larger than about 10 nm [16,17].

The evolution of the maximum MR value as a function of the Co content is shown in Fig. 7(2). As the Co content is increased, the number of scattering centres at

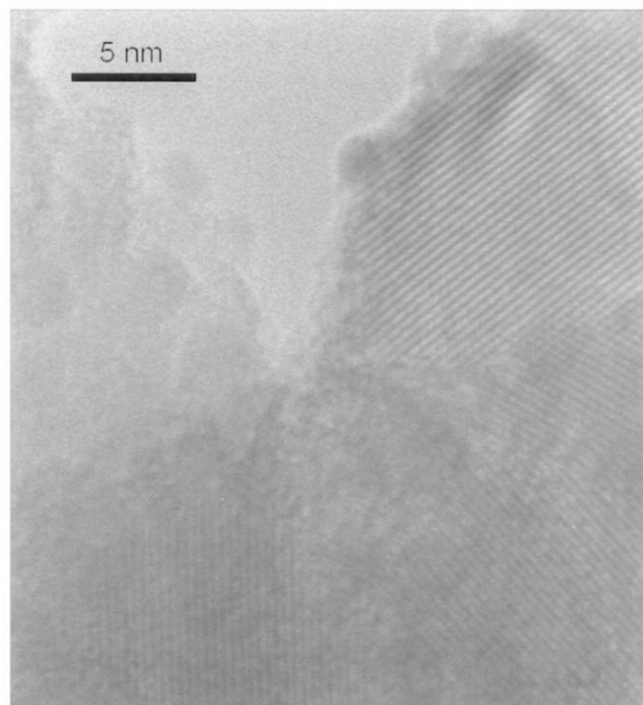

Fig. 6. Bright field high resolution TEM image of the deposit of Fig. 5B.

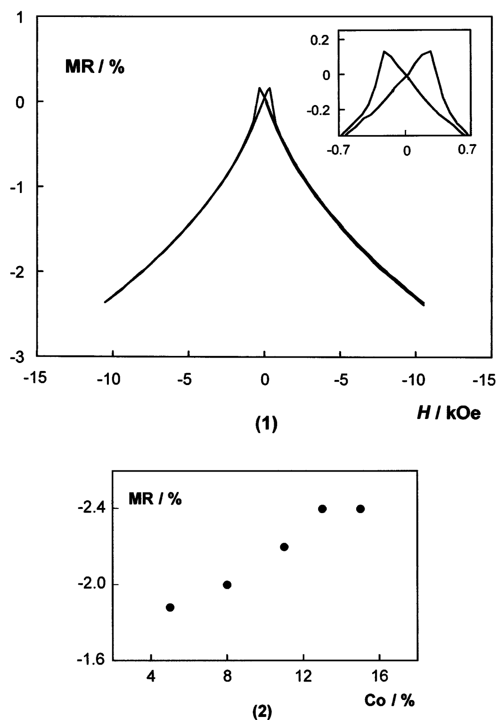

Fig. 7. (1) ΔMR vs. in-plane applied field in parallel geometry at 27 K for a 15% Co deposit. Inset: detail of the low field region. (2) ΔMR at 11 kOe as a function of the cobalt percentage.

the interface between the particles and the matrix increases as the size of the Co-rich particles increases (as confirmed by TEM), giving rise a quasi-linear increase of the MR maximum, which saturates at about 13%, as the optimum size of the segregated Co particles is reached. This compositional dependence of the MR maximum is analogous to the behaviour observed in as-prepared sputtered films of similar compositions [11,16].

All these facts indicate that our electrodeposited films are comparable to films prepared by other classical techniques (sputtering), both from the structural point of view and their magneto-transport properties. The relatively low MR signal and the harder magnetic response (higher values of the magnetic field are necessary to achieve magnetic saturation) as compared, for instance, to the corresponding results for Co + Ag granular films, are due to the existence of non-sharp interfaces surrounding Co-rich clusters, as a consequence of the high degree of dilution (alloying) of Co atoms within the Cu-rich matrix, in comparison with the Co + Ag case.

4. Conclusions

An ITO/glass substrate is sufficiently conductive to allow the electrodeposition of Co + Cu alloys directly onto it, and also allows the magnetoresistance to be measured without separating the films from the substrate. Thus the ITO film over a glass surface is useful for the deposition of Co + Cu alloy directly onto it, although only thin films can be obtained due to problems of poor adherence for thicker coatings. From stripping and diffraction experiments, Co + Cu films electrodeposited on ITO substrate seem to correspond to a solid solution of variable cobalt percentage, as a function of the experimental conditions. The cobalt percentage in the coatings can be increased either by increasing Co (II) concentration and/or by making the current density more negative. However, deposition conditions which lead to high cobalt percentages imply substantial hydrogen evolution, which induces the cracking of the deposits.

Although solid solutions seem to be obtained, a MR signal is observed for all the Co + Cu coatings studied, even without the annealing of the samples. This fact demonstrates the existence of nanometric cobalt-rich ferromagnetic regions distributed within the film. As can be deduced from TEM experiments, the MR value depends on the size of the magnetic clusters of cobalt and their distribution on the Co + Cu matrix. The reason for the increase of the MR ratio for the Co + Cu films when the cobalt percentage increases in the deposit seems to be that the mean size of the cobalt particles increases to an appropriate value.

References

[1] J.R. Childress, C.L. Chien, Phys. Rev. B 43 (1991) 8089.
[2] J.R. Childress, C.L. Chien, J. Appl. Phys. 70 (1991) 5885.
[3] H.J. Blythe, V.M. Fedosyuk, Phys. Stat. Sol. (a) 146 (1994) K13.
[4] H.J. Blythe, V.M. Fedosyuk, Phys. Condens. Matter. 7 (1995) 3461.
[5] R. López, J. Herreros, A. García-Arribas, J.M. Barandiarán, M.L. Fdez-Gubieda, J. Magn. Magn. Mater. 196 (1999) 153.
[6] A.E. Berkowitz, J.R. Mitchell, M.J. Carey, A.P. Young, S. Zhang, F.E. Spada, F.T. Parker, A. Hutten, G. Thomas, Phys. Rev. Lett. 68 (1992) 3745.
[7] J.Q. Xiao, J.S. Jiang, C.L. Chien, Phys. Rev. Lett. 68 (1992) 3749.
[8] M. Tsunoda, K. Okuyama, M. Ooba, M. Takahashi, J. Appl. Phys. 83 (1998) 7004.
[9] V.M. Fedosyuk, O.I. Kasyutich, D. Ravinder, H.J. Blythe, J. Magn. Magn. Mater. 156 (1996) 345.
[10] H. Zaman, A. Yamada, H. Fukuda, Y. Ueda, J. Electrochem. Soc. 145 (1998) 565.
[11] A.D.C. Viegas, J. Geshev, J.E. Schmidt, E.F. Ferrari, J. Appl. Phys. 83 (1998) 7007.
[12] G.N. Kakazei, A.F. Krovetz, N.A. Lesnik, M.M. Pereira de Azevedo, Yu.G. Pogorelov, G.V. Bondorkova, V.I. Silantiev, J.B. Sousa, J. Magn. Magn. Mater. 196 (1999) 29.
[13] Y. Ueda, T. Houga, H. Zaman, A. Yamada, J. Solid State Chem. 147 (1999) 274.
[14] E. Gómez, A. Llorente, E. Vallés, J. Electroanal. Chem. 495 (2000) 19.
[15] H. Baker (Ed.), Alloy Phase Diagrams, ASM Handbook, vol. 3, ASM International, Ohio, 1992.
[16] V. Franco, X. Batlle, A. Labarta, J. Magn. Magn. Mater. 210 (2000) 295.
[17] V. Franco, X. Batlle, A. Labarta, J. Appl. Phys. 85 (1999) 7328.

4.2. Control de la heterogeneïtat dels dipòsits Co-Cu mitjançant electrodeposició

En aquest capítol s'ha estudiat la possible obtenció per electrodeposició de dipòsits de Co-Cu heterogenis, essent uniformes en morfologia i composició, a partir del tipus de bany escollit. S'intenta trobar la relació entre la composició del bany i la heterogeneïtat del dipòsit.

S'ha treballat amb dissolucions contenint $CuSO_4$ i $CoSO_4$, de concentracions 0.9 a 2 mol dm^{-3} de $CoSO_4$, 0.01 a 0.1 mol dm^{-3} $CuSO_4$, en presència de H_3BO_3 i amb concentracions de citrat de sodi entre 0 i 1 mol dm^{-3}, a pH=3.5, a temperatura de 20ºC, sobre elèctrodes de carboni vitri i Ni. Les concentracions mes baixes de citrat afavoriran la menor complexació dels cations metàl·lics i per tant facilitaran la deposició separada d'ambdós metalls.

S'analitzarà l'efecte de la concentració del citrat de sodi en la resposta electroquímica, la morfologia (SEM) i l'estructura (XRD) dels dipòsits de Co-Cu.

S'estudiarà si els resultats electroquímics (voltamètrics i d'*stripping*) i els resultats de XRD permeten establir la composició òptima del bany i les condicions d'electrodeposició per les que sigui possible obtenir dipòsits de Co-Cu heterogenis, no-dendrítics, i uniformes en morfologia i composició.

Els resultats d'aquest capítol s'inclouen en el següent article:

-*Electrodeposition for obtaining homogeneous or heterogeneous cobalt-copper films*

J. Sol. Stat. Electrochem., publicat *on-line* el 23-09-2003

Electrodeposition for obtaining homogeneous and heterogeneous Co-Cu films

Abstract

Direct electrodeposition of heterogeneous deposits may be an alternative method of preparing Co-Cu coatings with magnetoresistive properties. Cobalt-copper electrodeposition was obtained in sulphate baths containing different citrate concentrations in order to prepare either homogeneous or heterogeneous Co-Cu deposits. X-ray diffraction (XRD) and voltammetric stripping analysis were used to study the kind of deposits formed.

Free-citrate baths produced heterogeneous films, although dendritic growth was observed, thus increasing the deposit's thickness. Increasing the Cu(II)/Co(II) ratio in solution enabled the formation of smoother deposits.

The presence of citrate at up to twice the total metallic concentration in the bath improved the morphological aspects of deposits, their structural heterogeneity being maintained. Higher citrate concentrations induced the loss of heterogeneity, and both electrochemical and diffraction peaks tended towards single peaks. Homogeneous cobalt-copper deposits, formed by a solid solution structure, were obtained in highly complexed citrate baths.

Keywords: cobalt-copper alloy films, electrodeposition, XRD

Introduction

In recent years, the preparation of magnetoresistive alloy thin films has been extensively studied in order to test their usefulness in sensor devices. The Co-Cu system is suitable for such a purpose because some heterogeneous Co-Cu alloys present high magnetoresistive values [1-10] when cobalt particles of a defined size are dispersed in a copper matrix.

Heterogeneous Co-Cu films are usually prepared by physical methods such as sputtering [1,2,6,11,12], nebulized spray pyrolysis [13], electron beam evaporation [8,9], rapid quenching [3,14] or mechanical milling of the elements [15,16].
A posterior annealing of the samples is usually performed in order to provide better separation of the cobalt granules from the copper matrix.

The electrodeposition technique has recently been used as an alternative method for preparing thin films of different alloys. However, despite the fact that the equilibrium phase diagram in the Co-Cu system allows negligible solubility of two metals at room temperature [17], electrodeposition has generally been found to produce a metastable solid solution when complexing agents are used for the simultaneous co-deposition of cobalt and copper. These homogeneous deposits require a posterior annealing of the samples in order to form cobalt precipitates in the matrix [4,7,18].

In previous electrodeposition studies [19,20] we obtained homogeneous Co-Cu films of different composition that corresponded to solid solutions. The present study aimed to test whether electrodeposition could be used for the direct preparation of uniform, adequate heterogeneous Co-Cu alloys, without the need for posterior annealing of the samples. To this end, different solutions were tested, with and without complexing agents, in order to induce the electrodeposition of Co-Cu heterogeneous alloys.

Experimental

Solutions were prepared from $CuSO_4 \cdot 5H_2O$, $CoSO_4 \cdot 7H_2O$ and H_3BO_3, with a constant boric concentration of 30 g dm^{-3}. High metallic concentrations were used to favour a high deposition rate. Different sodium citrate ($Na_3C_6H_5O_7 \cdot 2H_2O$) concentrations between 0 and 1 mol dm^{-3} were used in order to control the simultaneous cobalt and copper co-deposition. All solutions were freshly prepared with water first doubly distilled and then treated with a Millipore Milli Q system. In all cases, pH was adjusted to 3.5 by suitable addition of H_2SO_4.

Before and during the experiments, solutions were de-aerated with argon. Deposition was performed at 20º C.

Electrochemical experiments were carried out in a conventional three-electrode cell using an Autolab with PGSTAT30 equipment and GPES software. Working electrodes were vitreous carbon (Metrohm) and nickel rods (John Matthey 99.99%), both with an area of 0.0314 cm^2. The vitreous carbon electrode was polished to a mirror finish using alumina of different grades (3.75 and 1.87 μm) and cleaned ultrasonically for 2 min in water before each experiment. The nickel electrode was polished before each experiment using 4000 grade paper and diamond of different grades (6 and 1 μm), and then ultrasonically rinsed for 2 min in water. The counter electrode was a platinum spiral. The reference electrode was a Ag | AgCl | NaCl 1mol dm^{-3} mounted in a Luggin capillary containing 0.5 mol dm^{-3} Na_2SO_4 solution. All potentials are referred to this electrode.

Voltammetric experiments were carried out at different scan rates between 5 and 50 mV s^{-1}, scanning at first to negative potentials. Only one cycle was run in each voltammetric experiment. Stripping analysis was always performed immediately after deposition, both in the deposition solution itself and in a blank solution (0.5 mol dm^{-3} Na_2SO_4). All deposits were obtained under stirring conditions (ω=100 rpm, magnetic stirrer).

The morphology of deposits was examined with a Hitachi S 2300 scanning electron microscope. Elemental composition was determined using an X-ray analyser incorporated into a Leica Cambridge Stereoscan S-360 (EDX).

XRD analysis was performed on a Philips MRD diffractometer in its parallel low-resolution optics. The Cu-K_α radiation (λ=1.5418 Å) was selected by means of a diffracted-beam flat graphite monochromator crystal. Two experimental conditions were used. Diffractograms for the initial qualitative analysis were from 20 to 100 ° 2θ with a step size of 0.05 ° 2θ, a measuring time of 5 s per step and a beam size of (1x1) mm^2. 2θ/θ detailed scans were recorded for some samples in the range of the

311 reflection with a step size of 0.05 $^{\circ}$ 2θ, measuring times between 35 and 80 s per step and a beam size of (0.7x0.2) mm^2.

Results and Discussion

Different sodium citrate concentrations were tested to obtain coherent and continuous heterogeneous Co-Cu deposits. For each solution, a voltammetric study was performed both on vitreous carbon and nickel electrodes in order to test the copper and cobalt co-deposition. Electrodeposition conditions were then selected to obtain Co-Cu coatings, whose morphology, composition and crystalline structure were analysed.

a) Free-citrate solutions

The Co-Cu electrodeposition from baths without complexing agent was analysed from two solutions containing different proportions of copper and cobalt sulphates. Due to the different equilibrium potential of the Cu^{2+} and Co^{2+} reduction reactions in an uncomplexed state, copper (II) was always maintained as the minority ion, its deposition potential being clearly more favourable than that of cobalt.

For the first solution studied, that containing 0.01 mol dm^{-3} of Cu (II) and 2 mol dm^{-3} of Co (II), voltammetric response under stationary conditions showed a clearly separate reduction process (Fig.1A): a first copper reduction peak, that at this low concentration became diffusion controlled (Fig.1B), followed by new reduction current related to the start of cobalt deposition was observed. When low cathodic limits were used, only one oxidation peak was detected, corresponding to copper oxidation. Decreasing the cathodic limit, a new oxidation peak was observed in the anodic scan, prior to copper oxidation. As the position of the copper oxidation peak was constant for different cathodic limits, it can be deduced that the reduction current in excess of the diffusion-limited current for copper deposition, detected from around –800 mV, was due to cobalt deposition. Similarly, the more negative oxidation peak can be assigned to the oxidation of the deposited cobalt.

Potentiostatic transients over the vitreous carbon electrode confirmed the behaviour demonstrated by voltammetric results. At low deposition potentials, only copper deposition was observed (Fig.2, curve a). Decreasing deposition potentials to sufficiently negative values produced a first peak in the j-t transient, followed by a second growth in the curve (Fig.2, curves b and c), revealing that cobalt deposition took place over the previous copper deposited.

Under quiescent conditions, galvanostatic transients at different current densities showed a clear change with respect to time. The potential first evolved to a value corresponding to copper deposition, and then reached a value at which cobalt deposition was possible. Under stirred conditions it was only possible to attain a stationary potential when the total applied current was lower than the diffusion-limited current for Cu deposition.

As in voltammetric experiments, the voltammetric stripping response of the deposits obtained under moderate stirring conditions, both potentiostatically and galvanostatically, always showed two separate oxidation peaks (Fig.3) whose relative height depended on the deposition potential. When current efficiency was close to 100%, the relative heights of the two peaks indicated the relative presence of cobalt and copper in the films, the first oxidation peak corresponding to cobalt oxidation and the more negative to copper oxidation.

Thicker deposits were obtained over nickel electrodes, as this metallic substrate favours their adherence. The dependence of film composition on agitation meant that uniform stirring over the substrate was required. Final deposits obtained from this solution were not very homogeneous in morphology, and became more dendritic with decreasing deposition potentials and increasing deposition time. Only low charges produced relatively uniform final deposits (Fig.4A). Structural analysis of these coatings revealed that the films were clearly heterogeneous, the diffractograms showing peaks corresponding to the face centred cubic (f.c.c.) copper and the f.c.c. cobalt structures (Fig. 4B).

Increasing the Cu(II)/Co(II) solution ratio, some differences were observed in both electrochemical and morphological results. For a solution containing 0.1 mol dm^{-3} of Cu (II) and 0.9 mol dm^{-3} of Co (II), and using similar scan rates as for the 0.01 mol dm^{-3} Cu (II)/ 2 mol dm^{-3} Co (II) solution, the voltammetric response showed a lower separation of the oxidation peaks. However, decreasing to 5 mV s^{-1} also produced a clear separation of peaks for both vitreous carbon and nickel electrodes (Fig.5). As the copper (II) concentration was increased with respect to the first solution, there was a simultaneous increase in copper deposition in the cobalt reduction zone. However, the position of the two oxidation maximums was not dependent on the cathodic limit used in the voltammetric scan, revealing that although copper and cobalt may codeposit in a defined potential zone, a heterogeneous copper+cobalt deposit was in fact formed.

The deposits obtained from this solution at low deposition charges consisted of polyhedral crystals of varying size (Fig.6A) and which showed a similar morphology to that observed for a higher [Co(II)]/[Cu(II)] ratio. X-ray diffractograms showed that heterogeneous deposits, formed by a mixture of cobalt and copper, were also obtained from this solution. The cobalt percentage in these thin deposits increased when either the deposition potential or the current density were made more negative. In contrast, increasing the level of agitation of the solution during deposition led to a decrease in the cobalt percentage, because the process of copper deposition is controlled by diffusion.

Increasing the deposition charge, it was observed non-uniformity in the deposits and copper-rich dendrites were observed over the first deposit (Fig.6B).

b) Sodium citrate additions

A range of sodium citrate concentrations were added to the 0.1 mol dm^{-3} Cu (II)/ 0.9 mol dm^{-3} Co (II) solution in order to favour the formation of more homogeneous and

less dendritic deposits. Citrate concentration values between 0.1 and 1 mol dm^{-3} were tested.

Voltammetric experiments, over both vitreous carbon and nickel electrodes, showed that an increase in citrate concentration brought the potential close to that at which the two metals were deposited (Fig.7). Copper reduction was clearly shifted (Fig.7B) towards more negative potentials, revealing an important copper complexation, whereas the start of cobalt codeposition was less modified for the different citrate concentrations used. The corresponding oxidation response tended toward a single oxidation peak when the citrate concentration was gradually increased (Fig.7A), demonstrating that such increases produce gradual changes in the deposition process.

For the highest citrate concentrations studied ([citrate]>0.5 mol dm^{-3}), voltammetric and stripping results showed that only one oxidation peak was ever obtained for the different cathodic limits applied. The position of this peak clearly moved towards the position of the pure-cobalt oxidation peak as the cathodic limit was gradually decreased (Fig. 8), this corresponding to the formation of a Co-Cu solid solution [19,20]. These results confirm that deposition through citrate complexes favours the simultaneous co-deposition of cobalt and copper and induces a homogeneous alloy.

The deposits obtained, both potentiostatically and galvanostatically, from each one of the analysed solutions were compared. The solutions containing low citrate concentrations produced rough deposits (Fig.9A), whereas increasing the citrate concentration led to observe more homogeneous and flat deposits (Fig.9B). Deposits became dendritic in free-citrate solutions, whereas non-dendritic homogenous deposits were produced by increasing the citrate concentration. The addition of citrate to solutions led to more uniform deposits being obtained, even for thick coatings.

In order to investigate the influence of the bath's citrate content on the heterogeneity of the deposits, and to follow the gradual structural changes of these deposits, X-ray diffraction analyses of deposits obtained at the same deposition charge from different

citrate concentration solutions were performed. Low deposition charges were used to avoid the formation of dendritic copper structures in the case of the free-citrate solution. In all cases, the signal corresponding to vitreous carbon was found to be superposed onto the signal of the Co-Cu layer. The evolution of the samples' diffraction peak positions and intensities was also analysed and detailed scans of the 311 reflections were obtained. This peak, obtained at high θ values, was chosen because it showed the greatest separation between copper and cobalt positions. Moreover, no substrate peaks (of vitreous carbon) were detected in this 2θ range.

Peak profile analysis was performed using pseudo-Voight functions. Table I lists the 2θ positions, the relative intensities of the Cu and Co peaks when both were observed, and the full width at half maximum (FWHM) of the adjusted peaks. This table shows that non-uniform composition is detected from solutions containing citrate concentrations lower than 0.2 mol dm^{-3}.

For deposits obtained from the free-citrate solution, two separate peaks were clearly observed, as with those obtained for different Co(II) and Cu(II) concentrations and thicker deposits (Fig.4B). The adjusted positions are close to those known to exist for Cu and Co fcc structures (89.93 for Cu and 92.23 for Co). Decreasing the deposition potential, an increase in the relative intensity of the Co peak is observed, indicating an increased cobalt percentage in the deposit.

All results indicated that increasing the citrate concentration in the baths enabled the evolution from double to single peaks to be observed. A concentration of 0.1 mol dm^{-3} revealed double peaks indicative of heterogeneous films, whereas at concentrations of 0.2 and 0.8 mol dm^{-3} single peaks were observed, indicative of solid solution formation. Similarly, the relative intensity of the Co peak increases with deposition potential in the 0.1 mol dm^{-3} baths. When solid solutions are formed, the position of the peak seems closer to the known Co position when the overall Co composition is higher.

Conclusions

Electrodeposition was shown to be a useful tool for preparing either homogeneous or heterogeneous deposits, depending on solution composition and electrodeposition conditions.

Electrodeposition from electrolytes containing Co(II) and Cu(II) ions in an uncomplexed or weakly-complexed enabled heterogeneous Co-Cu deposits to be prepared, in which copper and cobalt deposited separately. However, these deposits were uniform and coherent at low deposition charges. When thicker deposits were prepared, even under stirring conditions, they developed a dendritic morphology, due to the fast and favoured deposition of copper over the initial Co-Cu deposit. Voltammetric and stripping curves provided an estimate of the cobalt and copper present in the prepared thin films.

When sodium citrate was used at concentrations higher than 0.2 mol dm^{-3}, the important complexation of ions, especially that of copper (II), slows copper deposition and favours simultaneous copper and cobalt codeposition. These solutions, regardless of the thickness, produced homogeneous and uniform deposits that correspond to a solid solution. The position of the peaks in X-ray diffractograms and voltammetric and stripping curves provide estimates of the cobalt percentage in the deposits.

Citrate concentrations around 0.1 mol dm^{-3} proved adequate for preparing granular heterogeneous Co-Cu coatings. However, this amount of sodium citrate in solution is not enough to complex all copper ions, as the manner that deposition occurs simultaneously from free and complexed ions. Although non-flat deposits were obtained in these conditions, sufficiently coherent and uniform deposits were prepared for coatings of a few microns.

Acknowledgements

The authors wish to thank the *Serveis Cientificotècnics* (*Universitat de Barcelona*) for providing equipment. This research was supported financially by contracts MAT 2000-0986 and MAT 2000-0858 from the Spanish *Comisión Interministerial de Ciencia y Tecnología* (CICYT) and by the *Comissionat* of the *Generalitat de Catalunya* under Research Project SGR 2000-017.

References

1.- Berkowitz AE, Mitchell JR, Carey MJ, Young AP, Zhang S, Spada FE, Parker FT, Huttem A, Thomas G (1992) Phys Rev Lett 68:3745

2.- Xiao JQ, Jiang JS, Chien CL (1992) Phys Rev Lett 68:3749

3.- Setna RP, Cerezo A, Hyde JM, Smith GDW (1994) Appl Surf Sci 76/77:203

4.- Fedosyuk VM, Kasyutich OI, Ravinder D, Blythe HJ (1996) J. Magn Magn Mat 156:345

5.- Schwarzacher W, Lashmore DS (1996) IEEE Trans Magn 32:3133

6.- Tsunoda M, Okuyama K, Ooba M, Takahashi M (1998) J Appl Phys 83:7004

7.- Zaman H, Yamada A, Fukuda H, Ueda Y (1998) J Electrochem Soc 145:565

8.- Viegas ADC, Geshev J, Schmidt JE, Ferrari EF (1998) J Appl Phys 83:565

9.- Kakazei GN, Krovetz AF, Lesnik NA, Pereira de Azevedo MM, Pogorelov YuG, Bondorkova GV, Silantiev VL, Sousa JB (1999) J Magn Magn Mater 196:29

10.- Ueda Y, Houga T, Zaman H, Yamada A (1999) J Solid State Chem 147:274

11.- Childress JR, Chien CL (1991) Phys Rev B 43:8089

12.- Childress JR, Chien CL (1991) J Appl Phys 70:5885,

13.- Parashar S, Raju AR, Rao CNR (1999) Mat Chem Phys 61:46

14.- Schmool D, Garcia-Arribas A, Abad E, Garitaonandia JS, Fdez-Gubieda ML, Barandiaran JM (1999) J Magn Magn Mat 203:73

15.- Dellogu F, Pintore M, Enzo S, Cardellini F, Contini V, Montone A, Rosato V (1997) Phil Magazin B 76:651

16.- Liu BX, Ma E, Li J, Huang LJ (1997) Nuc. Inst. Meth. Phys. Res. B19/20:682

17.- Alloy phase diagrams, in: Hugh Baker (Eds.), ASM Handbook, vol.3, ASM International, Ohio,1992

18.- Blythe HJ, Fedosyuk VM (1996) J Magn Magn Mat 155:352

19.- Gómez E, Llorente A, Vallés E (2000) J Electroanal Chem 495:19

20.- Gómez E, Labarta A, Llorente A, Vallés E (2001) J Electroanal Chem 517:63

Table I. Influence of citrate concentration and deposition potential on the positions and relative intensities of the diffraction peaks

[citrate]/ mol dm^{-3}	*E / mV*	*% Co*	*2θ (Cu)*	*% Intensity (Cu)*	*2θ (Co)*	*% Intensity (Cu)*	*FWHM*
-	-1000	32-63	90.37	40	91.91	60	1.29
-	-1100	40-80	90.68	24	92.08	76	1.13
0.1	-1000	30-56	90.85	54	91.59	46	1.06
0.1	-1100	37-42	90.37	19	91.58	81	1.20
0.2	-1000	55	91.35				1.24
0.2	-1100	72	91.65				1.28
0.8	-1000	50	91.05				1.23

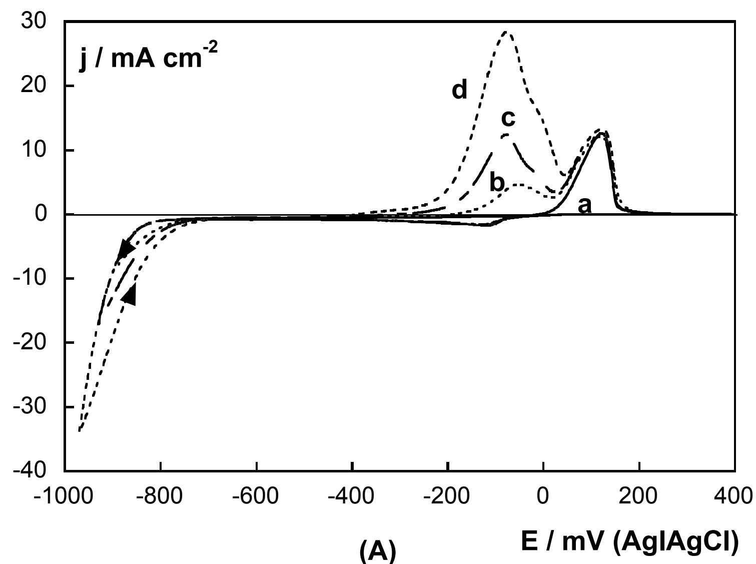

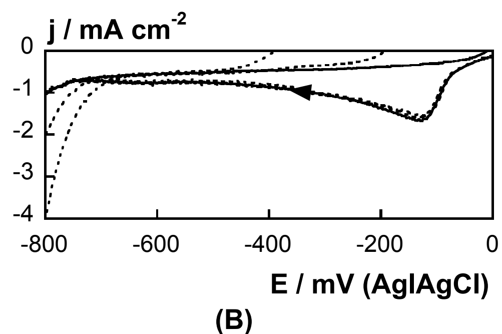

Figure 1.- Cyclic voltammograms of a 2 mol dm^{-3} $CoSO_4$ + 0.01 mol dm^{-3} $CuSO_4$ + 30 g dm^{-3} H_3BO_3 solution. 50 mV s^{-1}. Vitreous carbon electrode. Starting potential: 100 mV. Cathodic limit: a) –800, b) –900, c) –930 and d) –970 mV.

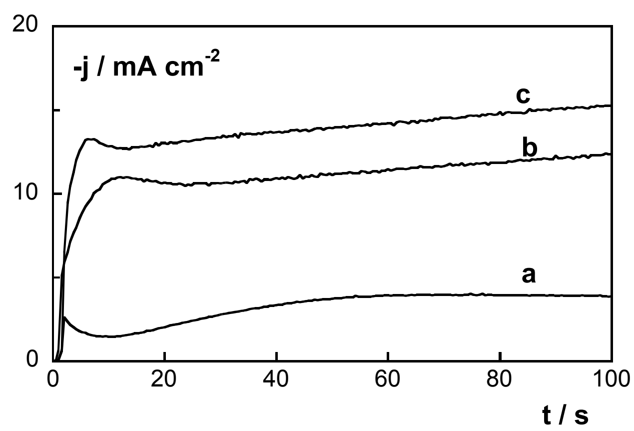

Figure 2.- Potentiostatic transients of the same solution and electrode as in Figure 1 at a) –800, b) –875 and c) –900 mV.

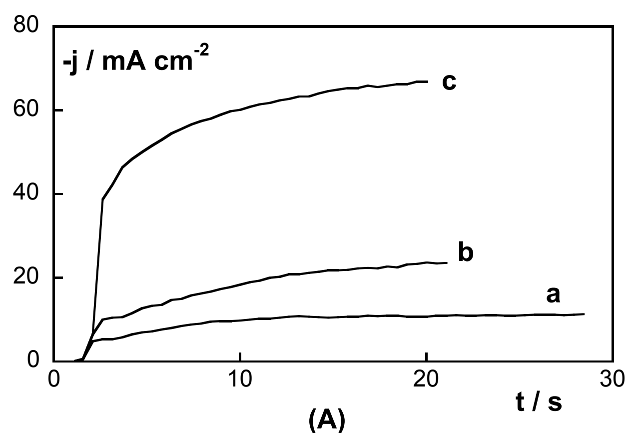

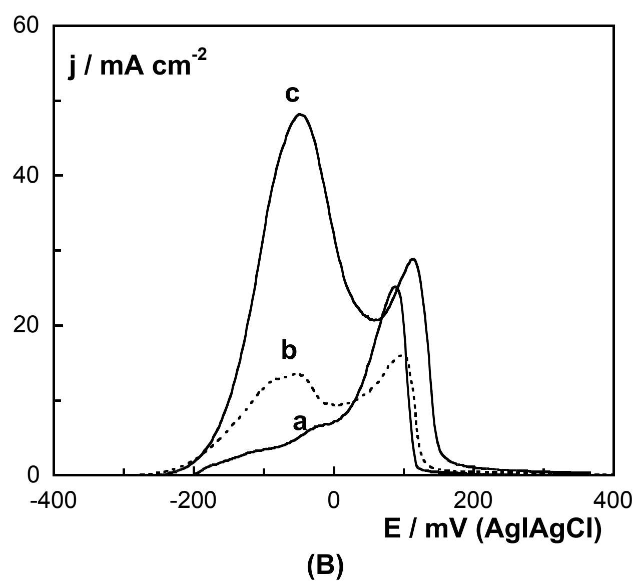

Figure 3

(A) Potentiostatic transients, obtained at 100 rpm, of the same solution and electrode as in Figure 1 at a) –850, b) –900 and c) –950 mV.

(B) Potentiodynamic stripping curves at 10 mV s^{-1} corresponding to deposits obtained from the j-t transients of Figure 3A.

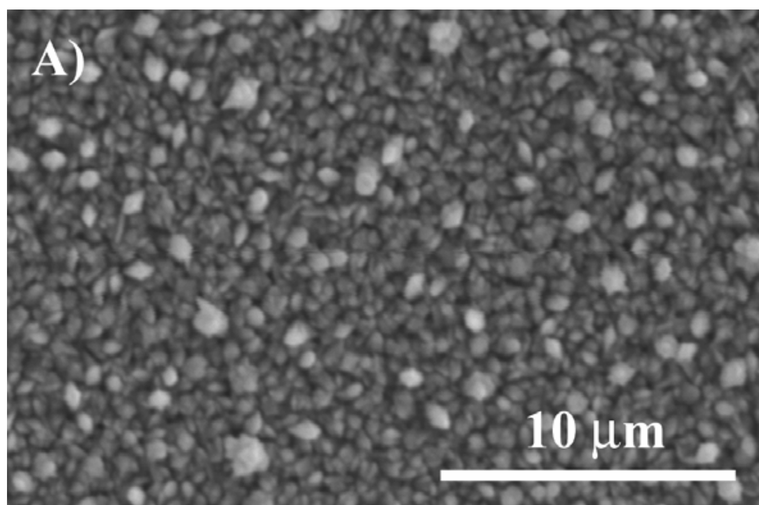

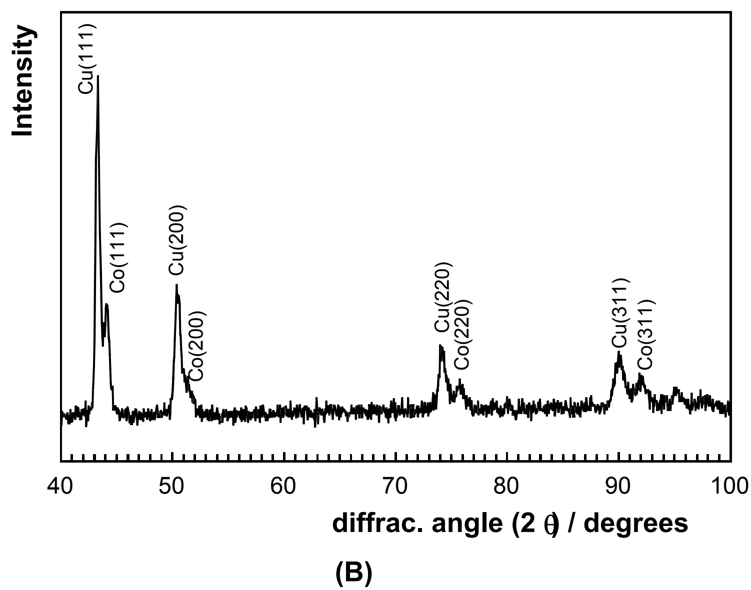

Figure 4

(A) SEM micrographs of a deposit obtained at –950 mV for 200 s from the solution of Figure 1. Nickel electrode. 100 rpm. 50 % Co.

(B) X-ray diffractogram of the deposit obtained under the same conditions as in Figure 4A, but for 1200 s.

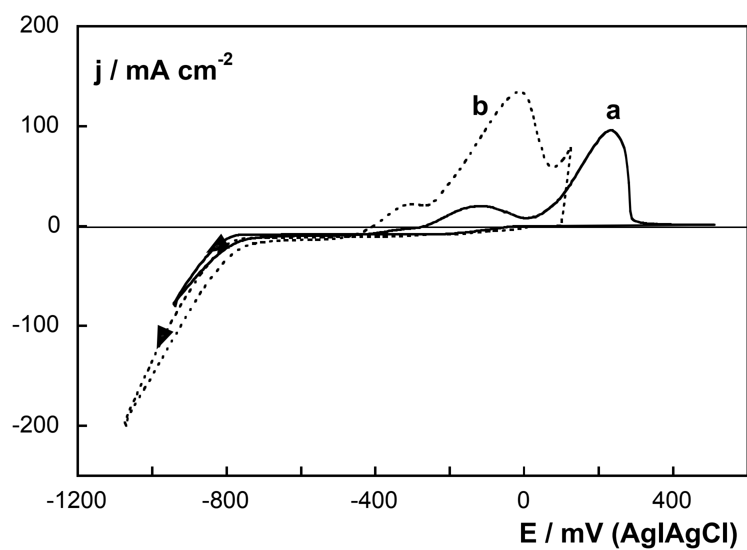

Figure 5.- Cyclic voltammograms of a 0.9 mol dm^{-3} $CoSO_4$ + 0.1 mol dm^{-3} $CuSO_4$ + 30 g dm^{-3} H_3BO_3 solution. 5 mV s^{-1}. a) Vitreous carbon electrode; and b) Nickel electrode.

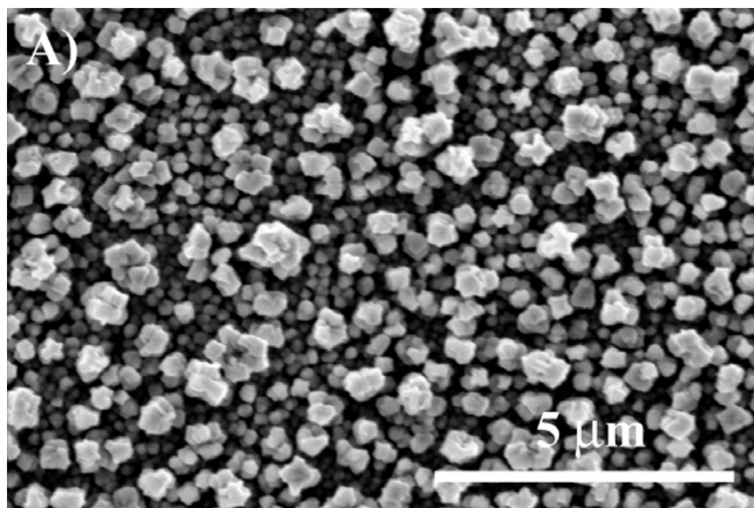

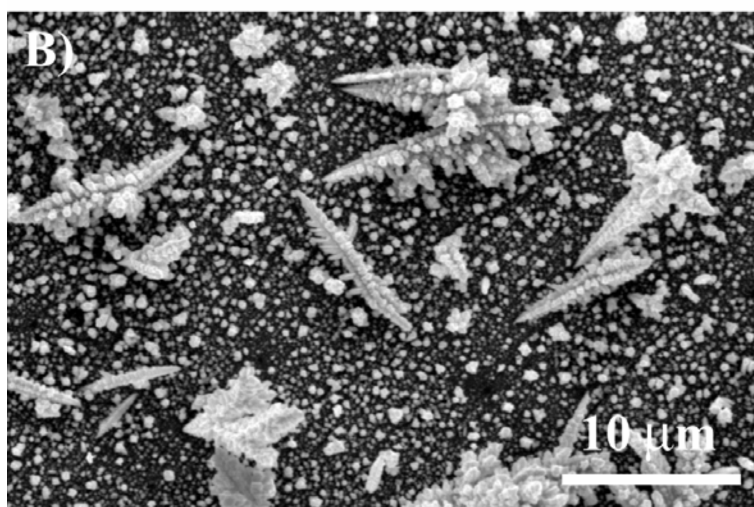

Figure 6.-SEM micrographs of the deposit obtained from the solution of Figure 5 at –1100 mV. Nickel electrode. 100 rpm.

(A) 50 s. 35 % Co

(B) 300 s.

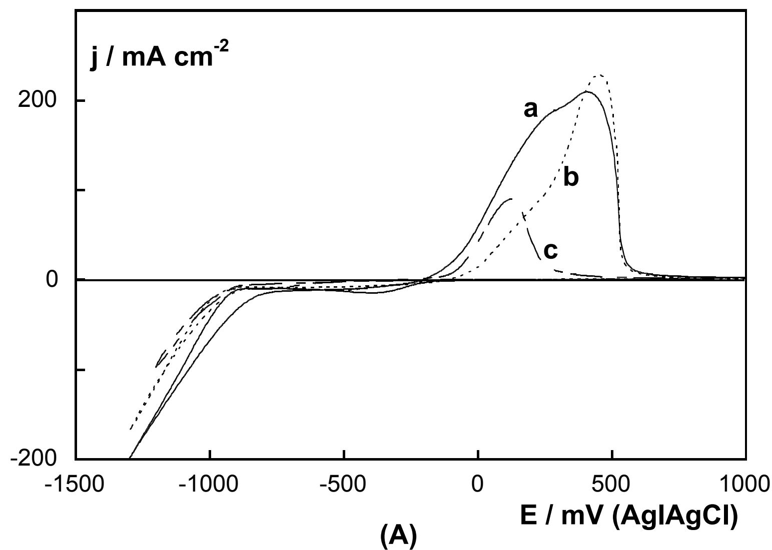

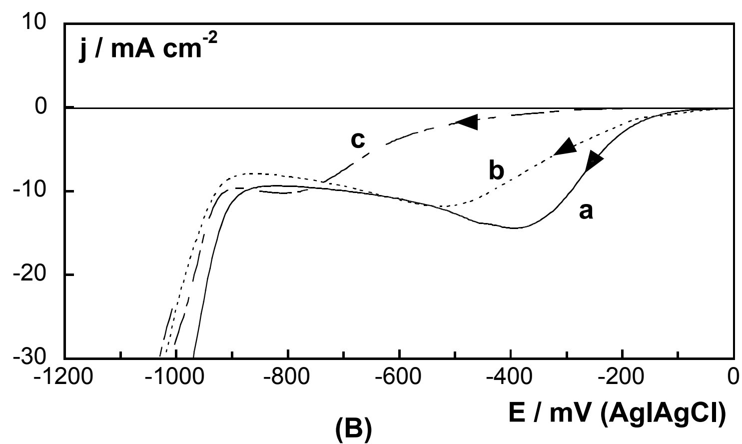

Figure 7.

(A) Cyclic voltammograms at 50 mV s^{-1} on vitreous carbon electrode. 0.9 mol dm^{-3} $CoSO_4$ + 0.1 mol dm^{-3} $CuSO_4$ + 30 g dm^{-3} H_3BO_3 + a) 0, b) 0.1 and c) 1 mol dm^{-3} $Na_3C_6H_5O_7$ solution.

(B) Detailed zone of the copper reduction peak.

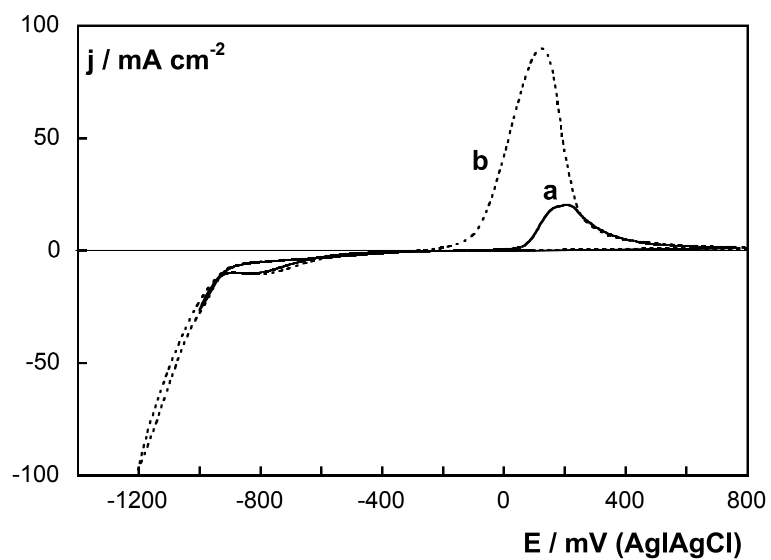

Figure 8.- Cyclic voltammograms of a 0.9 mol dm^{-3} $CoSO_4$ + 0.1 mol dm^{-3} $CuSO_4$ + 30 g dm^{-3} H_3BO_3 + 1 mol dm^{-3} $Na_3C_6H_5O_7$ solution. 50 mV s^{-1}. Vitreous carbon electrode. Cathodic limit: a) –1000 and b) –1200 mV.

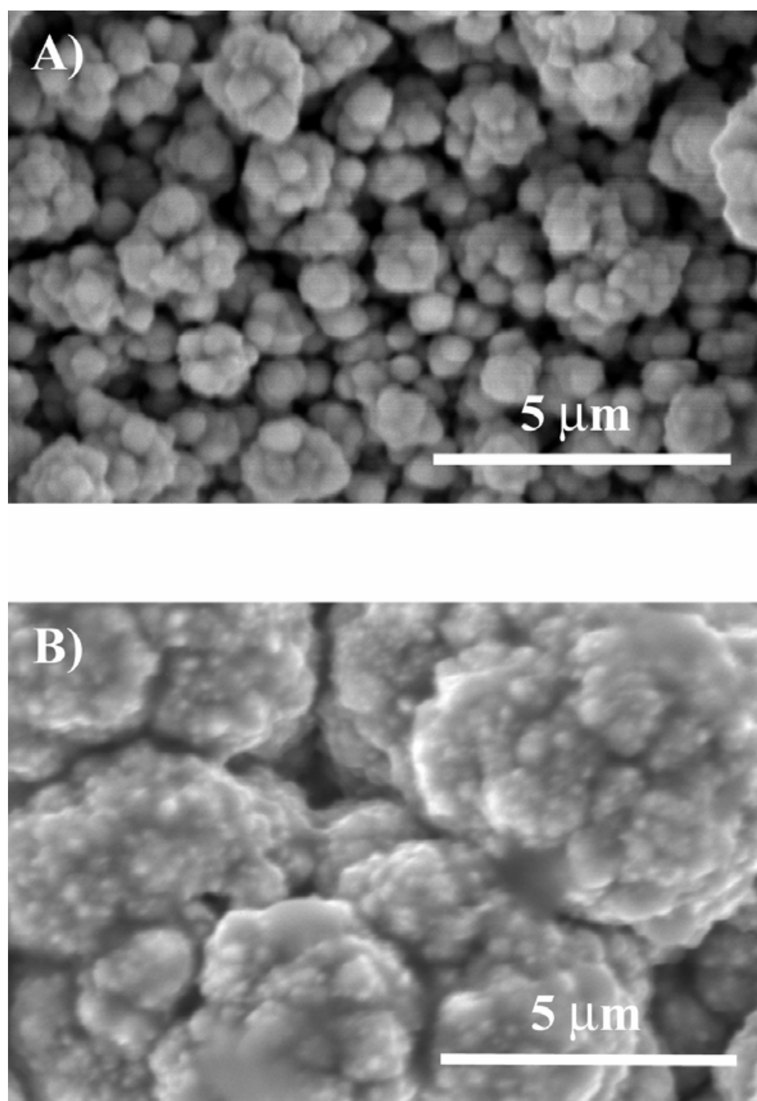

Figure 9.

(A) SEM micrographs of a deposit obtained from a 0.9 mol dm^{-3} $CoSO_4$ + 0.1 mol dm^{-3} $CuSO_4$ + 30 g dm^{-3} H_3BO_3 + 0.1 mol dm^{-3} $Na_3C_6H_5O_7$ solution. Nickel electrode. 100 rpm. –950 mV for 1000 s. 37 % Co.

(B) SEM micrographs of a deposit obtained from a 0.9 mol dm^{-3} $CoSO_4$ + 0.1 mol dm^{-3} $CuSO_4$ + 30 g dm^{-3} H_3BO_3 + 1 mol dm^{-3} $Na_3C_6H_5O_7$ solution. Nickel electrode. 100 rpm. –1000 mV for 2000 s. 50 % Co.

4.3. Estudi de la influència del recuit en làmines Co-Cu obtingudes per electrodeposició

En aquest capítol s'ha estudiat l'efecte del recuit en la morfologia, estructura i propietats de transport (MR) de mostres de Co-Cu obtingudes per electrodeposició. L'objectiu de fer el recuit és afavorir una millor separació de precipitats rics en cobalt dins la matriu de Co-Cu.

S'ha treballat amb una solució 0.15 mol dm^{-3} $CoSO_4$, 0.05 mol dm^{-3} $CuSO_4$, 0.5 mol dm^{-3} de citrat de sodi i 30 g dm^{-3} de H_3BO_3 a pH=5.3 i a temperatura constant (25ºC). Els dipòsits s'han preparat sobre elèctrodes de vidre/Cr i Si/capa llavor; aquests substrats s'han provat com els mes adients per mesurar directament sobre ells la magnetoresistència i alhora, resistir les elevades temperatures del forn.

S'han preparat dipòsits de diferents percentatges de cobalt en funció de la composició del bany i de la densitat de corrent aplicada. Per cada tipus d'elèctrode s'establirà la relació entre la densitat de corrent o potencial aplicat i la composició del dipòsit.

S'acotarà els percentatges de cobalt per als quals els dipòsits presentin MR. D'aquests dipòsits s'analitzarà l'efecte del procés de recuit en la morfologia i estructura cristal·lina mitjançant experiments de SEM, TEM i XRD. També s'estudiarà la influència de la temperatura de recuit en la cristal·linitat dels dipòsit.

S'estudiarà la influència del temps i la temperatura de recuit en les propietats de transport en funció del percentatge de cobalt. Es buscarà la temperatura de recuit òptima per a cada percentatge de cobalt per aconseguir els màxims valors de MR. Es relacionarà els valors de MR amb la possible segregació de precipitats rics en cobalt durant el procés de recuit.

Els resultats d'aquest capítol s'inclouen en el següent article:

-*Annealing of Co-Cu films obtained by electrodeposition*

Enviat per a la seva publicació al Journal of The Electrochemical Society.

Annealing of Co-Cu films obtained by electrodeposition

E. Gómez[1], A: Labarta[2], A. Llorente[1], and E. Vallés[1*]

[1]Electrodep, Departament de Química Física, Universitat de Barcelona, Martí i Franquès 1, 08028 Barcelona, Spain

[2]Departament de Física Fonamental, Universitat de Barcelona, Martí i Franquès 1, 08028 Barcelona, Spain

* author to whom correspondence should be addressed

Phone: 34 93 402 12 34

Fax: 34 93 402 12 31

E-mail: e.valles@ub.edu

Abstract

Co-Cu films showing giant magnetoresistance (GMR) have been obtained by electrodeposition and posterior annealing of the samples. Homogeneous cobalt-copper electrodeposits were obtained in sulphate+citrate bath at pH=5.3 using glass/Cr or Si/Ti-Ni seed layer substrates. These substrates are appropriate to measure directly the magnetoresistance of the Co-Cu films. Annealing conditions have been optimised to increase the magnetoresistance of the films. Moderate current densities (in the range .–2.7 to –3.7 mA cm^{-2}) were appropriate to prepare deposits with a 10-25% Co that present, after annealing, values of MR around 6-8%. The analysis of the microstructure resulting from the annealing process has been performed by means of TEM and XRD.

Keywords: cobalt-copper alloy films, electrodeposition, annealing, magnetoresistance

Introduction

During the last years, magnetoresistive alloys in the form of thin films have been extensively studied for different applications such as the development of magnetic field sensors and magnetoresistive devices. With respect to this, one of the most promising candidates is the heterogeneous Co-Cu system due to the high magnetoresistive values observed for some compositions after appropriate annealing treatment [1-10]. Usually, these Co-Cu films are prepared by physical methods (sputtering, electron beam evaporation, mechanical milling…) and a posterior annealing of the samples is usually performed in order to provide better separation of cobalt precipitates within the copper matrix. However, the electrodeposition technique has demonstrated to be a simple alternative method for obtaining thin films of different alloys. When electrodeposition is used to prepare Co-Cu films, usually complexing agents are necessary to induce the simultaneous deposition of cobalt and copper and a metastable solid solution is generally found. These homogeneous deposits require a posterior annealing in order to segregate the cobalt precipitates within the matrix [4,7,11].

In previous works we have electrodeposited homogeneous Co-Cu films over different substrates when a sufficient complexing agent was used [12,13]. The composition of the Co-Cu films was varied as a function of the solution composition and deposition parameters. Although solid solutions seemed to be obtained, a MR signal was observed even without annealing treatment, revealing the existence of nanometric cobalt-rich ferromagnetic regions distributed within the film [13]. This work aims at studying the effect of post-annealing on the morphology, structure and transport properties of electrodeposited Co-Cu samples. To measure directly the magnetoresistance of the films, low conductive substrates, such as covered glass plates or Si/seed layers are used to carry out electrodeposition. The effect of different annealing conditions on the properties of Co-Cu coatings is also analysed.

Experimental

Chemicals used were $CuSO_4 \cdot 5H_2O$, $CoSO_4 \cdot 7H_2O$, sodium citrate ($Na_3C_6H_5O_7 \cdot 2H_2O$) and H_3BO_3. Solutions containing $CoSO_4$ 0.15 mol dm^{-3} + $CuSO_4$ 0.05 mol dm^{-3} + 0.5 Na_3citrate + 30 g dm^{-3} H_3BO_3 were used All solutions were freshly prepared with water first doubly distilled and then treated with a Millipore Milli Q system. In all cases, pH was maintained at 5.3 and temperature at 25 ^{o}C. Before and during the experiments, solutions were de-aerated with argon.

Electrochemical experiments were carried out in a conventional three-electrode cell using an Autolab with PGSTAT30 equipment and GPES software. Working electrodes were vitreous carbon (Metrohm) of 0.0314 cm^2, plates of glass/sputtered Cr and silicon wafers with titanium/nickel (100/50 nm) seed layer. The vitreous carbon electrode was polished to a mirror finish by using alumina of different grades (3.75 and 1.87 μm) and ultrasonically cleaned for 2 min in water before each experiment. The other working electrodes were first cleaned with acetone and later with water. The counter electrode was a platinum spiral. The reference electrode was a Ag | AgCl | NaCl 1mol dm^{-3} mounted in a Luggin capillary containing 0.5 mol dm^{-3} Na_2SO_4 solution. All potentials are referred to this electrode

Voltammetric experiments were carried out at 50 mV s^{-1}, scanning at first to negative potentials. Only one cycle was run in each voltammetric experiment. All deposits were obtained under galvanostatic and stirring conditions (ω=60 rpm, magnetic stirrer).

The morphology of deposits was examined with a Hitachi S 2300 scanning electron microscope. Films composition was determined by means of an electron probe microanalysis (EPMA), performed on a cameca SX-50 electron microprobe. The microstructure of deposits was examined with a Philips CM-30 transmission electron microscope. The thickness of the deposits were measured using a Zeiss Axiovert 405 M Microscope or from a TEM image of the transversal section of the samples.

XRD analysis was performed on a Siemens D-500 diffractometer. The Cu-K_α radiation (λ=1.5418 Å) was selected by means of a diffracted-beam flat graphite monochromator crystal. Diffractograms were obtained with $^o2\theta$ ranging from 10° to 100° with a step size of 0.05^o and a measuring time of 5 s per step.

Magnetoresistance (MR) was measured by an alternating current four-point probe technique at 27 and 293 K in magnetic fields up to 11 kOe, wich was applied in the film plane and parallel to the current. The MR ratio was calculated as $\Delta R/R_0$, where $\Delta R = R(H)-R_0$ is the change in the electrical resistance due to the application of the magnetic field and R_0 is the maximum resistance at the coercive field.

Results and Discussion

1.-Electrochemical preparation of deposits

Figure 1 shows cyclic voltammograms corresponding to the chosen solution on different electrodes. In all cases, a small first current due to copper reduction was observed in the negative scan, followed by a greater current related to alloy deposition [12,13]. Simultaneous copper and cobalt deposition took place from around –1000 mV in all electrodes. Only one peak was detected in the anodic scan corresponding to alloy oxidation. The three electrodes studied presented similar behaviour, although the electrodes containing seed layers were less active than vitreous carbon substrate, due to their lower electrical conductance. The position of the oxidation peak was dependent on the cathodic limit used, revealing a variable alloy composition. Oxidation peak displacement from copper to cobalt oxidation position, as the lower potential limit is made more negative, reveals the increase of cobalt percentage in the deposit.

From voltammetric results, the potentials or current densities more suitable to induce alloy deposition were selected. Galvanostatic technique was chosen to prepare the coatings with easy control of the deposition charge. Figure 2 shows the galvanostatic curves of the deposition process at different current densities and fixed charge, for all

electrodes tested. In all cases, galvanostatic curves show the nucleation spike followed by stabilisation of the potential, which decreased as the current density was made more negative. For each electrode used, a relation between the applied current density, the stabilisation potential in the galvanostatic curve and the alloy composition was found. Figure 3 shows the stabilisation potential (E_{est}) and the cobalt percentage in the alloy for each current density applied for one of the electrodes used. A gradual increase of the cobalt percentage in the alloy was observed decreasing current density. The adjust of the applied current led to the preparation of Co-Cu films with a variable metal percentages. Similar qualitative behaviour was observed for the three types of electrodes used. However, for vitreous carbon substrate lower current densities were necessary to obtain similar cobalt percentages than using glass/Cr or Si/Ti-Ni electrodes.

Consequently, glass/Cr and Si/Ti-Ni substrates were chosen to prepare Co-Cu films to test their magnetoresistive behaviour, although lower adherence of the films was observed on glass/Cr substrates. The low conductance of these electrodes allows us to measure directly the MR value without separating the films from the electrode. To prepare the films, moderate current densities (between –2 and –5 mA cm^{-2}) were used to avoid the simultaneous hydrogen evolution and assure a high efficiency of the process. Current densities less negatives than –2 mA cm^{-2} led to quasi pure copper deposits. Deposition charge was maintained at about 5 C cm^{-2} to prepare films of 1-2 μm thickness. The coating thickness (*h*) was calculated from deposition charge, assuming high efficiency, and by using the expression:

$$h = \left(Q \cdot V\right) \frac{N_A}{2 \cdot F \cdot A} \qquad (1)$$

where Q is the deposition charge, V is the average atomic volumes in the fcc crystalline lattice, N_A is the Avogadro's number, F is the Faraday constant and A is the electrode area. The calculated h value was in agreement with experimental determinations of the coating thickness (±0.2 μm) revealing a high efficiency of the deposition process (Fig.4). A moderate stirring of the solution was maintained during

the deposition in order to avoid the depletion of the electroactive species towards the electrode. The analysis of the deposits obtained reveal that cobalt percentages ranged from 2 to 40% were obtained for the current densities applied.

The magnetoresistance of the as-deposited samples containing different cobalt percentages was measured both at room and low (27K) temperatures. The results are shown in Figure 5. The electrodeposited films for a cobalt percentage between 10 and 25% display a moderate negative MR signal, which was below -2% when MR was measured at low temperature under magnetic fields up to 11 kOe. However, for samples with cobalt percentages higher than around 30%, a strong decrease of the MR signal was observed and even positive MR values were measured at low applied fields. These results were in agreement to those reported for other granular films grown by sputtering of similar compositions [14]. At these cobalt percentages, the weak ferromagnetism due to the cobalt content alloyed with the copper matrix yields an anisotropic magnetoresistance (AMR), which is dominant at low applied fields and gives a positive contribution. At high applied fields, AMR saturates and its contribution is overcome by the negative MR coming from the Co-rich particles, but being the absolute value of the MR signals much lower than those values corresponding to Co contents below 25% Co.

2.-Annealing of the samples

A study of the effect of the annealing treatment on the samples was carried out. The effect of the annealing temperatures and times on the morphology, structure and transport properties of the Co-Cu films was analysed. Samples with cobalt percentages ranging from 5 and 25% were studied as they presented an appreciable negative MR value before annealing.

Figure 6 shows the effect of annealing treatment on the MR value of two samples with different cobalt percentage and obtained with different type of electrode. A clear increase of the MR value with the annealing was shown, especially in the low temperature measurements. In both cases, the coatings presented giant

magnetoresistance. Electrodeposition and posterior annealing have demonstrated to be a good method of preparation of Co-Cu magnetoresistive films.

In table I, it is reported the maximum MR value at 11 kOe for 20% Co as a function of the annealing time at a fixed annealing temperature of 450 ºC. MR increases with the annealing time reaching an almost constant value for annealing times longer or equal than 30 minutes. Consequently, 30 minutes has been selected as an appropriate value of the annealing time to enhance the magnetoresistive behaviour of the as-deposited samples. A further study of the influence of the annealing temperature on the MR properties of samples with different Co content was carried out. The results for two compositions, 10% Co and 20% Co, are shown in Table II. The MR values at 11 kOe for both compositions increased with the annealing temperature, reaching a maximum between 6% and 8% at low temperature for an optimal annealing temperature, which depends on the composition (450 ºC for 10% Co and 550 ºC for 20% Co). A further increase of the annealing temperature produced a progressive reduction of the MR

The changes on the MR signal reported in Tables I and II can be understood by analysing the structural evolution of the electrodeposited samples, caused by the annealing process.

Figure 7 shows SEM micrographs obtained for as-deposited and annealed samples containing 13% of Co. The SEM micrograph for the as-deposited sample (Fig. 7A) showed a homogeneous nodular deposit with a grain size of about 0.9 μm. After annealing of these samples during 30 minutes, a clear decrease of the grain size was observed (Fig. 7, B and C), which was more pronounced at high annealing temperatures. Besides, a more structured deposit was obtained after annealing at 550 ^{o}C (Fig. 7C), which might indicate the segregation of Co-rich regions within the Cu matrix.

The study of the structural evolution due to annealing processes was complemented by means of X-ray diffraction and bright field TEM. Figure 8 shows the XRD

obtained for 22% Co samples prepared over silicon/seed layer substrate. All diffractograms for as-deposited samples showed two peaks related to the substrate response: a small peak at 44.5 $^{o}2\theta$ corresponding to Ni seed layer and a broad peak at around 69 $^{o}2\theta$ corresponding to silicon. The rest of the peaks corresponds to a fcc structure of the Co-Cu film and were located at diffraction angles between the lines corresponding to pure fcc copper and cobalt. The position of the Co-Cu diffraction peaks leads to a 21% Co accordingly to Vegard's law, corroborating the analysis obtained by EPMA. When samples were annealed, higher and narrower peaks developed, this effect being more pronounced as the annealing temperature increased, likely as a consequence of the formation of larger crystals. The position of the main diffraction peaks, which can be attributed to the Co-Cu matrix, was slightly shifted from that of pure cobalt. This effect may be due to the existence of some degree of alloying of cobalt with the copper matrix, even in the Co-rich regions. However, no clear shoulders associated with cobalt segregation were detected in diffraction peaks for the annealed samples.

Electron diffraction patterns confirmed the fcc structure. The as-deposited films showed diffuse diffraction rings, whereas in the annealed films, the rings were better defined (Fig. 9) as a consequence of a higher degree of crystallinity.

The bright field TEM images of the as-deposited samples show crystallites with a distribution of sizes, in the range 10-20 nm (Fig. 10 A). Crystallographic contrast is strongly related to the local atomic number. For the system under investigation light regions are expected to be Cu-rich ones, while dark regions correspond to Co-rich areas, although the latter can not be attributed only to pure cobalt. An increase of the crystal sizes and the contrast between the dark and the light regions is clearly observed after annealing, which is more pronounced as the annealing temperature is increased (Fig. 10 B, C). Besides, the definition of the grain boundaries was also enhanced with the annealing temperature.

Consequently, the results of the structural analysis suggest the segregation through annealing of Co-rich regions within the Co-Cu matrix, which are responsible for the

increase in the negative MR signal reported in Tables I and II. As annealing temperature is risen, the size of these regions increases reaching a critical value, for which the incipient magnetic correlations among Co grains start to reduce the MR response. The increase in the size of the Co-rich grains through annealing is also evidenced in the MR curves measured as a function of the magnetic field which is depicted in Figure 6 for two samples with different cobalt percentage and obtained with different type of electrodes. In both cases and after annealing, the magnetic hardness decreases and, the coercive field and the MR signal increase, which also confirms the existence of larger Co-rich grains in the annealed samples with respect to those present in the as-deposited films.

Conclusions

A citrate-sulphate bath in boric acid leads to prepare Co-Cu electrodeposits with variable composition as a function of the applied current density. Similar electrodeposits are obtained over different type of substrates, although depending on the substrate activity, different current densities must be applied in each case to obtain similar alloy compositions. Si-seed layer substrate is an adequate electrode to prepare the alloy films due to the good adherence of the deposited films. Moreover, the low conductivity of the seed layer allows us to measure directly the magnetoresistance of the Co-Cu films.

Uniform and coarse-grained deposits are obtained, presenting low values of MR when measures are made at low temperature. Annealing of the samples causes an increase of the size of the Co-rich grains, an increase of the crystal size and consequently a clear increase of the magnetoresistance. Giant magnetoresistance, with values around 6-8%, at 11 kOe and 27 K is observed for annealed samples containing 8-25% Co. Samples with higher cobalt percentages show zero or even positive magnetoresistance at low fields due to the AMR contribution associated with the formation of a weakly ferromagnetic matrix. The optimal annealing temperature varies as a function of the cobalt percentage in the film.

Acknowledgements

The authors wish to thank the *Serveis Cientificotècnics* (*Universitat de Barcelona*) for providing equipment. This research was supported financially by contracts MAT 2000-0986 and MAT 2000-0858 from the Spanish *Comisión Interministerial de Ciencia y Tecnología* (CICYT) and by the *Comissionat* of the *Generalitat de Catalunya* under Research Project SGR 2000-017.

References

1.-A.E. Berkowitz, J.R. Mitchell, M.J. Carey, A.P Young, S. Zhang , F.E. Spada, F.T. Parker, A. Huttem and G. Thomas, *Phys. Rev. Lett*.,**68**, 3745 (1992).

2.- J.Q. Xiao, J.S. Jiang and C.L. Chien, *Phys. Rev. Lett*., **68**, 3749 (1992).

3.- R.P. Setna, A. Cerezo, J.M. Hyde and G.D.W. Smith, *Appl. Surf. Sci*., **76/77**, 203 (1994).

4.- V.M. Fedosyuk, O.I. Kasyutich, D. Ravinder and H.J. Blythe, *J. Magn. Magn. Mater.* **156**, 345 (1996).

5.- W. Schwarzacher and D.S. Lashmore, *IEEE Trans. Magn*., **32**, 3133 (1996).

6.- M. Tsunoda, K. Okuyama, M. Ooba and M. Takahashi, *J. Appl. Phys*., **83**, 7004 (1998).

7.- H. Zaman, A. Yamada, H. Fukuda and Y. Ueda, *J. Electrochem. Soc*., **145**, 565 (1998).

8.- A.D.C. Viegas, J. Geshev, J.E. Schmidt and E.F. Ferrari, *J. Appl. Phys*., **83**, 565 (1998).

9.- G.N. Kakazei, A.F. Krovetz, N.A. Lesnik, M.M. Pereira de Azevedo, Yu.G. Pogorelov, G.V. Bondorkova, V.L. Silantiev and J.B. Sousa, *J. Magn. Magn. Mater*., **196**, 29 (1999).

10.- Y. Ueda, T. Houga, H. Zaman and A. Yamada, *J. Solid. State Chem*., **147**, 274 (1999).

11.- H.J. Blythe and V.M. Fedosyuk, *J. Magn. Magn. Mater*, **155**, 352 (1996).

12.- E. Gómez, A. Llorente and E. Vallés, *J. Electroanal. Chem*., **495**, 19 (2000).

13.- E. Gómez, A. Labarta, A. Llorente and E. Vallés, *J. Electroanal. Chem*., **517**, 63 (2001).

14.-V. Franco, X. Batlle and A. Labarta, *J. Appl. Phys*., **95**, 7328 (1999).

Table I.- Influence of the annealing time on the MR value. 20%Co. 1.8 μm. $T_{annealing}$ = 450 °C.

$t_{annealing}$ / min	MR (at 293K) / %	MR (at 27K) / %
0	-0.5	-1.0
15	-0.9	-2.0
30	-1.5	-4.6
60	-1.5	-4.6

Table II.- Influence of the annealing temperature on the MR value. 1.8 μm. $t_{annealing}$ = 30 min.

10% Co	$T_{annealing}$ / ^{o}C	MR (at 293K) / %	MR (at 27K) / %
	as-deposited	-0.3	-1.5
	350	-0.4	-3,8
	400	-1.4	-5.4
	450	-1.0	-6.6
	550	-0.7	-3.6

20% Co	$T_{annealing}$ / ^{o}C	MR (at K) / %	MR (at K) / %
	as-deposited	-0.4	-1.0
	450	-1.5	-4.1
	500	-1.8	-5.3
	550	-2.5	-7.5
	600	-1.5	-4.2

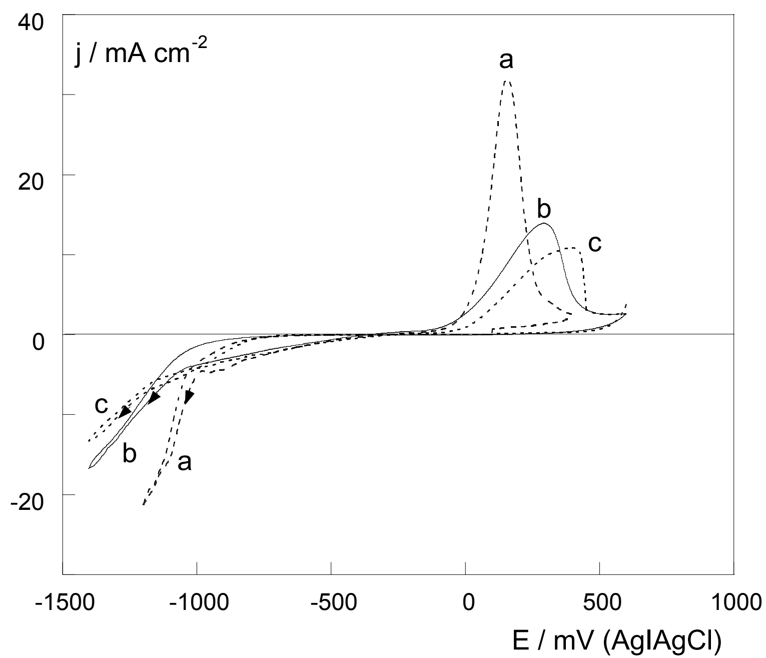

Figure 1.- Cyclic voltammograms recorded at 50 mV s^{-1} on different substrates: a) vitreous carbon, b) glass/Cr and c) Si/seed-layer.

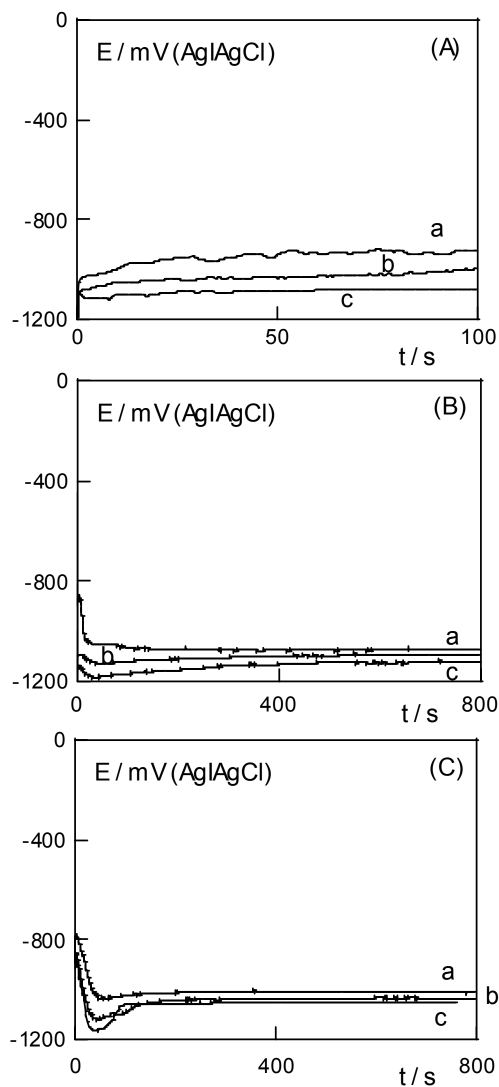

Figure 2.- Galvanostatic curves obtained over different substrates.

(A)- vitreous carbon. a) –4.8, b) –9.6 and c) –15.9 mA cm^{-2}.

(B)- glass/Cr. a) –4.2, b) –5.0 and c) –6.7 mA cm^{-2}.

(C)- Si/seed layer. a) –3.5, b) –3.7 and c) –5.0 mA cm^{-2}.

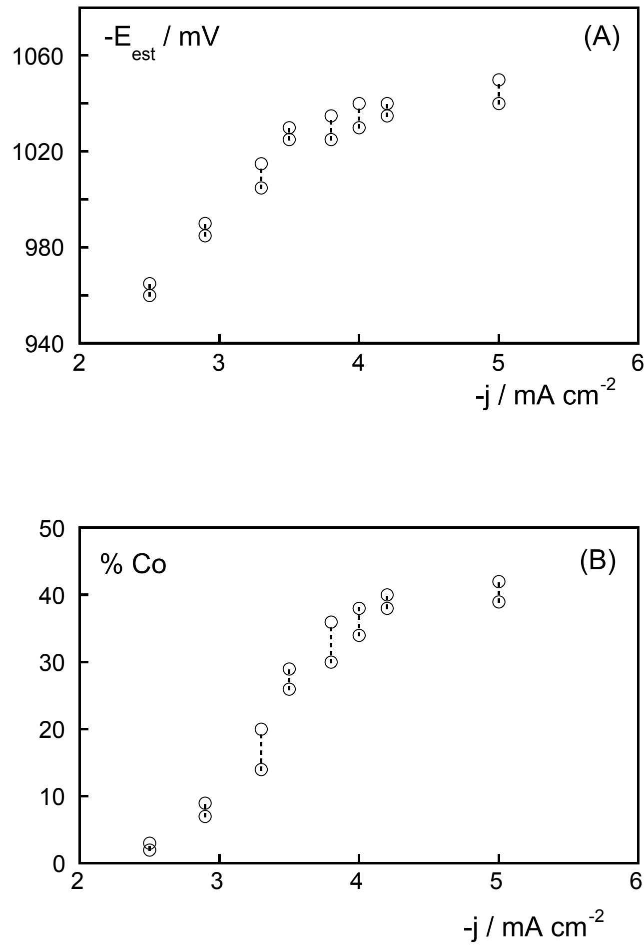

Figure 3.- Relation between the applied current density, the stabilization potential and the cobalt percentage in the deposits obtained over Si/seed layer.

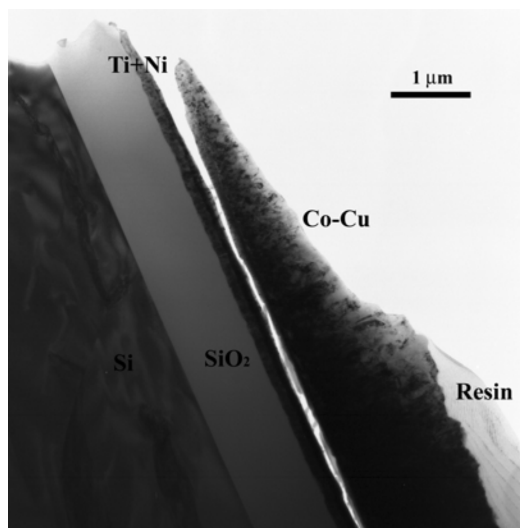

Figure 4.- Bright field TEM image of a transversal section of a deposit of 20% Co obtained over Si/ (Ti+Ni) electrode.
Measured thickness: 1.6 μm, theoretical thickness: 1.8 μm.

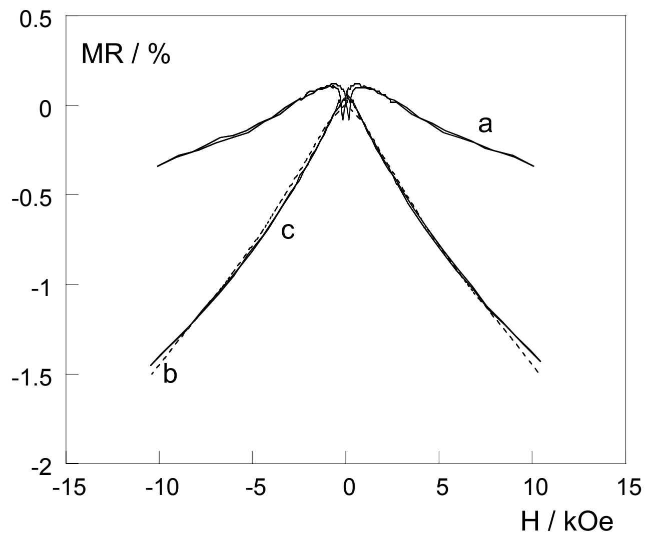

Figure 5.- ΔMR vs. in-plane applied field in parallel geometry at 27 K for Co-Cu deposits containing a) 30%, b) 21% and c) 11% Co.

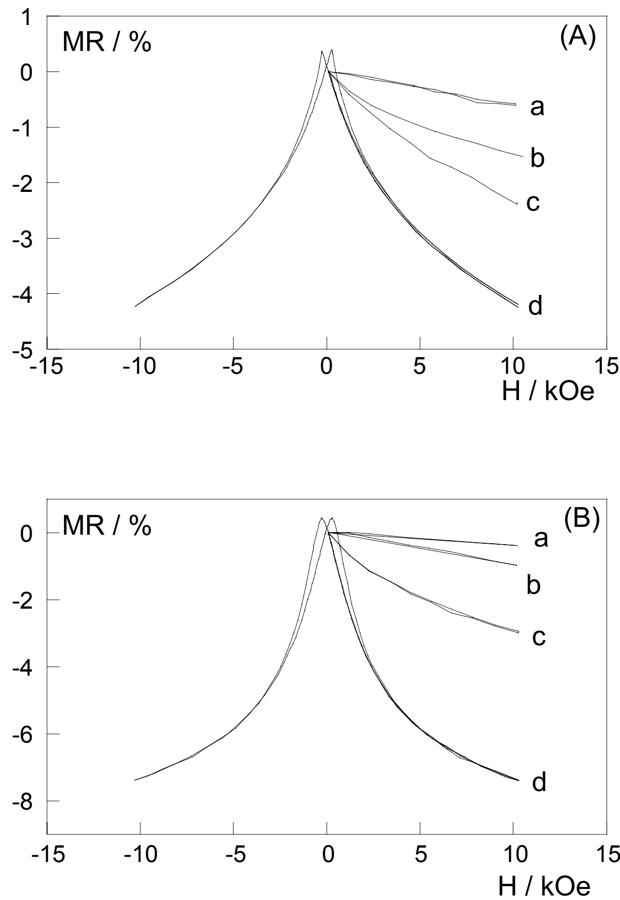

Figure 6.- ΔMR vs. in-plane applied field in parallel geometry.

(A).- Co-Cu films of 2 μm with 10% Co. glass/Cr electrode. a) as-deposited, room temperature, b) as-deposited, 27 K, c) annealed at 550 ^{o}C during 30 min, room temperature, d) annealed at 550 ^{o}C during 30 min, 27 K.

(B).- Co-Cu films of 1.8 μm with 21.5%. Si/seed layer electrode. a) as-deposited, room temperature, b) as-deposited, 27 K, c) annealed at 550 ^{o}C during 30 min, room temperature, d) annealed at 550 ^{o}C during 30 min, 27 K

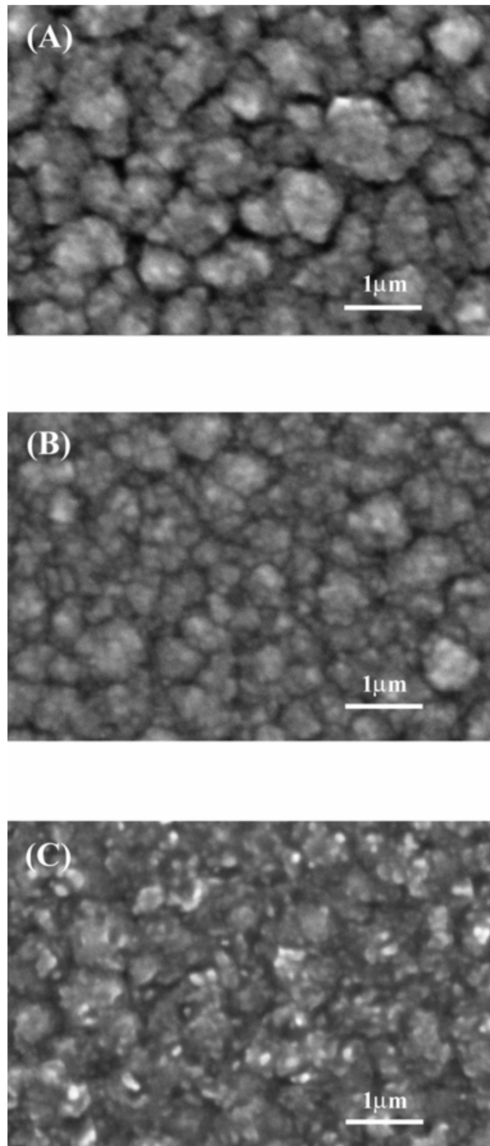

Figure 7.- SEM micrographs of Co-Cu films of 13.3% Co obtained over Si/seed layer electrode. (A).- as-deposited, b) after annealing at 350 ^oC during 30 min, c) after annealing at 550 ^oC during 30 min.

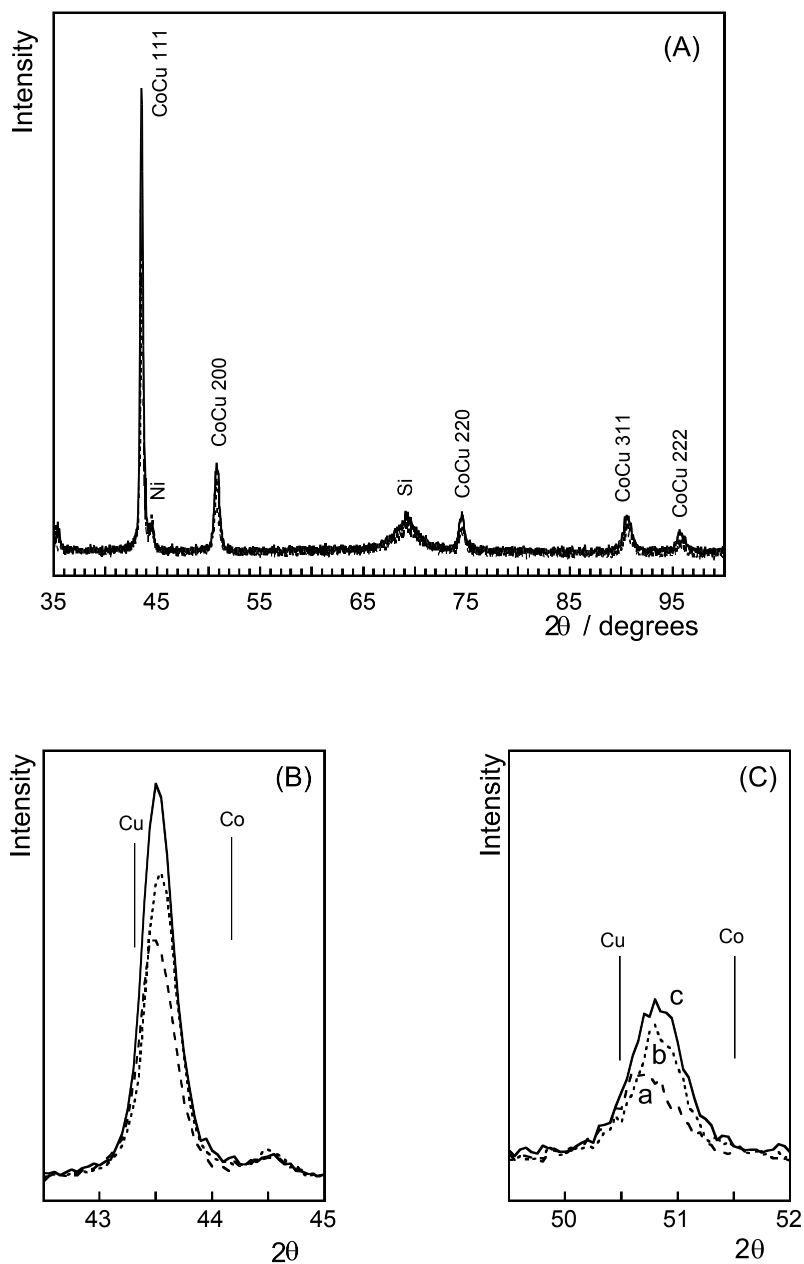

Figure 8.- X-ray diffractograms of a Co-Cu deposit of 22% Co obtained over Si/seed layer electrode. (A).- general diffractogram, (B) and (C) magnified details of two of the peaks. a) as-deposited sample, b) after annealing at 350 ^{o}C during 30 min, c) after annealing at 550 ^{o}C during 30 min.

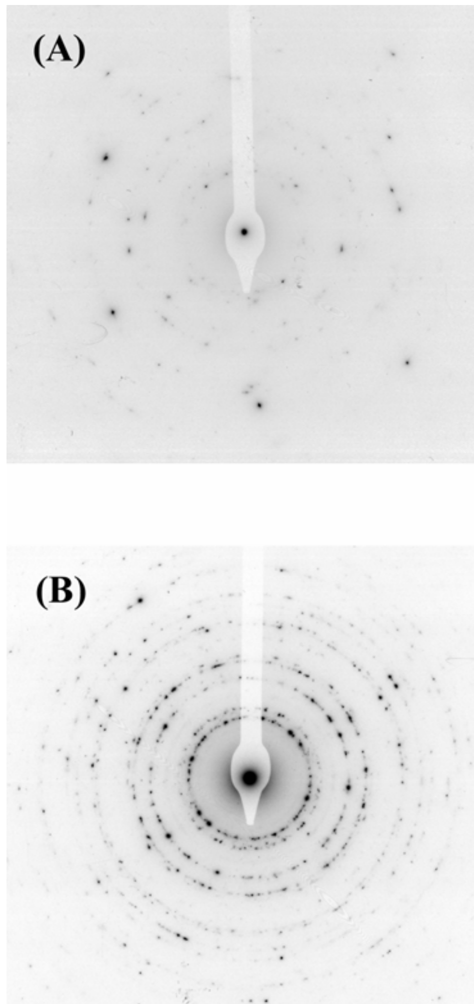

Figure 9.- TEM selected area diffraction pattern of of Co-Cu deposits of 18% Co obtained over Si/seed layer electrode.
(A).- as-deposited, (B) after annealing at 350 ^{o}C during 30 min.

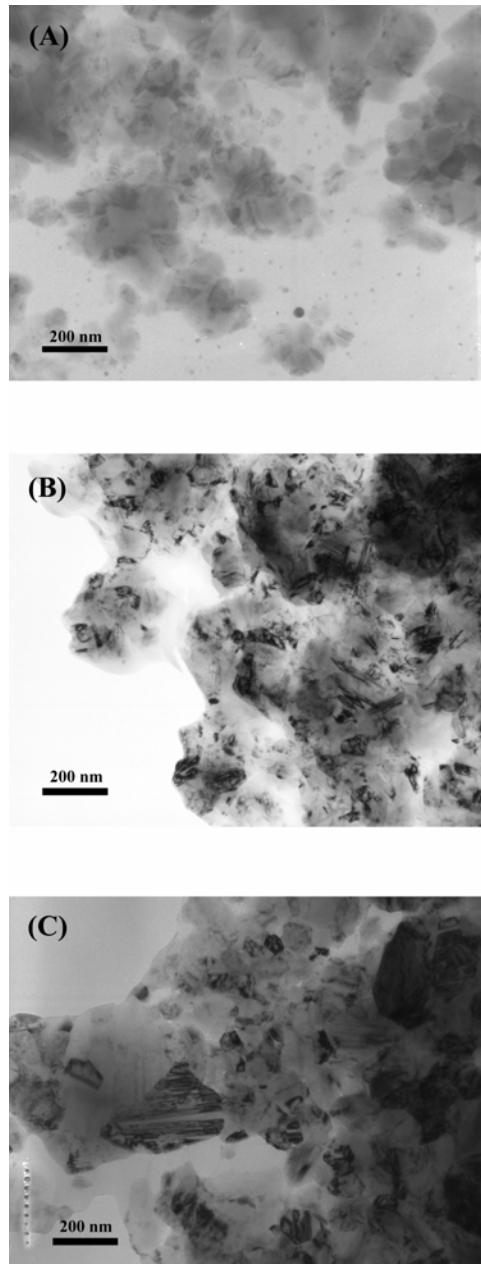

Figure 10.- Bright field TEM images of Co-Cu deposits of 18% Co obtained over Si/seed layer electrode. (A)-as-deposited, (B) after annealing at 350 ^{o}C during 30 min, (C) after annealing at 550 ^{o}C during 30 min.

4.4. Preparació i caracterització de multicapes de cobalt/coure electrodipositades

En aquests capítols s'han establert les condicions d'electrodeposició per a la preparació de multicapes de Co/Cu a partir d'una dissolució única, sobre diferents substrats en medi citrat, a pH de preparació (4.7) i a temperatura de 25ºC. S'ha analitzat la deposició d'aquests metalls a partir de dissolucions de $CuSO_4$ i $CoSO_4$, de concentració 0.7 mol dm^{-3} $CoSO_4$ i de 0.004 a 0.008 mol dm^{-3} $CuSO_4$, mantenint la concentració de citrat sòdic a 0.25 mol dm^{-3}.

S'ha realitzat un estudi previ del procés de deposició mitjançant voltametria cíclica per escollir els potencials mes adients per a preparar capes alternes d'ambdós metalls. Les multicapes Co/Cu s'han preparat mitjançant deposició per polsos de potencial, controlant la càrrega de les capes individuals. Es preveu la obtenció de multicapes de gruixos variables en funció de la relació de [Co(II)]/[Cu(II)] en solució, els potencials de deposició E_{Cu} i E_{Co} , i la duració dels polsos (t_{Cu} i t_{Co}.).

S'establirà el mètode de preparació per a la observació de les multicapes per SEM. S'intentarà establir un mètode que, a partir de les imatges de SEM i del càlcul de les càrregues de deposició, permeti predir els gruixos de les multicapes formades per les bicapes de menor gruix.

S'estudiarà la resposta de MR en la regió de camps baixos per ajudar a establir les condicions òptimes de preparació que assegurin la bona formació de les capes alternades. També s'estudiarà la dependència del senyal de MR amb els gruixos de les capes i el gruix total del dipòsit, a fi d'aconseguir el màxim valor de senyal de MR per a multicapes formades sota les condicions estudiades.

Es testaran les possibilitats de diferents mètodes de caracterització (TEM, XRD, TMAFM) per obtenir informació sobre les multicapes formades. Es provarà de relacionar els resultats electroquímics (*stripping*) amb els resultats obtinguts a partir de les tècniques de caracterització.

Els resultats detallats d'aquest capítol s'inclouen en els següents articles:

-*Characterisation of cobalt / copper multilayers obtained by electrodeposition*

Surf. Coat. Technol. 153 (2002) 261

-*Electrochemical behaviour and physical properties of Cu/Co multilayers*

Electrochim. Acta 48 (2003) 1005

ELSEVIER

Surface and Coatings Technology 153 (2002) 261–266

SURFACE & COATINGS TECHNOLOGY

www.elsevier.com/locate/surfcoat

Characterisation of cobalt/copper multilayers obtained by electrodeposition

E. Gómez[a], A. Labarta[b], A. Llorente[a], E. Vallés[a,*]

[a]Laboratori de Ciència i Tecnologia Electroquimica dels Materials (LCTEM), Departament Química Física, Facultat de Química, Universitat de Barcelona, Martí i Franquès, 1, 08028 Barcelona, Spain
[b]Departament Física Fonamental, Facultat de Física, Universitat de Barcelona, Martí i Franquès, 1, 08028 Barcelona, Spain

Received 1 August 2001; accepted in revised form 21 November 2001

Abstract

Electrodeposition of Co/Cu compositionally modulated multilayers was studied, using a single bath under potentiostatic conditions. The structure of the multilayers was characterised by scanning electron microscopy (SEM) and X-ray diffraction (XRD). Co/Cu multilayers with different sublayer thickness can be produced from a single bath as a function of different pulse potentials and deposition charges, avoiding cobalt oxidation at the start of each copper deposition. Copper sublayers are constituted of pure copper whereas 'cobalt' sublayers contain a low copper percentage ($\leq 2\%$). The multilayered Co/Cu deposits exhibit giant magnetoresistance when the thickness of the bilayers is approximately a few nanometers. © 2002 Elsevier Science B.V. All rights reserved.

Keywords: Plating; Multilayer; Scanning electron microscopy; X-Ray diffraction; Cobalt–copper; Giant magnetoresistance

1. Introduction

Materials known as composition modulated alloy (CMA) or multilayer films have been the subject of numerous recent studies since some multilayer coatings have improved physico-mechanical, optical, electrical, magnetic and magnetic-optic properties compared with traditional alloys. Such materials consist of alternate layers of different metals or alloys. The most common methods of multilayer preparation used is physical deposition, particularly by sputtering, and molecular beam epitaxy (MBE) [1–5]. Multilayer films, both of micrometric layers [6–9] and of nanometric layers [10–14] can also be prepared by electrodeposition. Electroplating offers the advantage of low cost production with respect to the deposition processes in gas phase, since electrodeposition requires only relatively simple and inexpensive processing equipment [15]. Moreover, electrodeposition is more suitable than vapour-phase deposition techniques for producing multilayers with a large area and arbitrary shape [16].

The interest in some of these multilayer systems is centred on their magnetoresistive properties. Magnetoresistance (MR) is the change in electrical resistance of a material in an applied magnetic field. Since the discovery of giant magnetoresistance (GMR), the largest magnetoresistance effect, in some metallic multilayer systems, investigation in magnetic multilayers has been greatly increased [17] due to their potential applicability to magnetoresistive sensor devices [18].

Magnetoresistance is very sensitive to the growth conditions and can be destroyed by intermixing magnetic and non-magnetic interfaces and also by poor crystalline quality of the layers. The aim of this study is both to investigate the electrodeposition from a single bath and to explore the characterisation methods of these multilayer systems. The interest was centred on obtaining Co/Cu alternate layers by means of electrodeposition. Different substrates were used in order to analyse both the influence of the substrates and the electrodeposition conditions on the structure of the multilayered systems formed. All substrates used for the multilayer preparation have a conductivity which hampers assessment of the magnetoresistance of the multilayers. For this reason,

*Corresponding author. Tel.: +34-93-4021324; fax: +34-93-402-1231.
E-mail address: e.valles@qf.ub.es (E. Vallés).

0257-8972/02/$ - see front matter © 2002 Elsevier Science B.V. All rights reserved.
PII: S0257-8972(01)01698-X

a seed layer of indium tin oxide (ITO) was selected as a less conducting electrode, since it allows magnetoresistance measurements to be carried out directly over the electrodeposited multilayers.

From the Co–Cu equilibrium phase diagram, it can be seen that cobalt and copper present inmiscibility and do not form any intermetallic compound, taking advantage of its very limited interdifussion.

2. Experimental

Chemicals used were $CuSO_4 \cdot 5H_2O$, $CoSO_4 \cdot 7H_2O$ and sodium citrate ($Na_3C_6H_5O_7 \cdot 2H_2O$). All solutions were freshly prepared with water first doubly distilled and then treated with a Millipore Milli Q system. The composition of the electrolyte is as follows: 0.25 mol dm^{-3} sodium citrate, 0.7 mol dm^{-3} $CoSO_4$ and a concentration of $CuSO_4$ which ranged between 0.004 and 0.008 mol dm^{-3}. Citrate medium was used to maintain the solution pH (which was found to be close to 4.7), in order to minimise hydrogen evolution during the deposition and also for its levelling action [19]. Before and during the experiments, solutions were deaerated with argon. Deposition was performed at 25 °C.

Electrochemical experiments were carried out in a conventional three-electrode cell using an EG&G 273 potentiostat/galvanostat controlled by a microcomputer. Multilayers were prepared using an analogue system Belport 105 potentiostat together with a EG&G 175 signal generator.

Different electrodes were used depending on the preparation or characterisation experiments: vitreous carbon (Metrohm) and copper (John Matthey 99.99%) were in the form of rods 2 mm in diameter; glass plates of 0.27 cm^2 covered with a gold layer of 200 nm obtained by sputtering and ITO thin films sputtered on glass plates (thickness of ITO layer = 25 nm and area = 0.2 cm^2). Vitreous carbon electrode was polished to a mirror finish using alumina of different grades (3.75 and 1.87 μm) and cleaned ultrasonically for 2 min in water. The copper electrode was polished to a mirror finish before each experiment using paper of 4000 grade and alumina (0.3 and 0.05 μm) suspended in distilled water and cleaned ultrasonically for 2 min in water. ITO electrodes were firstly cleaned with acetone and then with water. The counter electrode was a platinum spiral. The reference electrode was an Ag|AgCl|NaCl 1 mol dm^{-3} mounted in a Luggin capillary containing 0.5 mol dm^{-3} Na_2SO_4 solution. All potentials are referred to this electrode.

Voltammetric experiments were carried out at 10 mV s^{-1}, scanning at first to negative potentials. Only one cycle was run in each voltammetric experiment. Multilayers were attempted by a potentiostatic pulse electrolysis, with a moderate stirring of solution using argon flow.

The morphology of multilayers was examined with a Leica Cambridge Stereoscan S-360 scanning electron microscope. For SEM characterisation, the sample was cut slowly in order to avoid damage of multilayers and was then resin-encased in a mould. Polishing was initiated with papers of coarse grain (1000 and 2400 grade) just to the appearance of the multilayers cross-section. At this moment accurate manual polishing was necessary. Fine paper of 4000 grade was used prior to using alumina of 0.3 and 0.05 μm suspended in distilled water. The samples were washed in distilled water between each polishing step. An average of 3 h was necessary to obtain a sample which could be observed.

Elemental composition was determined using a Cameca SX-50 electron microprobe.

X-Ray diffraction (XRD) analysis was performed on a Siemens D-500 diffractometer. The CuKα radiation ($\lambda = 1.5406$ Å) monochromatiser was selected by means of a diffracted beam flat graphite crystal. $2\theta/\theta$ diffractograms were obtained in the range of $2\theta = 10–100°$ with a step range of $2\theta = 0.05°$ and a measuring time of 5 s per set, for general diffractograms. For detailed diffractograms, $2\theta = 30–100°$ with a step range of $2\theta = 0.02°$ and a measuring time of 7 s per set were used.

Magnetoresistance (MR) was measured by an alternating current four-point probe technique at 27 and 300 K in magnetic fields up to 11 kOe, applied parallel to the current.

3. Results and discussion

3.1. Electrodeposition

Co/Cu multilayers are grown by electrodeposition from a single electrolyte containing both Co(II) and Cu(II) ions under potentiostatic control. Due to the different ratio between the metallic components of the bath, moderate stirring of the solution was used in order to maintain the contribution of copper towards the electrode. As copper is one of the most noble metals it only requires a small negative potential for reduction to occur, whereas cobalt requires a more negative potential. For the multilayer growth a E_{Cu} potential was firstly applied, during a time t_{Cu} to deposit the Cu layer followed by a shorter period t_{Co} at potential E_{Co} to grow the Co layer. This Co/Cu cycle is repeated during some minutes for the multilayer growth (Fig. 1).

In order to select the deposition potentials adequate to prepare good alternate layers of cobalt and copper, a previous voltammetric study at low scan rate was made, using vitreous carbon electrode. Fig. 2 shows the voltammetric curve for [Co(II)]/[Cu(II)] = 175 ratio in solution. For all voltammetric curves, the sharp change in current density during the negative scan is related to the start of the cobalt deposition process, previously to this, only copper was deposited. As the [Co(II)]/

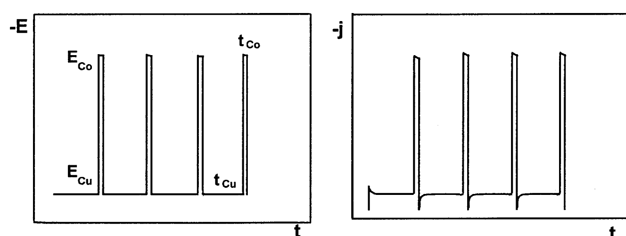

Fig. 1. Applied potential and current density response for potential pulses from E_{Cu} (during a time t_{Cu}) to E_{Co} (during a time t_{Co}).

[Cu(II)] ratio in solution is decreased, the rate of copper deposition becomes greater at low potentials, where cobalt does not deposit, agreeing with the higher copper concentration in solution.

For all [Co(II)]/[Cu(II)] ratios in solution studied, when the negative-proceeding scan is reversed previous to the beginning of cobalt deposition only one main oxidation peak is recorded (Fig. 2a). Reversing the scan at more negative potentials, a more cathodic peak appeared corresponding to cobalt oxidation (Fig. 2b).

Using different substrata, the general trends observed in the voltammetric curves were similar. However, for a fixed solution composition, the observed reduction of current density (j) from the same potential was: metal, vitreous carbon > glass/gold > glass/ITO substrates, indicating that different deposition rate is attained to the different analysed electrodes.

According to the voltammetric results, the potentials at which copper and cobalt will be deposited are selected. E_{Cu} is a potential for which pure Cu layer is formed and the deposition rate is sufficiently low to favour the formation of non-dendritic deposits. Moreover, the E_{Cu} is chosen such that no or very low oxidation of the cobalt layers occurs at the start of the deposition of each copper layer. The E_{Co} is held at a value at which cobalt is predominantly deposited, although a small copper percentage is detected in these layers ($\leq 2\%$). Small negative potential values were used in order to minimise simultaneous hydrogen evolution.

Upon varying conditions such as metal concentration, applied potential and step deposition time, it was possible to attain multilayers of variable thickness.

3.2. SEM characterisation

For scanning electron microscopy (SEM) observations, different Co/Cu multilayers were grown over different electrodes. The first requirement for successful imaging is to deposit on low roughness substrates, since imperfections extend to the multilayer system. However, as multilayer observation requires cross-section imaging, experience has demonstrated that better results are obtained after polishing when the mechanical properties of both the substrate and the multilayers are similar. Gold seed layer results are very soft and during the polishing step become deformed and cover the multilayer, hindering observation. Also, depending upon the type of glass used for supporting the seed layer, the different hardness of the substrate and the multilayers becomes a problem, as hard particles of glass might scratch the multilayers during polishing. A copper substrate offers similar hardness to the multilayers and improves its adherence to the substrate, being a suitable substrate for SEM observation.

After multilayer deposition a sheath of pure copper was electrodeposited so that the multilayers were protected between bulk copper. Copper deposition over the multilayers up to a thickness of 10 μm was induced galvanostatically at very low current density, from a $CuSO_4$ 0.2 mol dm^{-3} + H_2SO_4 0.5 mol dm^{-3} solution.

SEM micrographs (Fig. 3) show that a Co/Cu multilayered structure has been prepared. The electron micrographs show the formation of metallic layers parallel to the substrate, although the increase of the deposition time promotes the development of a roughness surface increase. As can be seen from the multilayer images, the bilayer thickness is 180–200 nm, whereas the bilayer thickness (h_b) calculated from deposition charges of cobalt and copper is approximately 195 nm suggesting 100% efficiency, not very different to the observed value. The bilayer thickness was calculated by means of Eq. (1) in which the small copper percentage in the cobalt layer was not considered:

$$h_b = (Q_{Cu}V_{Cu} + Q_{Co}V_{Co})\frac{N_A}{2FA} \quad (1)$$

where Q_{Cu} and Q_{Co} are the deposition charges corre-

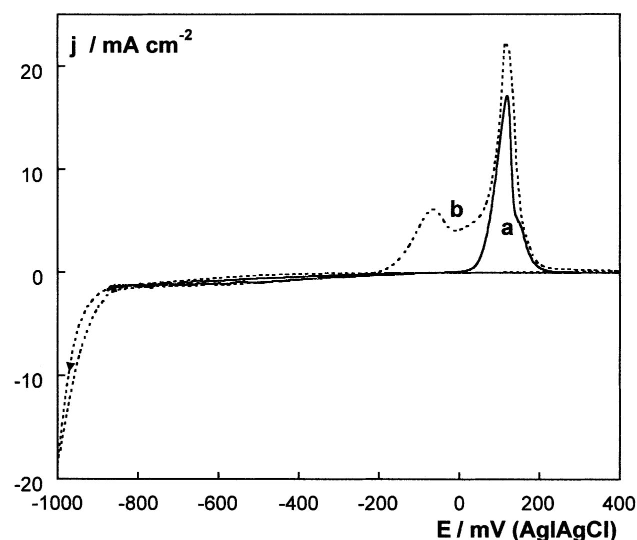

Fig. 2. Cyclic voltammograms of a 0.7 mol dm^{-3} $CoSO_4$ + 0.008 mol dm^{-3} $CuSO_4$ + 0.25 mol dm^{-3} $Na_3C_6H_5O_7$ solution, 10 mV s^{-1}. Vitreous carbon electrode. Starting potential: 0.1 V. Cathodic limit: (a) −0.9 V, (b) −1.0 V.

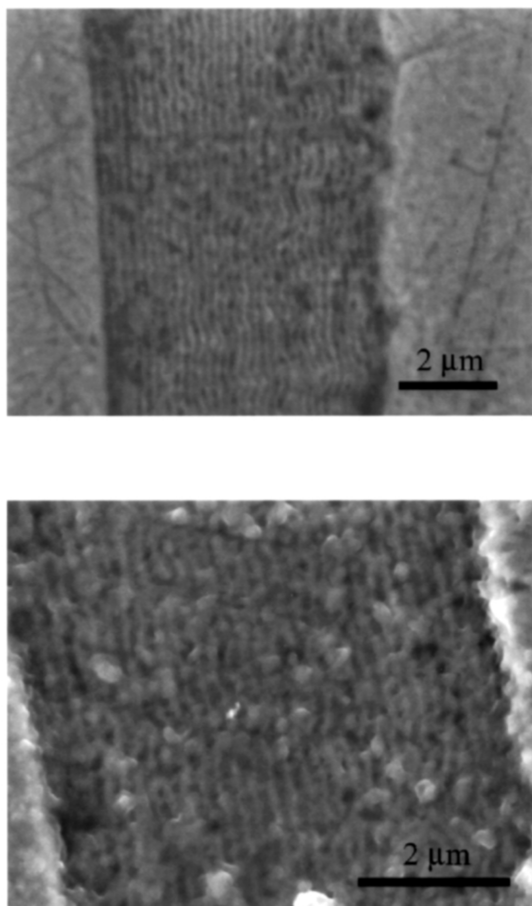

Fig. 3. SEM micrographs of the Co/Cu multilayers obtained by pulses at $E_{Cu} = -450$ mV, $t_{Cu} = 55$ s, $E_{Co} = -1172$ mV, $t_{Co} = 5$ s, from a 0.7 mol dm^{-3} $CoSO_4$ + 0.004 mol dm^{-3} $CuSO_4$ + 0.25 mol dm^{-3} $Na_3C_6H_5O_7$ solution. Copper electrode.

sponding to one layer of copper and cobalt, respectively, V_{Cu} and V_{Co} are the atomic volumes in the crystalline lattice, N_A is the Avogadro's number, F is the Faraday constant and A is the electrode area.

Therefore, the calculus can be used to estimate the thickness of the thinner bilayers by assuming that deposition took place at high current efficiency and when no cobalt oxidation was observed. The growth of the multilayers was shown to be dependant on the deposition potentials and its corresponding deposition times.

3.3. XRD characterisation

For the structural characterisation of $[Co(x)/Cu(y)]_n$ multilayers (x and y being the Co and Cu layer thickness in nanometers, respectively, and n the total number of bilayers) using XRD, glass/gold substrates were used. Gold showed a non-overlapping XRD response with cobalt or copper. Fig. 4 shows the XRD pattern from $[Co(18)/Cu(9)]_{60}$. Next to the peaks corresponding to the gold substrate, four well-defined main peaks are observed, corresponding to the coating response at approximately 44, 51, 75 and 91 2θ°, indicating good crystallisation structure. All indexed peaks correspond to a fcc structure and appear at diffraction angles between the lines corresponding to electrodeposited fcc copper and fcc cobalt. Similar results have been found for NiFe/Cu multilayers [20]. For the multilayered coating of Fig. 4, the adjustment of the cell parameters led to an 'a' value of 0.357 nm, intermediate between the parameter of fcc copper (0.361 nm) and fcc cobalt (0.354 nm). Upon varying the layer thickness ratio (x/y), the position of the diffraction peaks clearly moved. This diffraction response is similar to that obtained when the formation of Co–Cu solid solution with variable copper percentage in the deposits takes place [21,22]. The relative position of the diffraction peaks with respect to the pure copper and pure cobalt positions, lead to estimation of the cobalt content in the coatings.

The comparison of the diffractograms of multilayers of different bilayer thickness obtained at fixed E_{Co}, E_{Cu} and t_{Co}/t_{Cu} ratio, maintaining the total deposition time might show two different responses: when E_{Cu} was selected in the manner that no cobalt oxidation was detected at the start of copper deposition, a similar position of the diffraction peaks was observed for all the samples studied. However, a shift in the peaks was detected (Fig. 5) when some cobalt oxidation was observed in the current–time profiles, revealing a variation of the x/y ratio. On decreasing the bilayer thickness, the cobalt content gradually decreased, revealing a lower Co/Cu ratio when the number of bilayers increased, due to the increased number of cobalt oxidations.

No clear satellite peaks are detected to calculate the superlattice period.

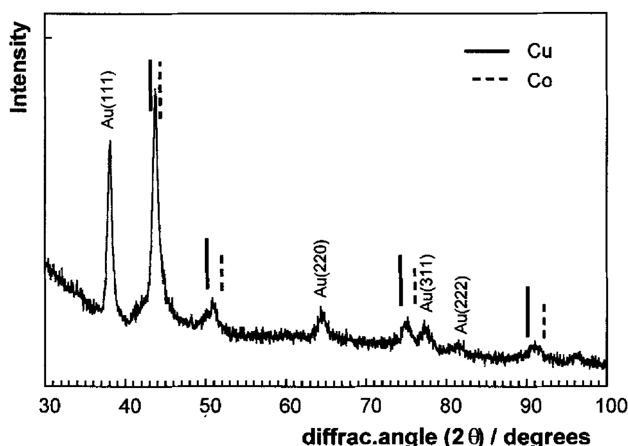

Fig. 4. X-Ray diffractogram of $[Co(18\ nm)/Cu(9\ nm)]_{60}$ multilayers obtained from a 0.008 mol dm^{-3} $CuSO_4$ + 0.7 mol dm^{-3} $CoSO_4$ + 0.25 mol dm^{-3} $Na_3C_6H_5O_7$ solution glass/gold electrode.

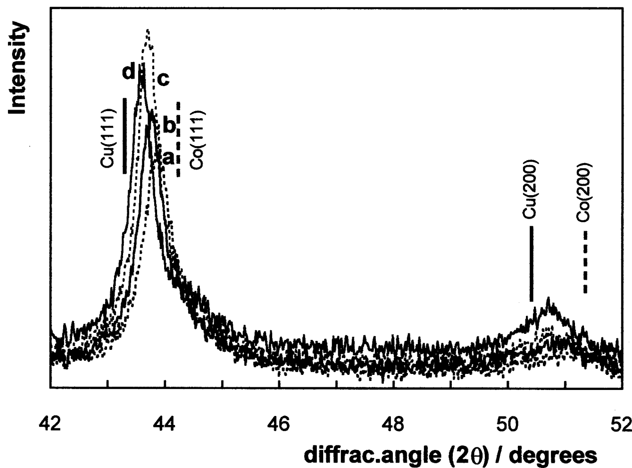

Fig. 5. Detail, between 42 and 52 2θ°, of X-ray diffractograms obtained from the same solution of Fig. 4 at E_{Cu} at which cobalt oxidation occurs. $E_{Cu} = -450$ mV, $E_{Co} = -1125$ mV. $t_{Cu}/t_{Co} = 11$. (a) $t_{Cu} = 22$ s, (b) $t_{Cu} = 11$ s, (c) $t_{Cu} = 5.5$ s, (d) $t_{Cu} = 2.2$ s. Total deposition time: 30 min.

3.4. Magnetoresistance

The MR ratio was calculated as $\Delta R/R_0$, where $\Delta R = R(H) - R_0$ is the change in the electrical resistance due to the application of the field H and R_0 is the maximum resistance at the coercive field.

The thickness of the copper layer has been found to be an important parameter which strongly affects the MR response of the Co/Cu multilayers obtained. When it is larger than 4 nm very low values of MR have been observed at 27 K, the signal being non-measurable at room temperature. For instance, for $[Co(5)/Cu(4)]_{15}$ MR was -1.2% at 27 K. MR increases monotonously as the thickness of the copper layer decreases suggesting that the optimum value is well below 4 nm. For this reason, we have decided to study the effect of the cobalt layer thickness on MR signal by preparing a set of multilayers with fixed copper layer thickness of 1 nm, which is a reasonable thickness for which a continuous layer can be obtained. The total deposition time for all these samples was 10 min, which ensures that internal stresses and excessive roughness do not appear.

In Fig. 6, it is shown the MR curves measured at 27 K for three samples of the form $[Co(x)/Cu(1)]_n$. All the curves display giant MR and irreversible behaviour in the low field region. Curves (a) and (b) show a coercive field of 300 Oe (which is in agreement with other values found in the literature for cobalt samples grown by electrodeposition [23,24]) with sharp peaks at H_c, which is indicative of the existence of continuous Co layers. However, curve (c) shows a coercive field of 200 Oe with rounded peaks at H_c, which could be explained in terms of the formation of Co isles of variable size. Therefore, for Co layer thicknesses above approximately 2 nm, the formation of continuous layers seems to be assured. However, for Co layer thicknesses less than approximately 1 nm, Co isles of variable size seem to be formed instead.

MR increases as the thickness of the Co layer decreases, -5.5% being the maximum value that was achieved for 1.3 nm. Further reduction of the thickness does not increase MR, indicating that probably below approximately 1 nm the continuity of the Co layer is lost.

It is worth noticing that although MR decreases with increasing temperatures, the measured value at room temperature is reduced only by a factor of two with respect to 27 K, in accordance with the expected reduction of the Co magnetisation in this range of temperatures.

4. Conclusions

In this paper, the preparation and characterisation of Co/Cu multilayers has been studied. Well-ordered multilayers have been prepared by pulse plating from a single bath upon different substrata. Although much work about the properties of multilayers is available in the bibliography, most of them take for granted the existence of well-ordered multilayers. Therefore, our interest was centred on the characterisation methods of these systems.

From SEM observation, bilayer thickness can be established, being similar to the theoretical value cal-

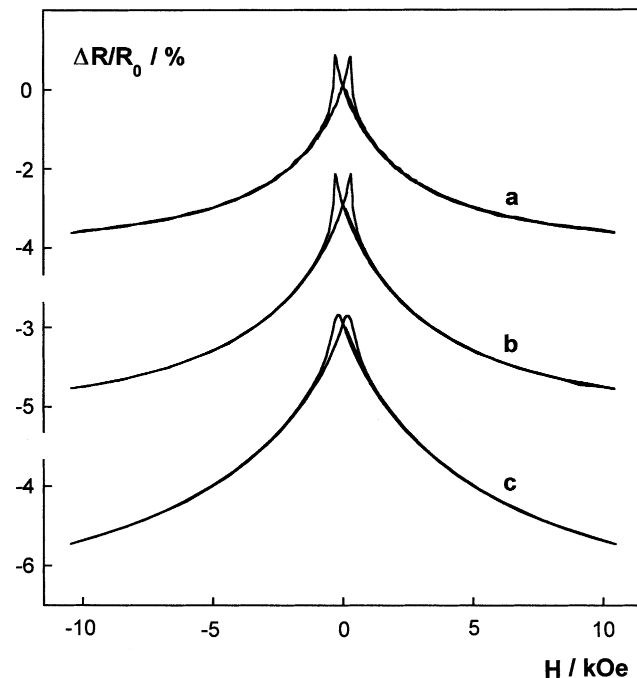

Fig. 6. $\Delta R/R_0$ vs. in-plane magnetic field applied parallel to the current at 27 K for a set of $[Co(x)/Cu(1)]_n$ multilayers being x: (a) 2.2, (b) 2.0 and (c) 1.3 nm.

culated from the deposition charges, although SEM observation becomes hard when reducing spacing thickness. However, the XRD technique can be an useful tool for controlling the adequate formation of multilayered systems of thin layers. The diffractograms obtained for different $[Co(x)/Cu(y)]_n$ multilayers with fixed layer thickness ratio (x/y) show invariant peak positions when high deposition efficiency and no cobalt oxidation during copper deposition takes place. However, when the diffraction peaks shift as the bilayer thickness are varied (for a theoretical fixed x/y ratio), it can inform us about the actual variable bilayer thickness ratio, due to non-desired processes as cobalt oxidation, hydrogen evolution or hydroxide formation.

Previous results [21,22] showed that electrodeposited Co–Cu alloy forms a fcc solid solution, for which is possible to estimate the composition by means of XRD position peaks (Vegard's law). The XRD response of multilayers of thin layer thickness is similar to that obtained from an homogeneous solid solution. Therefore, the analysis of the XRD results allows us to estimate the global cobalt content in the multilayer system using Vegard's law. It has been found that the cobalt percentages calculated from Vegard's law agree with the theoretical values obtained from the deposition charges. Therefore, by means of XRD analysis it is possible both to detect unexpected behaviour during the multilayer formation and to estimate the global cobalt content.

Electrodeposition in the bath tested allow us to obtain multilayered Co/Cu coatings displaying giant magnetoresistance both at low and room temperature. GMR values of approximately 5% are obtained when the thickness of copper and cobalt layers are 1 and 2 nm, respectively. MR increases as the cobalt layer thickness is reduced, however, below 1 nm MR does not further increase, probably indicating that the continuity of the Co layer is lost. The evolution of the coercive field with the thickness of the Co layer reinforces this conclusion.

Acknowledgments

The authors thank the Serveis Cientificotècnics (Universitat de Barcelona) for equipment availability. This research was supported financially by contract MAT 2000-0986 and MAT 2000-0858 of the Comisión Interministerial de Ciencia y Tecnología (CICYT) and by the Comissionat of the Generalitat de Catalunya under Research Project SGR 2000-017.

References

[1] M.P. Johansonn, N. Hellgren, T. Berlind, E. Broitman, J. Hultman, J.E. Sundgren, Thin Solid Films 360 (2000) 17.
[2] Y. Massiani, A. Medjahed, P. Gravier, J.P. Croussier, Thin Solid Films 217 (1992) 31.
[3] F. Hamelmann, S.H.A. Petri, A. Klipp, , et al., Thin Solid Films 338 (1999) 70.
[4] M.H. Kryder, Thin Solid Films 216 (1992) 174.
[5] X. Ming, Ch. Chai, G. Luo, T. Yang, Z. Mai, W. Lai, Thin Solid Films 375 (2000) 205.
[6] I. Kirilova, I. Ivanov, St. Rashkov, J. Appl. Electrochem. 28 (1998) 637–1359.
[7] J.D. Jensen, D.R. Gabe, G.D. Wilcox, Surf. Coat. Technol. 105 (1998) 240.
[8] G. Chawa, G.D. Wilcox, D.R. Gabe, Trans IMF 76 (1998) 117.
[9] M.R. Kalantary, G.D. Wilcox, D.R. Gabe, Br. Corrosion J. 33 (1998) 197.
[10] A.M. Herman, M. Mansour, V. Badri, , et al., Thin Solid Films 361/362 (2000) 74.
[11] A.A. Pasa, W. Schwarzacher, Phys. Stat. Sol. 173 (1999) 73.
[12] E. Toth Kadar, L. Peter, T. Becsei, W. Schwarzacher, J. Electrochem. Soc. 147 (2000) 3311.
[13] Y. Jyoko, S. Kashiwabara, Y. Hayashi, W. Schwarzacher, Electrochem. Solid Stat. Lett. 2 (1999) 67.
[14] Y. Ueda, T. Houga, H. Zaman, A. Yamada, J. Solid Stat. Chem. 147 (1999) 274.
[15] D. Landolt, Electrochim. Acta 39 (1994) 1075.
[16] M. Datta, D. Landolt, Electrochim. Acta 45 (2000) 2535.
[17] W. Schwarzacher, D.S. Lashmore, IEEE. Trans. Magn. 32 (1996) 3133.
[18] M. Suzuki, T. Ohwaki, Y. Taga, Thin Solid Films 304 (1997) 333.
[19] C. Bonhote, D. Landolt, J. Electrochim. Acta 42 (1997) 2407.
[20] E. Chassaing, P. Nallet, M.F. Trichet, J. Physique IV 6 (1996) C7–C13.
[21] H. Zaman, A. Yamada, H. Fukuda, Y. Ueda, J. Electrochem. Soc. 145 (1998) 565.
[22] E. Gómez, A. Llorente, E. Vallés, J. Electroanal. Chem. 495 (2000) 19.
[23] J.L. Bubendorff, E. Beaurepaire, C. Mény, P. Panissod, J.P. Bucher, Phys. Rev. B 56 (1997) R7120.
[24] L. Cagnon, T. Devolder, R. Cortes, , et al., Phys. Rev. B 63 (2001) 104419.

PERGAMON

Available online at www.sciencedirect.com
SCIENCE DIRECT®

Electrochimica Acta 48 (2003) 1005–1013

ELECTROCHIMICA Acta

www.elsevier.com/locate/electacta

Electrochemical behaviour and physical properties of Cu/Co multilayers

E. Gómez [a,1], A. Labarta [b], A. Llorente [a], E. Vallés [a,2,*]

[a] Laboratori de Ciència i Tecnologia Electroquímica dels Materials (LCTEM), Departament Química Física, Facultat de Química, Universitat de Barcelona, Martí i Franquès 1, 08028 Barcelona, Spain

[b] Departament Física Fonamental, Facultat de Física, Universitat de Barcelona, Martí i Franquès 1, 08028 Barcelona, Spain

Received 17 September 2002; received in revised form 2 December 2002

Abstract

Cobalt/copper multilayer formation was analysed over different substrates in order to control the bilayer thickness and quality of coatings. Using a sulphate–citrate bath, at pH 4.7, electrodeposition conditions were optimised to prepare good alternate Cu/Co layers with high efficiency, by minimising the oxidation of cobalt layers during copper deposition. For multilayers with cobalt and copper layers of several nanometers, direct observation by scanning electron microscopy (SEM) or tapping mode-atomic force microscopy (TMAFM) gives layer thickness in agreement with the value calculated from deposition charges. Therefore, this calculation has been used to estimate the thickness of the thinner layers for which direct observation was difficult or impossible. A relation between the response of different characterisation methods was found. When the thickness of each layer in Cu/Co multilayers is >1.8–2 nm, potentiodynamic stripping experiments show separate peaks related to cobalt and copper oxidation. In these conditions, magnetoresistance of the coating is low. For thinner layers, the stripping response shows overlapping peaks or even a single oxidation peak. In these conditions the magnetoresistance begin to increase.

© 2002 Elsevier Science Ltd. All rights reserved.

Keywords: Cobalt–copper; Multilayers; Electrodeposition; Stripping

1. Introduction

Multilayer materials have received increasing attention in recent years because of their special properties (mechanical, optical, electrical, magnetic) with respect to traditional alloys. In recent years electrodeposition has proved to be an alternative technique for preparing alternate micrometric [1–4] or nanometric layers [5–9]. In this line, Cu/Co multilayers present a great interest because of their possible transport properties [10–17] and several authors report their preparation from different baths [10,11,14,16,18,19]. A serious difficulty in electrodeposition multilayer preparation is to test when experimental deposition conditions lead to good alternate layers, especially when thin layers are desired. Scanning electron microscopy (SEM) and transmission electron microscopy (TEM) techniques have been used to characterise some electrodeposited multilayers [19–22] although a hard sample preparation is necessary in successful multilayer observation. However, the direct observation of bilayers of few nanometers is very difficult or not feasible by means SEM and TEM and, most of studies take the presence of well-ordered multilayers for granted.

The properties of multilayered systems depend on bilayer thickness, global thickness and good multilayer formation. Therefore, it is important to control the electrodeposition conditions that lead to good deposit formation and to measure the response of the multilayered system to different characterisation methods depending on the bilayer thickness of the coatings.

Our final interest will be the preparation of Cu/Co multilayers for their potential applicability in microsystems (MST). As different materials might be used as

* Corresponding author. Tel.: +34-93-402-1234; fax: +34-93-402-1231.

E-mail address: e.valles@qf.ub.es (E. Vallés).

[1] ISE member.

[2] ISE member.

0013-4686/02/$ - see front matter © 2002 Elsevier Science Ltd. All rights reserved.
doi:10.1016/S0013-4686(02)00814-9

components of the devices, several substrates were investigated. The first goal of the present work is to monitor, on different substrates, the conditions of electrodeposition that lead to the formation of good alternate Cu/Co layers with high efficiency, avoiding, the oxidation of the less noble metal (cobalt) during the deposition of the more noble metal (copper).

The second objective proposed was to relate the information provided by means of electrochemical methods (stripping analysis) with that obtained from physical characterisation techniques as SEM, TEM, X-ray diffraction (XRD), TMAFM and magnetoresistance measurements (MR) of the prepared coatings. In this way, the electrochemical analysis can be useful to predict the goodness of the multilayer formation and also useful to inform about the magnetoresistive behaviour.

2. Experimental

Chemicals used were $CuSO_4 \cdot 5H_2O$, $CoSO_4 \cdot 7H_2O$ and sodium citrate ($Na_3C_6H_5O_7 \cdot 2H_2O$), all of analytical grade. All solutions were freshly prepared with water first doubly distilled and then treated with a Millipore Milli Q system. The bath contained 0.7 mol dm^{-3} $CoSO_4$ and $CuSO_4$ ranging between 0.004 and 0.008 mol dm^{-3}. Citrate medium 0.25 mol dm^{-3} was added to each solution, maintaining the pH close to 4.7. Before and during the experiments, solutions were de-aerated with argon. Deposition was performed at 25 °C with stirring at 60 rpm.

Electrochemical experiments were carried out in a conventional three-electrode cell using both an EG&G 273 potentiostat/galvanostat controlled by a microcomputer and an Autolab with PGSTAT30 equipment and GPES software. Multilayers were prepared using an analogical system Belport 105 potentiostat together with a EG&G 175 signal generator and the Autolab PGSTAT30 equipment.

Different electrodes were used depending on the preparation or characterisation experiments: vitreous carbon rod (Metrohm), copper and nickel rods (John Matthey 99.99%), indium tin oxide (ITO) thin films sputtered on glass plates (thickness of ITO layer = 25 nm) and silicon wafers with titanium/nickel (100/50 nm) seed layers. Vitreous carbon electrode was polished to a mirror finish using alumina of different grades (3.75 and 1.87 μm) and cleaned ultrasonically for 2 min in water. Copper and nickel electrodes were polished to a mirror finish before each experiment using paper of 4000 grade and alumina (0.3 and 0.05 μm) suspended in distilled water and cleaned ultrasonically for 2 min in water. Glass/ITO and Si/seed layer electrodes were first cleaned with acetone and later with water. The counter electrode was a platinum spiral. The reference electrode was an Ag | AgCl | NaCl 1mol dm^{-3} mounted in a Luggin capillary containing 0.5 mol dm^{-3} Na_2SO_4 solution. All potentials refer to this electrode.

Voltammetric experiments were carried out at 10 mV s^{-1}, scanning at first to negative potentials. Only one cycle was run in each voltammetric experiment. Stripping analysis was always performed immediately after deposition. All potentiodynamic-stripping experiments were made at a scan rate of 10 mV s^{-1} and an initial potential at which deposition did not occur was chosen. Multilayers were attempted by potentiostatic pulse electrolysis.

SEM examined multilayers morphology with a Leica Cambridge Stereoscan S-360 scanning electron microscope. For a successful SEM observation it was necessary to follow an accurate sample preparation. The sample was cut slowly in order to avoid damage of multilayers and then was resin-encased in a mould. Polishing was initiated with papers of coarse grain (1000 and 2400 grade) until the multilayers cross-section appeared. At this point accurate manual polishing was necessary. Fine paper of 4000 grade was used prior to using alumina of 0.3 and 0.05 μm suspended in distilled water. The samples were washed in distilled water between each polishing step.

TMAFM studies were performed with a Multimode microscope stand controlled by Nanoscope III electronics, both from Digital Instruments. The cantilever probes were made on silicon and microfabricated by Nanosensors. For TMAFM observation of the multilayers, it was necessary, after performing the same sample preparation procedure of SEM characterisation, to attack one kind of layers selectively, in order to create a relief of the surface that allowed us to distinguish the individual layers. Selective chemical etching of copper was performed for 5 s in a Nital solution (HNO_3 65 wt.% solution in ethanol). The samples were washed in distilled water before TMAFM observation.

Microstructure was examined using a transmission electron microscope Philips CM-30. TEM-selected area diffraction was used.

Electron probe microanalysis (EPMA) was performed on a Cameca SX-50 electron microprobe. X-ray photoelectron spectroscopy (XPS) measurements were performed with a PHI 5600 multitechnique system and Auger spectroscopy measurements were done with a PHI 670 scanning Auger nanoprobe system.

XRD analysis was performed on a Siemens D-500 diffractometer. The Cu-K_α radiation ($\lambda = 1.5406$ Å) monochromatiser was selected by means of a diffracted beam flat graphite crystal. $2\theta/\theta$ diffractograms were obtained in the range of $2\theta = 10$ or 30–100° with a step range of $2\theta = 0.05°$ and a measuring time of 3 or 6 s per set.

Magnetoresistance was measured by an alternating current four-point probe technique at 27 and 300 K in

magnetic fields up to 11 kOe, applied parallel to the current.

3. Results and discussion

3.1. Voltammetric study

In order to select the deposition potentials adequate to prepare good alternate layers of cobalt and copper, a previous voltammetric study was made. For each selected electrode, a starting potential at which no current is detected was used. On all electrodes tested, similar behaviour was observed: For low cathodic limits, only copper was deposited and a single oxidation peak was detected (Fig. 1, curve a). It was necessary to decrease the negative limit to induce the start of the cobalt deposition process. The peak which appeared during the positive scan previous to copper oxidation corresponded to cobalt oxidation (Fig. 1, curve b).

Although the qualitative behaviour of the deposition process was similar on the different substrates, different deposition rates were attained from the different analysed electrodes. Both metallic substrates and vitreous carbon were more active than Si/seed-layer, glass/ITO being the less active substrate (Fig. 2).

3.2. Multilayers formation and stripping experiments

Multilayer preparation was performed using potentiostatic pulses ranging from a potential at which only copper deposited (E_{Cu}) to a potential at which mainly cobalt deposited (E_{Co}). A time t_{Cu} was applied to deposit the Cu layer followed by a much shorter period t_{Co} at potential E_{Co} to grow the Co layer. This Cu/Co cycle was repeated for some minutes to allow the desired multilayer growth.

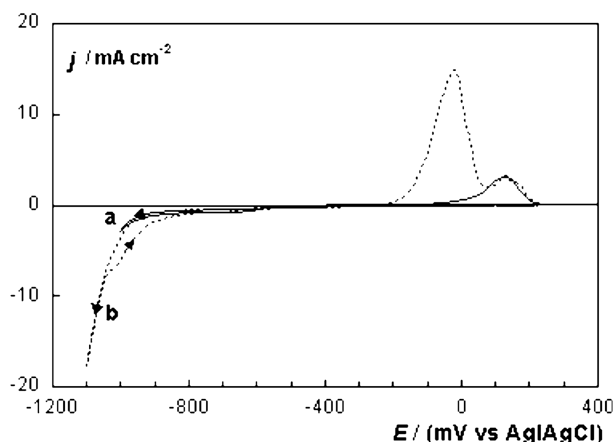

Fig. 1. Cyclic voltammograms of a 0.7 mol dm^{-3} $CoSO_4$+0.008 mol dm^{-3} $CuSO_4$+0.25 mol dm^{-3} $Na_3C_6H_5O_7$ solution. 10 mV s^{-1}. Si/seed layer electrode. Starting potential: −0.4 V. Cathodic limit: (a) −1.0 V, (b) −1.1 V.

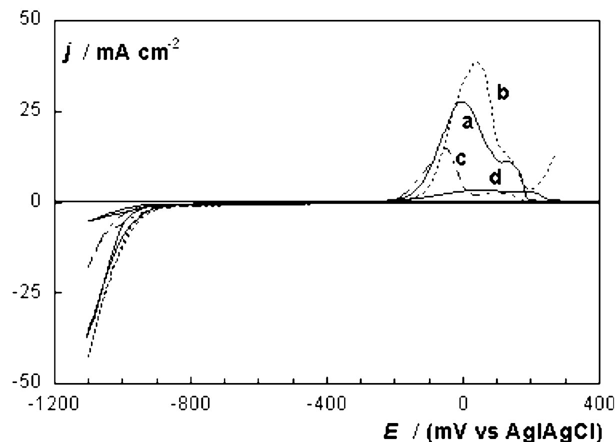

Fig. 2. Cyclic voltammograms of a 0.7 mol dm^{-3} $CoSO_4$+0.008 mol dm^{-3} $CuSO_4$+0.25 mol dm^{-3} $Na_3C_6H_5O_7$ solution. 10 mV s^{-1}. Different electrodes: (a) Vitreous carbon, (b) Copper, (c) Si/seed layer electrode, (d) glass/ITO.

Related to the voltammetric results, appropriate E_{Cu} and E_{Co} values for each substrate were selected as the manner that: At E_{Cu} the deposition rate was low enough to favour the formation of non-dendritic deposits thus ensuring the formation of the continuous copper layer, but not too positive that the oxidation of the cobalt layers occurred at the start of the deposition of each copper layer. At E_{Co}, cobalt was predominantly deposited and low simultaneous hydrogen co-evolution took place. EPMA analysis showed that a small percentage of copper ($\leq 2\%$) was always detected in deposits obtained at E_{Co} potential. By controlling the deposition parameters: (copper concentration, applied potential and step deposition time) multilayers of variable thickness were prepared.

Potentiodynamic stripping was tested as an electrochemical method able to allow information about the electrodeposited multilayers formation. In order to avoid interferences in the response due to the possible substrate oxidation, a vitreous carbon electrode was selected to perform these experiments. The oxidation of deposits had been made, both in the deposition solution itself and in a blank solution (0.7 mol dm^{-3} Na_2SO_4 dm^{-3}+0.25 mol dm^{-3} Na_3citrate, pH 4.7). In all experiments, the oxidation scan was started at a potential value for which no deposition occurred. A similar response was obtained from both solutions.

Fig. 3A shows the oxidation of both Cu/Co and Co/Cu bilayers, next to the oxidation of copper and quasi-pure cobalt layers (curves b and a). When one bilayer was deposited, their oxidation showed different responses depending on whether copper or cobalt was the upper metal. The oxidation of the Cu/Co bilayer appeared in the form of two clear separate peaks (curve c), the more cathodic, corresponding to the oxidation of the cobalt (the upper metal), and the second one corresponding to the oxidation of the copper.

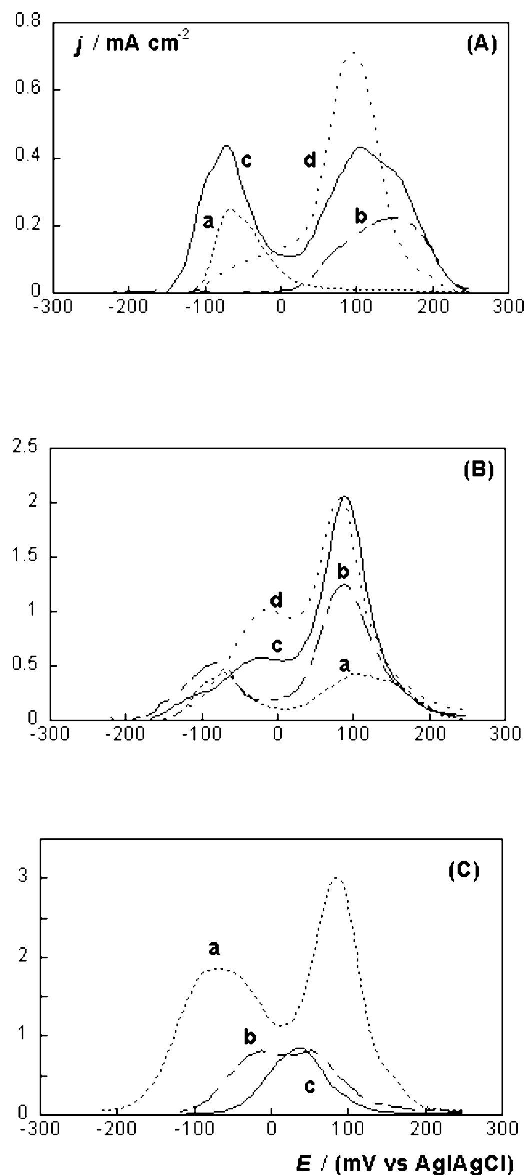

Fig. 3. Potentiodynamic stripping curves at 10 mV s^{-1} of alternate layers systems obtained on vitreous carbon electrodes at $E_{Co} = -1.10$ V, $E_{Cu} = -0.45$ V. Same solution of Fig. 2. (A) (a) Cobalt layer $t_{Co} = 0.4$ s, (b) Copper layer $t_{Cu} = 20$ s., (c) Cu/Co bilayer $t_{Cu} = 20$ s, $t_{Co} = 0.4$ s. (d) Co/Cu bilayer, $t_{Co} = 0.4$ s, $t_{Cu} = 20$ s. (B) Comparison between different numbers of alternate layers $t_{Cu} = 20$ s, $t_{Co} = 0.4$ s: (a) Cu/Co $t_{Cu}+t_{Co} = 20.4$ s, (b) $[Cu/Co]_2$ $t_{Cu}+t_{Co} = 40.8$ s (c) $[Cu/Co]_2Cu$ $t_{Cu}+t_{Co} = 60.8$ s and (d). $[Cu/Co]_3Cu$ $t_{Cu}+t_{Co} = 81.2$ s. (C) $[Cu/Co]_3Cu$ layers obtained at (a) $t_{Co} = 0.4$ s, $t_{Cu} = 20$ s, $t_{Cu}+t_{Co} = 81.2$ s (b) $t_{Co} = 0.2$ s, $t_{Cu} = 10$ s, $t_{Cu}+t_{Co} = 40.6$ s (c) $t_{Co} = 0.2$ s, $t_{Cu} = 5$ s, $t_{Cu}+t_{Co} = 20.6$ s.

However, when a Co/Cu bilayer was electrodeposited, stripping response showed a small peak followed by a great oxidation peak at more positive potentials (curve d). The charge involved in this stripping curve ($Q_{ox} = 2.40 \times 10^{-4}$ C) was similar than the reduction charge measured during bilayer deposition ($Q_{red} = -2.52 \times 10^{-4}$ C). This result indicates that, practically all the Co/Cu bilayer was oxidised in the stripping experiment, although some of the cobalt was oxidised at potentials more positive than those corresponding to pure-cobalt oxidation. Then, the presence of the thin copper layer over the first layer of quasi-pure cobalt hindered, but did not prevent, the complete cobalt oxidation, which occurred at more positive potentials. An increase in the deposition charge of the upper copper layer makes the cobalt oxidation more difficult.

When samples of different number of layers were prepared, a generalised behaviour was observed in the stripping response (Fig. 3B). Cobalt oxidation occurred at two different potentials: When cobalt was the upper layer, the oxidation of this cobalt layer occurred at the same potential at which the oxidation of a single layer of cobalt occurred (curves a and b), revealing the goodness of the cobalt layer formation, even after a few number of cycles. The oxidation of the other cobalt layers took place at more positive potentials (curves c and d), since in this case cobalt oxidation was hindered by the presence of the copper layers. Copper was always oxidised at the same position, although at potentials slightly more negative than that corresponding to pure copper. This is probably because the copper remaining after cobalt oxidation had a more porous structure than a compact copper layer.

When a set of samples were prepared at fixed deposition potentials by gradually reducing the thickness of the layers, the stripping response tended towards the appearance of only one oxidation peak at an intermediate position between cobalt and copper oxidation (Fig. 3C). In these conditions, the stripping peak moved according to the relative proportions of cobalt and copper presence in the layered system. For example, maintaining the deposition charge of the copper layers and increasing the deposition charge for the cobalt layers, the position of the stripping peak moved to cobalt oxidation position, as a consequence of a presumed increase in the global content of cobalt in the layered system. In this case, a similar stripping response was observed to that obtained for the oxidation of a Co–Cu solid solution electrodeposited [23].

Therefore, the stripping of multilayer samples showed different kind of responses depending on the thickness of the layers prepared. Different oxidation peaks were recorded for the thicker layers, whereas only one oxidation peak was observed when reducing the thickness of the layers electrodeposited. Similar results were obtained in all tested substrates.

The stripping method also allowed us to check the optimality of the electrodeposition conditions selected. Only conditions that lead to high Q_{ox}/Q_{red} ratio, higher than 0.9 were considered to prepare multilayers.

3.3. Morphological characterisation and analysis of the deposits

The checking of multilayer formation was firstly attempted by SEM. For this purpose, different Cu/Co multilayers had been grown over different electrodes. In all cases, after multilayer deposition pure-copper was electrodeposited to protect the multilayers between bulk copper. As multilayer observation requires cross-section imaging, better results were obtained when the mechanical properties of both the substrate and the multilayers were similar. For glass/ITO and Si/seed layer substrates, hard particles of substrate might scratch the multilayers during polishing. Copper substrate proved to be a good substrate for SEM observation, because it has similar hardness to the multilayers and improves its adherence to the substrate.

Observation of prepared samples by SEM revealed that metallic layers parallel to the substrate were obtained (Fig. 4), although the increase in the deposition time produced an increase in surface roughness. Co/Cu bilayer thickness measured from the images logically depended on the pulse duration, leading to 180 nm from Fig. 4A and 70 nm for Fig. 4B. The bilayer thickness observed was similar to that calculated from deposition charges of cobalt and copper accepting high efficiency (171 nm for conditions of Fig. 4A and 65 nm for conditions of Fig. 4B). The bilayer thickness (h_b) was calculated by means the equation (1) in which the small copper percentage in cobalt layer was not considered:

$$h_b = (Q_{Cu} \cdot V_{Cu} + Q_{Co} \cdot V_{Co}) \frac{N_A}{2 \cdot F \cdot A} \quad (1)$$

where Q_{Cu} and Q_{Co} are the deposition charges corresponding to one layer of copper and cobalt, respectively, V_{Cu} and V_{Co} are the atomic volumes in the crystalline lattice, N_A is the Avogadro's number, F is the Faraday constant and A is the electrode area. High current efficiency is a condition assessed by stripping results.

In a parallel way TMAFM was used to analyse the Cu/Co multilayer formation. TMAFM imaging of the prepared samples at different points of the section coating showed alternated multilayered structure (Fig. 5). The profile of the surface of the cross-section showed a periodic variation in the z direction due to the selective chemical etching, the copper layers being lower than the cobalt layers, revealing the good selectivity of the etching procedure. Individual layers were clearly distinguished, showing an average value of bilayer thickness (from the start of one cobalt layer to the end of next etched copper layer) of 140 nm. This value was similar to that calculated from deposition charges ($h_b = 136$ nm). However, it was not possible to get evidence of multilayers of lower bilayer thickness by TMAFM,

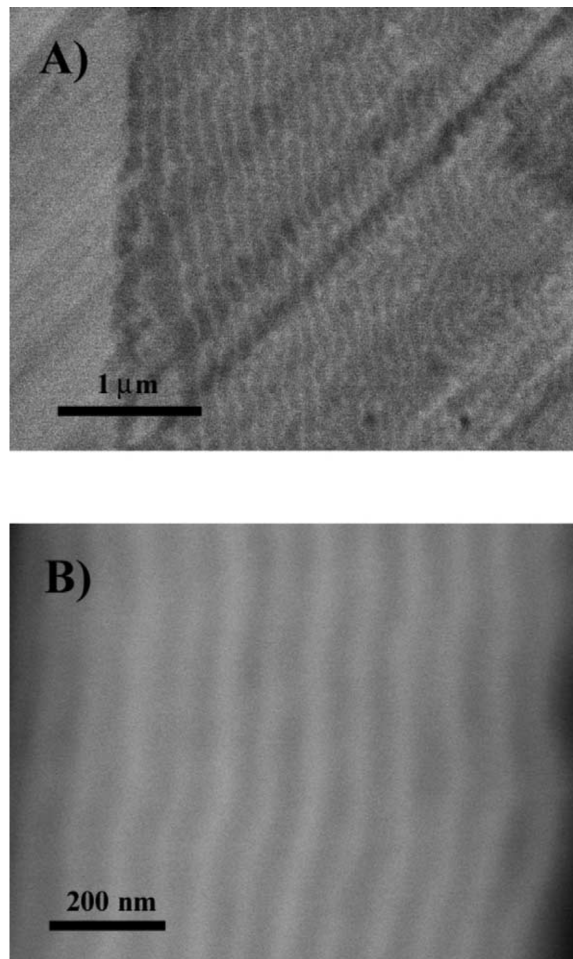

Fig. 4. SEM micrographs of the Cu/Co multilayers obtained by pulses at (A) $E_{Cu} = -0.45$ V, $t_{Cu} = 55$ s, $E_{Co} = -1.175$ V, $t_{Co} = 5$ s, from a 0.7 mol dm^{-3} $CoSO_4$+0.004 mol dm^{-3} $CuSO_4$+0.25 mol dm^{-3} $Na_3C_6H_5O_7$ solution. Copper electrode. (B) $E_{Cu} = -0.50$ V, $t_{Cu} = 22$ s, $E_{Co} = -1.15$ V, $t_{Co} = 2$ s, from a 0.7 mol dm^{-3} $CoSO_4$+0.008 mol dm^{-3} $CuSO_4$+0.25 mol dm^{-3} $Na_3C_6H_5O_7$ solution. Copper electrode.

probably due to non-selective chemical etching of the copper layers when these were too thin.

Cu/Co multilayer deposition took place with low hydrogen evolution and avoiding cobalt dissolution during copper deposition. The estimation of the thickness from the deposited charge was possible. When the objective is to prepare multilayers of very thin layers, for which direct observation is not possible, it is fundamental to adjust the electrodeposition conditions to high current efficiency.

EPMA analysis allowed determining the global composition of the prepared multilayers. Measured values were compared with the calculated values obtained from Faraday's law from the electrodeposited charge. The sufficient concordance between both results aided to use the theoretical spaced calculation. Then, a non-destructive method such as EPMA allowed us to contrast the

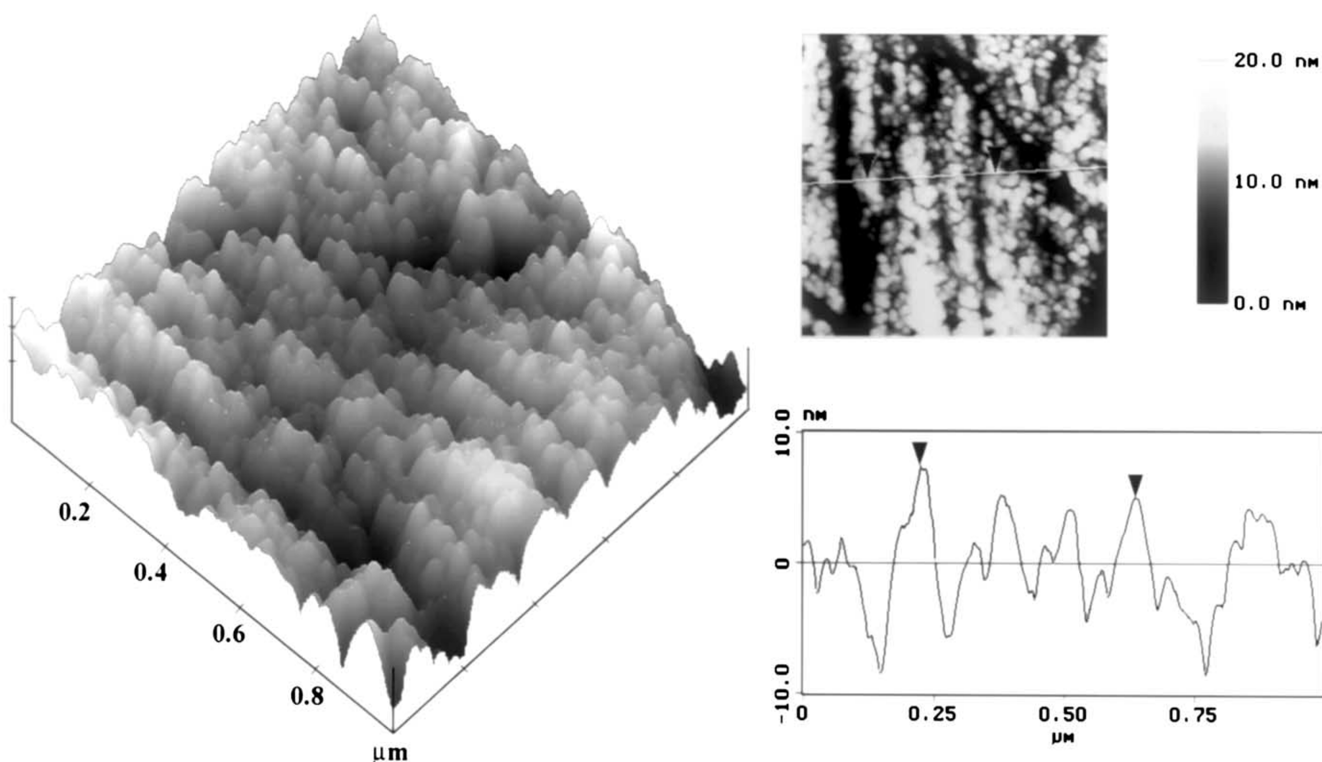

Fig. 5. TMAFM images of electrodeposited multilayer obtained at $E_{Cu} = -0.45$ V, $t_{Cu} = 55$ s, $E_{Co} = -1.125$ V, $t_{Co} = 5$ s, from a 0.7 mol dm^{-3} $CoSO_4$+0.008 mol dm^{-3} $CuSO_4$+0.25 mol dm^{-3} $Na_3C_6H_5O_7$ solution. Copper electrode.

calculated thickness by means the electrodeposition charge involved in each of the layers.

The analysis of the multilayered coatings, obtained over Ni substrate, using XPS and Auger techniques showed that both experimental methods were unable to detect the cobalt and copper alternance in the deposits. From these techniques global composition was always obtained. The metal percentages obtained from these experiments were similar to those obtained by means of EPMA measurements and were also similar to values obtained by means of the theoretical calculations from the deposition charges of copper and cobalt.

3.4. Structural characterisation

Cu/Co multilayers of different layer thickness were also analysed using XRD. For this purpose, glass/ITO and Si/seed layer were mainly selected due to the absence of intensity at 2θ values next to copper or cobalt responses.

Fig. 6A shows a typical diffractogram on glass/ITO substrate. Next to the response of the substrate, four main peaks were detected corresponding to the coating response at around 44, 51, 75 and 91° 2θ. All indexed peaks correspond to a fcc structure and appeared at diffraction angles between the lines corresponding to electrodeposited fcc copper and fcc cobalt. Moreover, XRD showed that the deposited multilayers consist of a highly (111) textured structure.

Upon varying the Q_{Co}/Q_{Cu} ratio, i.e. the global coating composition, the position of the diffraction peaks moved clearly. Fig. 6B and C show the magnification of the peak (111) of coatings obtained both on glass/ITO and Si/seed layer substrates. The position of each diffraction peak shifted towards the position of the cobalt line as the Q_{Co}/Q_{Cu} ratio increased. This diffraction response was similar to that obtained when the formation of Co+Cu solid solution with variable cobalt percentage in the deposits took place [23,24]. The analysis of the global composition of the coatings studied by XRD allowed us to corroborate that the diffraction peak position from multilayers response varies as a function of Vegard's law, in a similar way to that of Co+Cu solid solution formation. From these results, the relative position of the diffraction peaks with respect to pure-copper and pure-cobalt position was another way of estimating the cobalt content in the coatings.

For all diffraction experiments made, no clear satellite peaks were detected to calculate the superlattice period.

Similar results were found when TEM-selected area diffraction was used to study the Cu/Co multilayers. Deposits obtained on Si/seed layer substrates led to spotty diffraction rings (Fig. 7). The measurement of the ring diameter ($2R_{hkl}$) related to the (hkl) reflection in the

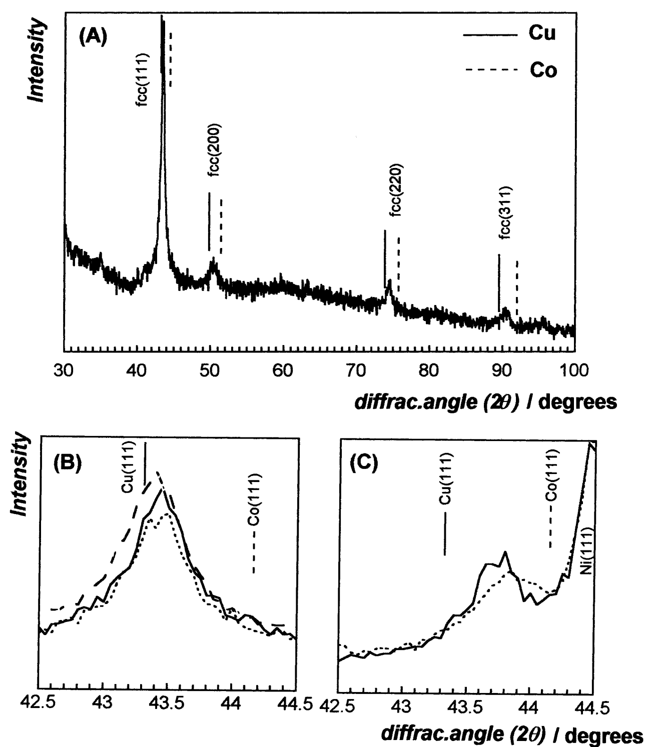

Fig. 6. (A) X-ray diffractogram of [Cu(4.3 nm)/Co(1.2 nm)]$_{50}$ multilayers obtained from a 0.008 mol dm^{-3} $CuSO_4$+0.7 mol dm^{-3} $CoSO_4$+0.25 mol dm^{-3} $Na_3C_6H_5O_7$ solution. Glass/ITO electrode. (B) Detail, between 42.5 and 44.5° 2θ, of X-ray diffractograms on glass/ITO electrode of Figure A. (a) [Cu(4.3 nm)/Co(1.2 nm)/]$_{50,}$ (b) [Cu(2.0 nm)/Co(0.4 nm)]$_{100,}$ (c) [Cu(1.1 nm)/Co(0.2 nm)]$_{200}$. (C) Detail, between 42.5 and 44.5° 2θ, of a X-ray diffractogram of (a) [Cu(2.2 nm)/Co(2.5 nm)]$_{50}$ and (b) [Cu(3.4 nm)Co(6.7 nm)]$_{25}$ multilayers obtained from a 0.008 mol dm^{-3} $CuSO_4$+0.7 mol dm^{-3} $CoSO_4$+ 0.25 mol dm^{-3} $Na_3C_6H_5O_7$ solution. Si/seed layer substrate.

diffraction patterns allowed us to assess the mean lattice parameter of the Cu/Co multilayer. Next to the rings

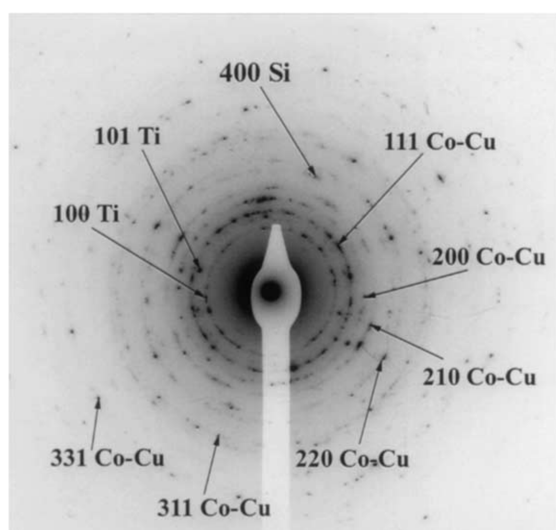

Fig. 7. TEM selected area diffraction pattern of [Cu(2.2 nm)/Co(2.5 nm)]$_{50}$ obtained at conditions of Fig. 6C.

identified as those corresponding to silicon or titanium of the substrate, six rings were assigned to the coating. Rings corresponding to the nickel seed layer were not detected. The coating rings corresponded to a fcc structure and they appeared at an intermediate position between those of pure-cobalt or pure-copper for all the multilayers analysed, corroborating the results obtained by XRD. A lattice parameter of the fcc structure, intermediate between the parameter of fcc copper (0.361 nm) and fcc cobalt (0.354 nm), was obtained.

3.5. Magnetoresistance values

The resistance of some Cu/Co multilayers, obtained on glass/ITO substrate, with a fixed copper layer thickness of about 1.2–1.3 nm was measured as a function of the external magnetic field, H, in samples with the thickness of the cobalt layer ranging from 0.7 to 3 nm. All thickness values were estimated from the deposition j-t transient obtained for each layer. As we have previously shown [25], a copper layer slightly greater than 1 nm thick is the optimum value, which ensures the continuity of the deposited layer, but it is not so large as to reduce the MR signal by decreasing the relative contribution to the total resistance of the Co–Cu interfaces with respect to that of the current flowing through the inner part of the Cu layers. The present work was aimed at elucidating the effect of the cobalt layer thickness on the MR response of these samples. Three sets of multilayers obtained after 5, 10 and 15 min of deposition time were prepared. These values of the deposition time, which lead to coatings ranging between 0.1 and 0.3 μm, guarantee that the obtained multilayers are free of internal stresses and have moderate surface roughness.

From the $R(H)$ measurements, the MR ratio was calculated as $\Delta R/R_0$, where $\Delta R = R(H) - R_0$ is the change of the resistance due to the application of H and R_0 is the maximum value of $R(H)$ at the coercive field. In Fig. 8, the value of the MR ratio at 27 K measured at a field of 11 kOe for the three sets of multilayers is depicted as a function of the thickness of the cobalt layer. The maximum MR for each curve is achieved for cobalt thickness in the range of 1–1.5 nm, irrespective of the deposition time (number of Cu/Co bilayers). In fact, the optimum value is in the middle point of this range, close to about 1.2 nm, which is the same value estimated for the optimum copper thickness [25].

Deeper insight into the morphology of the cobalt layer may be gained by analysing the MR curves in the vicinity of the coercive field. In Fig. 9, a detail of the MR curves for samples with cobalt thickness of 1 and 1.5 nm, both obtained after 15 min of deposition time, are compared. For a cobalt thickness of 1 nm (curve b) the MR curve shows rounded peaks centred at a

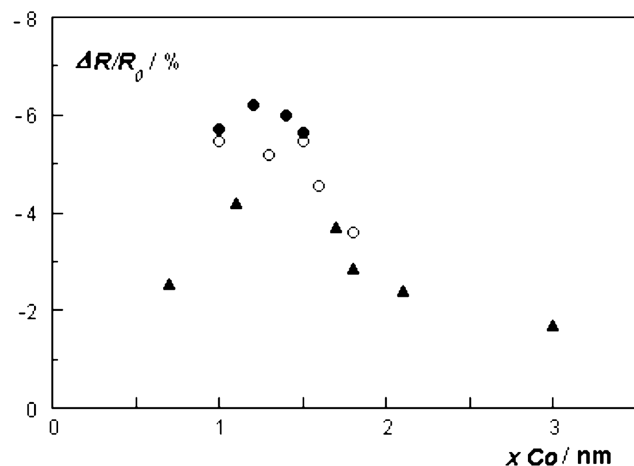

Fig. 8. $\Delta R/R_0$ at 11 kOe and 27 K as a function of the Co layer thickness for three sets of multilayers of fixed Cu layer thickness (1.2 nm) and total deposition time of 5 (▲), 10 (m) and 15 (●) min.

coercive field of about 200 Oe, indicating the existence of a distribution of Co isles of variable size (lost of continuity of the Co layer). In contrast, the MR curve for a cobalt thickness of 1.5 nm (curve a) shows sharper peaks located at about 300 Oe, which is in agreement with the values of the coercive field observed in other cobalt samples grown by electrodeposition [26,27]. This is consistent with the formation of a continuous Co-rich layer with magnetic response similar to that of the bulk material. Consequently, the maximum value of MR occurs at the minimum Co thickness (about 1.2 nm) for which a continuous Co-rich layer appears.

The MR curves measured at 27 and 300 K, respectively, in a multilayer with 1.2 nm of cobalt thickness obtained after 15 min of deposition are shown in Fig. 10. The MR at 27 K and with an applied field of 11 kOe is −6.2%, the maximum value. MR at 11 kOe is reduced as the temperature increases, the value observed at room temperature being −2.4%. This reduction is associated with the thermal demagnetisation of the cobalt present at the interfaces. Moreover, the electrodeposition method produces a high degree of dilution of the cobalt atoms at the interfaces with the copper layers, which is responsible for the moderate MR values observed, both at low and room temperatures, as compared with those corresponding to similar samples prepared, by another nonequilibrium techniques such as sputtering, especially over a buffer layer [28–30].

4. Conclusions

Electrodeposition was used to obtain Cu/Co multilayers on different substrates. Voltammetric and stripping studies were used to select deposition conditions that lead to a Q_{ox}/Q_{red} ratio greater than 0.9 even on the low active substrates. Under these conditions, the

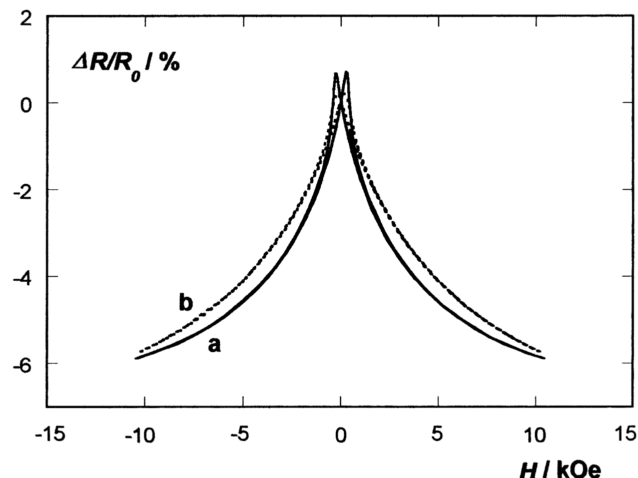

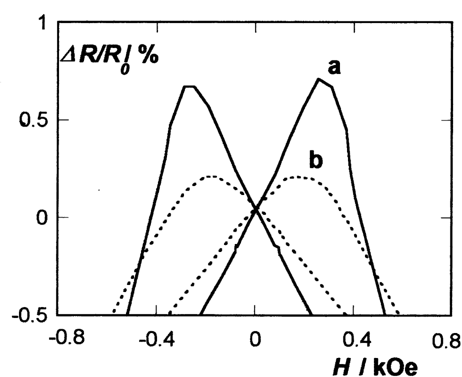

Fig. 9. $\Delta R/R_0$ vs. in-plane applied field in parallel geometry, and detail of the low field region, at 27 K for the multilayers: (a) $[Cu(1.2)/Co(1.5)]_{120}$ and (b) $[Cu(1.2)/Co(1.0)]_{140}$.

recorded current response during layer deposition allowed us to estimate the layer thickness (h_b) because for the thickest bilayers prepared this theoretical calculation lead to similar values to those obtained from direct observation of multilayers from SEM or

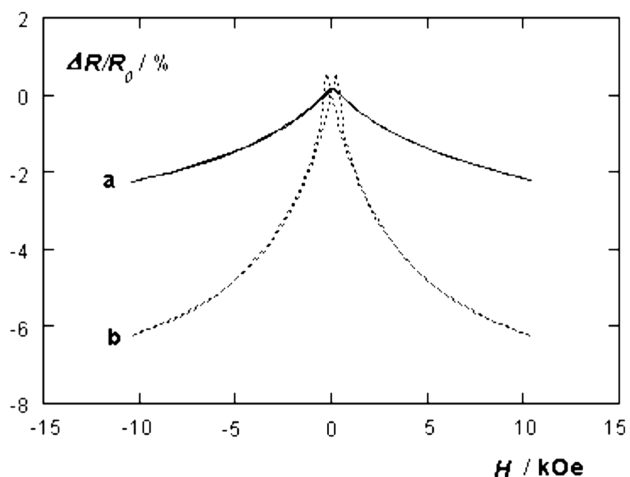

Fig. 10. $\Delta R/R_0$ vs. in-plane applied field in parallel geometry, for a $[Cu(1.2)/Co(1.2)]_{130}$, measured at (a) 27 K and (b) 300 K.

TMAFM experiments. Therefore, it was demonstrated that when thin layers (of 0.5–3 nm) are prepared to measure magnetoresistance, the theoretical calculation can be used, with low error, to assess the bilayer thickness.

It has been found that stripping responses of multilayered systems can inform us about the thickness of cobalt and copper layers able to show magnetoresistive response. For the Cu/Co multilayers prepared, when the layers were not so thin (greater than 1.8–2 nm) and different peaks were obtained in the stripping response, the measured values of magnetoresistance are low. In contrast, when stripping response evolved into overlapped peaks or only one peak, a clear increase in the magnetoresistance of the corresponding Cu/Co coating was observed. However, very thin layers, below 1 nm, lead, again, to a clear decrease in the magnetoresistance of the material, revealing that very short deposition times were not able to obtain well-formed alternate layers.

XRD, XPS and Auger experiments allowed us to detect the global composition in the multilayered system. XRD showed a similar response to that obtained for a solid solution formation. Cobalt percentages calculated from Vegard's law agree with the theoretical values obtained from the deposition charges.

Magnetoresistance results of the Cu/Co samples analysed indicate that similar arguments used to justify the optimum value of the copper thickness [25] also might be applied to the cobalt layers, fact which demonstrates that MR in these multilayers is mainly associated with electron scattering at the Co–Cu interfaces. Consequently, the optimum cobalt thickness must be enough to ensure the formation of well-defined Co–Cu interfaces, but not as large as to produce an intermediate cobalt layer without copper intermixing which would act as a nonmagnetoresistive channel. Besides, for a fixed thickness of the copper layers, MR increases with the deposition time, accordingly with the increasing number of Co–Cu interfaces.

Acknowledgements

The authors thank the Serveis Cientificotècnics (Universitat de Barcelona) for equipment availability. This research was supported financially by contract MAT 2000-0986 and MAT 2000-0858 of the Comisión Interministerial de Ciencia y Tecnología (CICYT) and by the Comissionat of the Generalitat de Catalunya under Research Project SGR 2000-017.

References

[1] I. Kirilova, I. Ivanov, S. Rashkov, J. Appl. Electrochem. 28 (1998) 637, 1359.
[2] J.D. Jensen, D.R. Gabe, G.D. Wilcox, Surf. Coat. Technol. 105 (1998) 240.
[3] G. Chawa, G.D. Wilcox, D.R. Gabe, Trans IMF 76 (1998) 117.
[4] M.R. Kalantary, G.D. Wilcox, D.R. Gabe, Br. Corrosion J. 33 (1998) 197.
[5] A.M. Herman, M. Mansour, V. Badri, B. Pinkhasov, C. Gonzales, F. Fickett, M.E. Calixto, P.J. Sebastian, C.H. Marshall, T.J. Gillespie, Thin Solid Films 361-362 (2000) 74.
[6] A.A. Pasa, W. Schwarzacher, Phys. Stat. Sol. 173 (1999) 73.
[7] E. Toth Kadar, L. Peter, T. Becsei, W. Schwarzacher, J. Electrochem. Soc. 147 (2000) 3311.
[8] Y. Jyoko, S. Kashiwabara, Y. Hayashi, W. Schwarzacher, Electrochem. Solid-State Lett. 2 (1999) 67.
[9] Y. Ueda, T. Houga, H. Zaman, A. Yamada, J. Solid Stat. Chem. 147 (1999) 274.
[10] Y. Jyoko, S. Kashiwabara, Y. Hayashi, W. Schwarzacher, J. Electrochem. Soc. 144 (1997) L5.
[11] E. Chassaing, P. Nallet, M.F. Trichet, J. Physique IV 6 (1996) C7–13.
[12] W. Schwarzacher, D.S. Lashmore, IEEE Trans. Magn. 32 (1996) 3133.
[13] M Suzuki, T. Ohwaki, Y. Taga, Thin Solid Films 304 (1997) 333.
[14] H. El Fanity, K. Rahmouni, M. Bouanani, A. Dinia, G. Shmerber, C. Meny, P. Panissod, A. Cziraki, F. Cherkaoui, A. Berrada, Thin Solid Films 318 (1998) 227.
[15] M. Schlesinger, K.D. Bird, in: Paunovic (Ed.), The Electrochemical Society Proceedings, The Electrochemical Proceeding Series, Pennington, NJ, vol. 94-31, 1994, p. 97.
[16] M. Shima, L. Salamanca-Riba, T.P. Moffat, R.D. McMichael, J. Mag. Mag. Mat. 198–199 (1999) 52.
[17] Y Ueda, N. Kikuchi, S. Ikeda, T. Houga, J. Mag. Mag. Mat. 198-199 (1999) 740.
[18] P. Nallet, E. Chassaing, M.G. Walls, M.J. Hytch, J. Appl. Phys. 79 (1996) 6884.
[19] P.E. Bradley, D. Landolt, Electrochim. Acta 45 (1999) 1077.
[20] T. Miyake, M. Kume, K. Yamaguchi, D.P. Amalnerkar, H. Minoura, Thin Solid Films 397 (2001) 83.
[21] Y. Jyoko, W. Schwarzacher, Electrochim. Acta 47 (2001) 371.
[22] K. Kudo, K. Kobayakawa, Y. Sato, Electrochim. Acta 47 (2001) 353.
[23] E. Gómez, A. Llorente, E. Vallés, J. Electroanal. Chem. 495 (2000) 19.
[24] H. Zaman, A. Yamada, H. Fukuda, Y. Ueda, J. Electrochem. Soc. 145 (1998) 565.
[25] E. Gómez, A. Labarta, A. Llorente, E. Vallés, Surf. Coat. Technol. 153 (2002) 261.
[26] J.L. Bubendorff, E. Beaurepaire, C. Mény, P. Panissod, J.P. Bucher, Phys. Rev. B 56 (1997) R7120.
[27] L. Cagnon, T. Devolder, R. Cortes, A. Morrone, J.E. Schmidt, C. Chappert, P. Allongue, Phys. Rev. B 63 (2001) 104419.
[28] D.J. Kubinski, H. Holloway, J. Mag. Mag. Mat. 165 (1997) 104.
[29] M. Suzuki, T. Ohwaki, Y. Taga, Thin Solid Films 304 (1997) 333.
[30] M. Angiolini, G. Carlotti, G. Gubbiotti, A. Montone, L. Palmieri, L. Pareti, G. Turilli, M. Vittori-Antisari, J. Mag. Mag. Mat. 198-199 (1999) 462.

5. Discussió i anàlisi de resultats

L'estudi electroquímic del procés de deposició de Co-Cu en un bany electrolític de sulfats i citrats mostra que quan la dissolució conté suficient quantitat de citrat per assegurar que tant coure(II) com cobalt(II) estiguin en forma de complexos cítrics, té lloc la deposició conjunta d'ambdós metalls, sempre que s'apliquin potencials o densitats de corrent suficientment negatives. L'interval de potencials als que comença la deposició es detecta a la voltametria cíclica amb un brusc increment de la intensitat de reducció i correspon a potencials intermedis entre els de deposició de coure i cobalt purs en el mateix medi. La oxidació del dipòsit es detecta en un únic pic d'oxidació tant a la voltametria cíclica com a l'*stripping* potenciodinàmic. Aquest pic es relaciona amb la oxidació de l'aliatge.

Les respostes cronoamperomètriques durant la deposició a potencial constant i cronopotenciomètrica durant la deposició a densitat de corrent fixa, demostren igualment la deposició no separada d'ambdós metalls.

La posició intermèdia del pic d'oxidació de l'aliatge entre els pics d'oxidació dels metalls purs i el desplaçament del pic des de la posició de coure cap a la del cobalt a mida que el potencial o la densitat de corrent es fan mes negatius es relaciona amb la formació d'una dissolució sòlida de composició variable.

L'*stripping* galvanostàtic dels dipòsits reflexa també aquest comportament, ja que detecta una variació gradual del potencial durant la oxidació fins a registrar l'inici de la oxidació del propi medi. La oxidació galvanostàtica de cada metall pur (coure i cobalt) es registra com un *plateau* de potencial constant.

La formació d'una dissolució sòlida Co-Cu es corrobora mitjançant l'anàlisi composicional i estructural dels dipòsits. L'aliatge format correspon a una estructura cristal·lina cúbica centrada a les cares (fcc), detectada per XRD, amb uns paràmetres

de xarxa que varien gradualment entre els de coure i cobalt (fcc) a mesura que augmenta la proporció de cobalt al dipòsit. El compliment d'una dependència lineal entre el paràmetre de xarxa i el percentatge de cobalt al dipòsit (llei de Vegard) permet estimar la composició del dipòsit a partir de la posició dels pics de difracció.

L'ajust de la relació [Co(II)]/[Cu(II)] en solució i del potencial o la densitat de corrent ha permès controlar la composició, morfologia i estructura de l'aliatge. Les condicions estudiades han conduït a dipòsits de percentatges de cobalt moderats (0-40%) i de morfologia variable en funció de la composició. Els dipòsits de percentatges mes baixos de cobalt presenten una morfologia nodular, que evoluciona cap a una morfologia mes arestada en augmentar el contingut de cobalt al dipòsit. L'anàlisi dels dipòsits mostra que per cada condició de deposició la composició del dipòsit és constant, tant en superfície com en profunditat.

No ha interessat preparar dipòsits amb percentatges de cobalt mes alts ja que l'estudi de les propietats magnètiques ha demostrat que els aliatges Co-Cu que contenien mes d'un 30% ja presentaven un comportament magnètic molt similar al del cobalt pur.

S'ha observat com tant la resposta electroquímica durant la deposició com els dipòsits obtinguts són similars per als diferents substrats testats (carboni vitri, coure, níquel, vidre/ITO, vidre/Cr o Si/capa llavor), encara que s'han d'ajustar les condicions de deposició per a cada substrat. Aquest fet ha permès utilitzar l'elèctrode mes adient per la preparació de dipòsits en funció del tipus de caracterització. Prèviament a l'estudi del procés ha estat necessari conèixer la resposta del propi elèctrode en una dissolució blanc i definir l'interval de potencials lliure de processos d'oxidació o reducció. Així, tant el carboni vitri com el vidre/ITO han estat els mes adients per a un estudi general del procés mitjançant voltametria cíclica o tècniques de stripping degut a la no oxidació del propi elèctrode en l'interval de potencials en els que es detecta la oxidació del dipòsit. Els elèctrodes metàl·lics (coure o níquel) han estat especialment útils per a la preparació de dipòsits gruixuts en facilitar la seva adherència.

Encara que els aliatges Co-Cu obtinguts responguin al comportament d'una dissolució sòlida tant a nivell electroquímic com a partir dels resultats de XRD, una observació acurada dels dipòsits a nivell nanomètric, utilitzant la microscòpia de transmissió electrònica, ha portat a detectar una certa heterogeneïtat dels dipòsits encara que es preparin a partir dels complexos cítrics de cobalt(II) i coure(II). Aquesta petita heterogeneïtat es manifesta en forma de *clusters* nanomètrics de cobalt distribuïts en la matriu.

A partir d'aquests resultats, el control de la quantitat de citrat sòdic a la dissolució ha permès obtenir dipòsits Co-Cu de diferent heterogeneïtat. La no complexació total dels cations metàl·lics en la dissolució permet la deposició mes separada de cobalt i coure. Però una molt baixa complexació condueix a dipòsits no uniformes (ni en composició ni en morfologia) i dendrítics a temps alts de deposició. La oxidació d'aquest tipus de dipòsits es reflexa en forma de dos pics clarament separats corresponents a la oxidació de coure i cobalt; la resposta de XRD mostra també els pics assignables als dos metalls, ambdós d'estructura fcc. Ha estat necessari l'ajust de la concentració de complexant per obtenir dipòsits de cobalt-coure d'aspecte uniforme i no dendrític, i amb una certa separació de pics tant a la resposta de oxidació electroquímica dels dipòsits com a l'espectre de difracció.

La concordança que s'ha trobat entre els resultats d'anàlisi ex-situ i els de *stripping* dels dipòsits cobalt-coure de diferent tipus ha permès corroborar la utilitat d'aquesta tècnica. *L'stripping* ha resultat útil per aquells elèctrodes en els que la oxidació del propi elèctrode no té lloc en la zona de potencials en la que es detecta la oxidació de l'aliatge. Ha resultat una eina ràpida de detecció de formació de dissolució sòlida Co-Cu o bé de dipòsits heterogenis, de determinació de la composició del dipòsit i de la comprovació de la seva constància amb el gruix del dipòsit. També ha permès obtenir informació sobre la eficiència del procés per a les diferents condicions de deposició.

Encara que la electrodeposició s'ha demostrat útil per a preparar directament dipòsits cobalt-coure uniformes en els que clarament es detecten ambdós metalls per separat,

és difícil mantenir la uniformitat d'aquests dipòsits en incrementar el temps de deposició. És per això que s'ha plantejat el fet de potenciar la segregació parcial del cobalt mitjançant el recuit controlat de mostres corresponents a aparents dissolucions sòlides.

El recuit de les mostres s'ha dut a terme a diferents temperatures i temps de recuit en un forn al buit per evitar la oxidació de les làmines. El forn dissenyat a tal fi ha funcionat correctament ja que no s'ha detectat la oxidació dels dipòsits preparats. El recuit de les mostres ha conduït a canvis morfològics i estructurals. S'observa un augment de la cristal·linitat del dipòsit així com la segregació de *clusters* rics en cobalt de diferents mides en funció del temps i de la temperatura de recuit. De totes maneres, la quantitat de cobalt segregat és massa petita com per que es pugui detectar per XRD i ha estat necessària la seva caracterització per TEM.

Una altra manera d'aconseguir electroquímicament un sistema heterogeni cobalt-coure ha estat la electrodeposició de multicapes mitjançant tècnica polsant a partir d'un únic bany contenint coure(II) i cobalt(II). En aquest cas es va utilitzar també un bany sulfat-citrat, però amb una menor quantitat de complexant a fi de possibilitar la deposició dels metalls a potencials suficientment separats. De totes maneres va ser necessària una certa quantitat de citrat per aconseguir que la deposició del coure tingués lloc a potencials mes negatius d'aquells als que s'oxida el cobalt acabat de dipositar i, d'aquesta manera, evitar/minimitzar la oxidació del cobalt durant la deposició del coure.

Degut a que el coure és un metall mes noble que el cobalt, diposita a potencials menys negatius, de manera que es pot dipositar coure pur escollint correctament el potencial. A mesura que el potencial aplicat es va fent mes negatiu, la deposició de cobalt va sent la reacció predominant, ja que la deposició del coure no pot excedir el corrent límit. Es va escollir una gran diferència de concentracions entre coure(II) i cobalt(II), mantenint molt baixa la de coure per minimitzar l'entrada d'aquest metall durant la deposició de cobalt. Es va decidir agitar suaument la dissolució durant la deposició, a fi de disminuir el temps necessari per a la formació de la capa i

simultàniament evitar els creixements dendrítics que es poden donar quan el creixement té lloc sota règim de difusió. En les condicions escollides el percentatge de coure en la capa de cobalt (determinat per EPMA) no va ser en cap cas superior al 2%.

La preparació de les multicapes es va testar sobre un ampli ventall de substrats: carbó vitri, grafit, coure, níquel, vidre/Cr, vidre/Au ,vidre/ITO, silici/capa llavor. Donada la diferent resposta electroquímica d'aquests substrats, per cada un d'ells es va fer un primer estudi voltamètric a fi de poder escollir els potencials de deposició de cobalt i coure adients per aconseguir, en cada cas, màxima eficiència de corrent i mínima oxidació del cobalt.

La caracterització d'aquests sistemes per tècniques com SEM o TEM implica una observació transversal del dipòsit, fet que comporta la necessitat d'un tall transversal de la mostra i un polit posterior. El tall de la mostra sense modificació de la mateixa es va aconseguir amb la serra adequada a la velocitat de tall adient; però aconseguir un bon polit de la mostra va ser mes dificultós: quan els dos materials, substrat i multicapes tenien propietats molt diferents, es produïa fàcilment el deteriorament de la mostra. Les partícules de vidre o de silici despreses durant el polit i procedents dels substrats, en tenir una duresa molt diferent de la de les multicapes, deterioraven la mostra, encara que el polit es realitzés manualment. Quan es va utilitzar com elèctrode una capa llavor de or sobre vidre, els problemes encara van ser mes greus degut a que l'or és un metall tou que durant el polit es deformava i acabava per cobrir la mostra. Les mostres que es van visualitzar amb millor resultat van ser les obtingudes sobre substrat metàl·lic.

D'altra banda es va observar que les multicapes es formaven mes paral·leles quan mes baixa era la rugositat del substrat. Els substrats de vidre rugosos milloraven l'adherència tant de la capa llavor com del dipòsit però promovien una elevada rugositat del dipòsit. El substrat que alhora afavoreix una baixa rugositat i elevada adherència dels dipòsits de multicapes és el Si/capa llavor.

Per les multicapes amb una mida superior a uns 50nm per bicapa va ser possible la observació per SEM. Però la disminució del gruix va fer que cada vegada la visualització fos mes difícil. Per les multicapes visualitzades per SEM es va fer un estudi comparatiu de la mida de cada bicapa en les imatges de SEM i del gruix teòric calculat a partir de la carrega que havia circulat durant la formació de cada una de les capes i del volum atòmic de cada metall a la xarxa cristal·lina. Els resultats van posar de manifest que l'eficiència del procés era molt propera al 100%. Aquest fet va permetre calcular amb fiabilitat el gruix de les capes preparades, en els casos en què no va ser possible visualitzar la mostra.

La microscòpia de forces atòmiques (TMAFM) es va demostrar útil per observar mostres tractades de la mateixa manera que per la visualització per SEM seguit d'un atac selectiu de les capes de coure a fi de crear el relleu necessari per evidenciar l'existència de les multicapes.

La tècnica de XRD ha estat utilitzada també com a eina de caracterització de les multicapes. Tots els pics indexats corresponen a una estructura fcc i apareixen a angles intermedis entre els corresponents a coure fcc i a cobalt fcc, resposta similar a la de una dissolució sòlida. Aquesta resposta s'ha utilitzat com a mètode de test per establir la correcta selecció dels potencials de deposició d'ambdós metalls. La posició del pic està relacionada amb la composició global de la multicapa, és a dir, amb la relació dels gruixos de les capes que composen la bicapa. Mostres preparades a potencial fix, igual temps global de deposició i relació t_{Cu}/t_{Co} constant però a partir de valors de t_{Cu} i t_{Co} diferents haurien de presentar els pics de difracció a la mateixa posició. Però per capes obtingudes amb polsos de potencial curts es va observar un desplaçament dels pics cap a la posició del coure que es va interpretar com l'existència d'un procés d'oxidació del cobalt durant la deposició del coure que provocava una disminució efectiva del gruix de la capa de cobalt. Aquests resultats indicaven la necessitat de corregir el potencial de deposició del coure a fi de minimitzar el procés d'oxidació del cobalt.

Els espectres de XRD a angles baixos de mostres obtingudes sobre elèctrodes amb capa llavor (per evitar la interferència del substrat metàl·lic) i que teòricament podrien haver aportat informació sobre els espaiats de les bicapes mai van donar resultats concloents, probablement degut a la elevada rugositat del substrat.

Donada la inversió de temps que implica la preparació de les mostres de multicapes per aconseguir la caracterització i donat que en moltes ocasions durant la preparació de la mostra aquesta es deteriora o es destrueix, es van analitzar les possibilitat de les tècniques electroquímiques per obtenir informació de les multicapes. El mètode es va aplicar a sistemes de multicapes que previsiblement tenien capes de pocs nanòmetres de gruix; aquests són sistemes de difícil visualització per microscòpia electrònica.

En analitzar la resposta de *stripping* de bicapes d'uns quants nanòmetres es va veure que si el coure era la primera capa dipositada no hi havia interferències entre les respostes d'ambdós metalls, confirmant la coherent formació de les capes. Si el coure era la darrera capa dipositada, la oxidació del cobalt es dificultava i tenia lloc majoritàriament a potencials propers a la oxidació del coure. Incrementant el nombre de capes es va comprovar que excepte quan el cobalt era la darrera capa dipositada, per la que s'observa la seva oxidació al potencial propi del cobalt, el coure dificulta la oxidació del cobalt que es retarda a potencials mes positius. L'estructura porosa en que deu quedar el coure després d'oxidar-se el cobalt facilita la oxidació del coure que té lloc a potencials mes negatius que els corresponents al coure dipositat.

Quan l'espaiat entre les capes era superior als 5 nm, en la resposta de *stripping* es van identificar dos pics corresponents a la oxidació dels dos metalls, però quan es redueixen les capes als 2-3 nm la oxidació tendeix a estar sota un sol pic, de posició depenent de la relació Co/Cu a la multicapa. Per capes per sota del nanòmetre es manté també un únic pic de *stripping*.

Per tots els sistemes preparats, tant en làmines continues com en multicapes es va testar la possible resposta de magnetoresistència. La mesura de les propietats de transport dels dipòsits de Co-Cu va implicar fer un estudi previ d'elecció dels

substrats mes adients, a fi de minimitzar la influència del substrat en la mesura de MR. S'ha comprovat que substrats formats per una base poc o gens conductora (vidre, silici) i una fina capa llavor conductora són útils tant per actuar com a elèctrodes per dipositar-hi les làmines de cobalt-coure com per mesurar directament sobre ells la magnetoresistència dels dipòsits, sense necessitat de separar-los del substrat. Per a cada un d'aquests elèctrodes l'estudi electroquímic ha permès establir les condicions òptimes de deposició, a les quals no es produeix ni deteriorament del substrat ni una important evolució de hidrogen. D'entre els diferents elèctrodes testats els mes útils han estat el vidre/ITO i el silici/capa llavor.

Per a mostres de Co-Cu de percentatges de Co inferiors al 30% i corresponents a una aparent dissolució sòlida, s'obtenen valors de MR petits, però no nuls. Aquest fet corrobora la presencia, en aquestes condicions, de petits *clusters* rics en cobalt detectats en una acurada observació per TEM. Percentatges superiors de cobalt donen lloc a una mesura de MR nul·la, relacionada amb el comportament ferromagnètic del material, similar al de cobalt pur.

El recuit d'aquest tipus de mostres ha conduït sempre a un increment del valor de MR relacionat amb la segregació de petits nous *clusters* de cobalt i, per tant, amb l'increment del nombre de fronteres entre partícules ferromagnètiques i matriu no magnètica. El valor concret de MR és funció del percentatge global de cobalt, de la temperatura i del temps de recuit. Per a cada composició es troba una temperatura de recuit òptima per la qual el valor de MR és màxim. Aquesta temperatura es relaciona amb la mida adient dels *clusters* rics en cobalt segregats durant el recuit.

Per al sistema de multicapes Cu/Co en les condicions de preparació escollides hi ha un espaiat mínim a partir del qual s'observa resposta magnetoresistiva. S'ha fixat la mida de la capa d'un metall i s'ha estudiat la influència de la variació del gruix de la capa de l'altre metall. S'ha vist que la mida òptima amb la que s'obtenen els valor mes alts de MR és quan l'espaiat de les capes està entre 1 i 2 nanòmetres. Valors mes baixos condueixen a una disminució de MR probablement com a conseqüència d'una no correcta formació de la capa.

De la mateixa manera es va estudiar la influència del gruix total de la mostra, observant-se que l'augment del gruix total estava relacionat amb un augment del valor de MR; Aquest increment no és lineal, ja que d'altra banda, l'augment del nombre de capes afavoreix l'augment de la rugositat, disminuint la bondat de les fronteres, factor que fa disminuir la MR.

En comparar els valors obtinguts de MR de les multicapes amb els resultats de *stripping*, es dedueix que la tècnica electroquímica ajuda a determinar els valors límits dels espaiats capaços de presentar magnetoresistència. El sistema comença a presentar senyal de MR per a espaiats tal que la resposta de *stripping* passa de ser de 2 pics a un pic únic; en reduir més els espaiats s'incrementa la senyal de MR.

Per tant, la tècnica electroquímica pot ser útil per determinar l'espaiat a partir del qual el material presenta resposta magnetoresistiva.

6.- Situació actual

Simultàniament al desenvolupament d'aquest treball, la recerca relacionada amb el sistema Co-Cu ha continuat en d'altres laboratoris d'arreu del món, donant lloc a un seguit de publicacions relacionades amb el tema.

Hi ha una gran activitat relacionada amb la preparació de mostres, majoritàriament de multicapes [1-3]. Normalment es continuen preparant a partir dels tradicionalment anomenats mètodes físics, ja que moltes de les propietats característiques d'aquest sistemes estan relacionades amb el món de la Física . Tot i això, en els últims anys s'ha acceptat que l'electrodeposició pot ser una eina útil per preparar capes primes de cobalt-coure. Això fa que vagi en augment el nombre de laboratoris que introdueixen la preparació electroquímica d'aquest sistema.

Un dels objectius prioritaris és l'estudi de la dependència de MR/GMR en funció tant de la tècnica com de les condicions de preparació, confirmant-se que l'estructura i la morfologia són factors més importants que la composició. S'ha comprovat que la utilització de diferents banys electrolítics pot conduir a dipòsits de la mateixa composició, però que presenten valors de MR molt diferents [4-8]. Això és degut a que cada tipus de bany condueix a dipòsits de cristal·linitat i de mida de gra diferent i té una diferent capacitat de mantenir pel·lícules continues de gruix nanomètric [9].

Uns altres estudis s'adrecen a relacionar els valor de MR amb la qualitat de les interfícies metall magnètic-metall no magnètic. Per això s'està abordant l'estudi tant de la rugositat de les capes (especialment en el cas de sistemes multicapes) [10-12] com de la interdifusió que té lloc entre les capes metàl·liques de coure i cobalt malgrat la teòrica immiscibilitat dels elements [13].

En els sistemes obtinguts per electrodeposició s'ha abordat la influència d'additius, tant orgànics com inorgànics, però s'ha trobat que els additius potencien el desordre estructural, el que es tradueix en una disminució de la GMR [14-17]. Un altre punt

que es considera quan s'utilitza deposició polsant és el control de les reaccions de desplaçament i la possible oxidació del cobalt durant la deposició del coure.

Donades les característiques del sistema cobalt-coure hi ha un interès especial en analitzar l'efecte dels tractament tèrmics sobre els dipòsits, incidint especialment en l'efecte sobre els valors de les propietats magnètiques i/o magnetoresistives. S'estudia la influencia tant de la temperatura com dels temps de recuit [10,11,18-25]. En el cas dels dipòsits tant granulars com de multicapes existeix un interval de temperatures de recuit en què s'observa un increment de MR, que sempre es relaciona amb la segregació de Co en la interfície, encara que en el cas dels sistemes formats per capes alternes, el recuit provoca el deteriorament de les multicapes a partir d'una certa temperatura.

S'han relacionat les propietats magnetoresistives amb els mètodes de preparació. Els valors de la temperatura de recuit i l'interval de temps per als que s'obtenen els millors valors de GMR depenen del mètode i de les condicions de preparació, tant si les mostres es preparen per mètodes físics com electroquímics [26-28].

D'altra banda, el desenvolupament dels sistemes tipus cobalt-coure va paral·lel al desenvolupament de les tècniques de caracterització, ja que l'estudi experimental de les propietats físiques dels nous materials requereix la seva caracterització. És necessari conèixer l'estructura del material (raigs X, microscòpia electrònica de transmissió, microscòpia de forces atòmiques), la seva composició, les propietats magnètiques (magnetització) i de transport (magnetoresistència). A mida que es van reduint els gruixos de les capes, els mètodes de caracterització han de ser mes sensibles i precisos, capaços de resoldre a nivell nanomètric.

Per exemple, donat que l'estructura cristal·lina i que l'orientació dels materials és important quan es determinen propietats magnètiques i de transport, un dels temes d'estudi actual és el possible control de la textura cristal·logràfica utilitzant substrats que indueixen una determinada orientació [29-31]. Hi ha grups en els que es treballa electrodipositant en condicions epitaxials, estudiant la capacitat de controlar

l'orientació en les capes subseqüents a partir de la informació obtinguda amb les tècniques de secció transversal per microscòpia electrònica de transmissió [1,9,31].

En aquest moment fabricar capes de pel·lícules individuals amb gruixos en el rang dels 10 nanòmetres com producte comercial és un repte, no només des del punt de vista de preparació d'aquestes capes si no també per la necessitat de controlar-ne l'estructura.

Referències

1.- M. Shima, L. Salamanca-Riba, R.D. Mc Michael, T.P. Moffat, J. Electrochem. Soc. 149(9) (2002) C439

2.- E. Chassaing, A. Morrone, J.E. Schmidt, Proc. Electrochem. Soc. 99-34, 2000 p. 235

3.- F. Spizzo, E. Angeli, D. Bisero, P. Vavassori, F. Ronconi, Appl. Phys. Letters 79 (2001) 3293

4.- T. Cohen-Hyams, W.D. Kaplan, D. Aurbach, Y.S. Cohen, J. Yahalom, J. Electrochem. Soc. 150 (2003) C 28

5.- A. Cziraki, M. Koteles, L. Peter, Z. Kupay, J. Padar, L. Pogany, I. Bakonyi, M. Uhlemann, M. Heruch, B. Arnold, J. Thomas, H. D. Bauer, K. Wetzig, Thin Solid Films 433 (2003) 237

6.- A. Paul, T. Danm, D. Burgler, S. Stein, H. Kohlstedt, P. Grunberg, J. Phys. Condensed Matter 15 (2003) 2471

7.- N.V. Myung, B.Y. Yoo, M. Schwartz, K. Nobe, Proc. Electrochem. Soc 2000-29 (Magnetic materials , Processes and devices VI) 2001 p.154

8.- T. Thomson, P.C. Riedi, Hyperfine Interactions 120 (1999) 23

9.- A. Cziraki, L. Peter, B. Arnold, J. Thomas, H. D. Bauer, K. Wetzig, I. Bakonyi, Thin Solid Films 424 (2003) 229

10.- S. Merkourakis, M. Hytch, E. Chassaing, M. Walls, Y. Leprince-Wang, J. Appl. Phys. 94 (2003) 3035

11.- K. Ratzke, M. J. Hall, D.B. Jardine, W.C. Shih, R.E. Somekh, A. L. Greer, J. Magn. Magn. Mat. 204 (1999) 61

12.- Y. Ueda, N. Kikuchi, S. Ikeda, T. Houga, J. Magn. Magn. Mat. 198-199 (1999) 740

13.- W. Weihnach, L. Peter, J. Toth, J. Padar, Zs.Kerner, G. M. Schneider, I. Bakonyi, J. Electrochem. Soc. 150 (2003) C 507

14.- B.L. Peterson, R. L. White, B.M. Clemens, Physica V: Condensed Matter 336 (2003) 157

15.- E. Chassaing, J. Electrochem. Soc. 148 (2001) C 690

16.- L. Peter, Z. Kupay, A. Cziraki, J. Padar, J. Toth, I. Bakonyi, J. Phys. Chem. 105 (2001) 10867

17.- J. J. Kelly, P.E. Bradley, D. Landolt, J. Electrochem. Soc. 147 (2000) 2975

18.- J. Thomas, A. John, K. Wetzig, Mikrochimica Acta 133 (2000) 131

19.- D. Kubinski, M. Parsons, J. Appl. Phys. 87 (2000) 4858

20.- R. García-Calderón, A. Yedra, A. García –Prieto, L. Fernández-Barquin, M.L. Fdez-Gubieda, J. Magn. Magn. Mat 262 (2003) 97-101

21.- M. Uhlemann, A. Gebert, M. Herrich, A. Kraure, A. Cziraki, L. Schultz, Electrochim. Acta 48 (2003) 3005

22.- M. Hecker, J. Thomas, D. Tretjen, S. Baunack, C.M. Schneider, A. Qiu, N. Cramer, R.E. Camley, Z. Celinski, J. Phys. D: Applied Physics 36 (2003) 564

23.- M. Urbaniak, T. Lucinski, F. Stobiecki, B. Szymanski, M. Schmidt, A. Slazak, Phys. Status Sol. A Applied Res. 196 (2003) 37

24.- L. Albini, G. Carlotti, G. Gubbiotti, L. Pareti, G. Socino, G. Turilli, J. Magn.Magn. Mat. 198-199 (1999) 363

25.- F. Prokert, J. Noetzel, N. Schell, E. Wieser, A. Gorbunov, Thin Solid Films 416 (2002) 114

26.- F. Casoli, F. Albertini, F. Bolzoni, L. Pareti, G. Turilli, E. Bontempi, F. Spizzo, L.E. Depero, J. Magn. Magn. Mat. 262 (2003) 69

27.- L. Van Loyen, D. Elefant, D. Tietjen, C.M. Schneider, M. Hecker, J. Thomas, J. Appl. Phys. 87 (2000) 4852

28.- E. Rozenberg, D. Mogilaynski, J. Pelleg, G. Gorodesky, R. Somekh, Thin Solid Films 342 (1999) 11

29.- M. Marszalek, J. Jaworski, J. Lekki, K. Marszalek, Z. Stachura, V. Voznyi, O. Bolling, B. Sulkio-Cleff, Surface Science 507-510 (2002) 346

30.- L. Cagnon, T. Devolver, R. Cortes, A. Morrone, J.E. Schmidt, C. Chappert, P. Allongue, Phys. Review B 63 (2001) 104419

31.- L. Peter, A. Cziraki, L. Pogany, Z. Kupay, I. Bakonyi, M. Uhlemann, M. Herrich, B. Arnold, T. Bauer, K. Wetzig, J. Electochem. Soc. 148 (2001) C168

7.- Conclusions

1.- Un bany electrolític tipus sulfat-citrat a pH moderadament àcid i amb complexació total dels cations metàl·lics porta a la electrodeposició d'aliatges de Co- Cu que corresponen a una dissolució sòlida d'estructura fcc. El control de les condicions d'electrodeposició permet l'obtenció d'aliatges Co-Cu de diferent composició i morfologia.

2.- El comportament del procés de deposició és similar per als diferents substrats utilitzats. Encara que el potencial en què s'inicia el procés és característic per a cada elèctrode, les característiques dels dipòsits finals són independents del tipus de substrat utilitzat.

3.- La tècnica de *stripping* s'ha provat com a mètode útil i ràpid tant per l'anàlisi de la composició dels dipòsits com per comprovar que la composició es manté constant al llarg de tot el gruix dels dipòsits.

4.- Els elèctrodes de vidre/ITO i silici/capa llavor han resultat adequats per preparar dipòsits dels quals se'n pugui mesurar directament la magnetoresistència. El valor de MR detectat en les làmines sense tractament tèrmic està relacionat amb la presencia de regions ferromagnètiques de mida nanomètrica dins la matriu no magnètica.

5.- L'electrodeposició a partir d'un bany que conté cations metàl·lics sense complexar permet obtenir dipòsits heterogenis, encara que la uniformitat d'aquests dipòsits es manté únicament per a làmines de poc gruix i ajustant la concentració de citrat per que la deposició d'ambdós metalls tingui lloc a potencials no molt separats.

6.- El tractament tèrmic dels dipòsits homogenis, controlant-ne la temperatura i el temps de recuit, dóna lloc a sistemes heterogenis que presenten MR. Les condicions òptimes de tractament es poden relacionar amb la mida i nombre de *clusters* ferromagnètics dins la matriu no magnètica.

7.- L'optimització d'un bany amb poc contingut de citrat i de les condicions d'electrodeposició ha permès preparar multicapes Co(Cu)/Cu amb eficiència propera al 100%. L'observació de les multicapes s'ha realitzat mitjançant SEM i AFM. La concordança entre els gruixos observats a les imatges de SEM i AFM i els teòrics calculats a partir de les càrregues de deposició permet estimar els gruixos de les capes més primes, de mida nanomètrica.

8.- Els valors de MR que presenten els dipòsits de multicapes són funció del gruix de les capes. El valor màxim de MR obtingut correspon a gruixos tant de la capa de coure com de la de cobalt al voltant d'un nanòmetre.